Probing living cells with the molecular force assay

Uta Wienken

Dissertation

München, Oktober 2013

Probing living cells with the molecular force assay

Dissertation

an der Fakultät für Physik

der Ludwig-Maximilians-Universität München

vorgelegt von

Uta Wienken
geb. Steinbach

aus Leipzig

München, Oktober 2013

Erstgutachter: Prof. Dr. Hermann E. Gaub

Zweitgutachter: Prof. Dr. Tim Liedl

Mündliche Prüfung am 12. Dezember 2013

Table of contents

Zusammenfassung

In der vorliegenden Arbeit wurde ein Analyseverfahren für Rezeptor-Ligand Systeme basierend auf dem Molekularen Kraft Assay (MFA) für die Anwendung auf lebenden Zellen weiterentwickelt und verfeinert. Mit dem MFA sind hoch parallele vergleichende Kraftmessungen möglich, die bisher aber nur an immobilisierten Molekülen auf festen Oberflächen durchgeführt wurden. Die molekulare Kraftwaage erlaubt es, die Bindungskräfte von Rezeptor-Ligand Interaktionen zu analysieren, indem die zu untersuchende Bindungskraft mit einer bereits bekannten Referenzkraft z.B. mit der Bindungskraft zwischen komplementären DNA-Strängen verglichen wird. Dabei werden die einzelnen Moleküle als Kraftsensoren verwendet, die in Serie zwischen zwei Oberflächen gespannt werden. Beim Separieren der Oberflächen reißt die schwächere der beiden Bindungen mit größerer Wahrscheinlichkeit. Am Referenzmolekül ist ein Fluoreszenzfarbstoff angebracht, der, je nach Ausgang des Experiments, auf der einen oder der anderen Oberfläche zu finden ist. Nach dem Separieren wird das Verhältnis der Fluoreszenzintensitäten der beiden Oberflächen analysiert.

Nachdem in einem modifizierten MFA Experiment bereits in Vorarbeiten grundsätzlich gezeigt wurde, dass es möglich ist, Liganden von einer Elastomeroberfläche auf Zellen zu transferieren, werden in dieser Arbeit aufwendigere Experimente vorgestellt. Um die Elastomerstempel zu funktionalisieren, müssen Proteine auf der Oberfläche immobilisiert werden. In diesem Zusammenhang wurde die Anwendung eines Microplotters für das Aufbringen von Proteinen optimiert. Auf diese Weise ist es möglich verschiedene Liganden auf einen Elastomerstempel zu platzieren und somit in nur einem Stempelvorgang mehrere Experimente parallel durchzuführen und zu vergleichen.

Auf menschlichen roten Blutzellen wurden die Interaktionen von dem N-Acetylgalactosamin (galNAc) terminierten Glykolipid mit dem Lektin *helix pomatia* Agglutinin (HPA) und eines CD47 Rezeptors mit einem Anti-CD47 Antikörper untersucht. Beide Liganden wurden in einem Schachbrettmuster auf den Stempel aufgebracht. Durch das Transferieren der Liganden gegen eine gewisse Referenzkraft werden unspezifische Wechselwirkungen vermieden, die das Ergebnis verfälschen können. Auf Zellen der Blutgruppe A werden beim Stempelprozess beide Liganden

übertragen. Zellen der Blutgruppe 0 hingegen fehlt galNAc, was dazu führt, dass beim selben Experiment auf diesen Zellen nur ein Fluoreszenzübertrag für den CD47 Rezeptor stattfindet. Dieses Experiment zeigt, dass der MFA auf lebenden Zellen eine wertvolle Methode ist, um ein paralleles Screening nach Rezeptoren auf der Zelloberfläche ohne unspezifische Wechselwirkungen durchzuführen.

Weiterführende Experimente auf roten Blutzellen zeigen, dass es der MFA auf Zellen ermöglicht, detaillierte vergleichende Kraftanalysen von Rezeptoren durchzuführen. In diesem Zusammenhang konnte durch Variation der DNA Referenzkraft ein Kraftäquivalent sowohl für die Wechselwirkung von galNAc mit HPA als auch für den CD47 Rezeptor und seinen Antikörper bestimmt werden. Die Messungen ergaben ein leicht niedrigeres Kraftäquivalent für den niederaffinen Liganden HPA verglichen mit dem CD47 Antikörper. Somit ermöglicht der MFA auf Zellen durch die detaillierte Kraftanalyse z.B. auch einen Zugang zu einer Kraftschwelle die nötig ist, um Moleküle spezifisch auf lebenden Zellen abzuliefern. Darüber hinaus konnte gezeigt werden, dass die hier beschrieben Kraftanalysetechnik nicht nur auf rote Blutzellen anwendbar ist, sondern auch für lebende Zellen in Kultur funktioniert. Dafür wurde auch auf M21 Melanomzellen das Kraftäquivalent für den CD47 Rezeptor und seinen Antikörper bestimmt.

Insgesamt zeigen die im Rahmen dieser Arbeit durchgeführten Experimente, dass der MFA auf Zellen eine sehr empfindliche und universelle Methode ist, um Informationen über Rezeptorprofile und Bindungseigenschaften von Rezeptoren auf lebenden Zellen zu erhalten. Der MFA auf Zellen kann somit zum Auffinden und Selektieren möglicher passender Liganden in der medizinischen Forschung und in der Medikamentenentwicklung beitragen.

Summary

In this thesis a live-cell receptor-ligand assay based on the molecular force assay (MFA) was advanced and extended. Previously, with the MFA high throughput comparative force measurements were only conducted on molecules immobilized at solid surfaces. The molecular force balance analyses binding forces of receptor-ligand interactions by directly comparing a binding force of interest to a known reference interaction e.g. the binding force of two complementary DNA strands. In the experiments single molecules are used as force sensors that are clamped in series between two surfaces. When separating the surfaces, the molecular complex with the weaker bond is more likely to rupture. A fluorescent label at the reference complex indicates the outcome of the experiment. After separation, the ratio of fluorescence intensity of both surfaces is analysed.

Coming from preliminary studies that demonstrated the capability of a modified MFA experiment to deliver ligands from an elastomer surface onto living cells, here, more complex experiments are introduced. For the functionalisation of the elastomer stamps, proteins have to be immobilised on the surface. In this context, the application of a microplotter is optimized for spotting proteins. This way, an elastomer stamp can be functionalised with several different ligands, which enables parallel and comparable experiments in one stamping process.

On human red blood cells, the interaction of the N-acetylgalactosamine (galNAc) terminated glycolipid with the lectin *helix pomatia* agglutinine (HPA) and of the CD47 receptor and its antibody is studied. For this experiment a chessboard like pattern of HPA and the CD47 antibody is deposited on the elastomer stamp. By delivering the ligands to the cell surface against a certain reference force, the method excludes unspecific interactions that might lead to biased results. On cells of blood group A, the stamping process yields a fluorescence transfer for both types of ligands, whereas on cells of group O lacking galNAc only the CD47 antibody is transferred. With this experiment, it is demonstrated that the MFA applied on living cells is a powerful method to do a parallel screening for receptors on living cells without unspecific interactions.

Further experiments prove that it is even possible to do detailed comparative force measurements on receptors of RBCs. In this context, a DNA force equivalent for the interaction of galNAc and HPA and for the CD47 receptor and its antibody is determined by the variation of DNA reference forces. The measurements yield a slightly lower DNA force equivalent for the low-affinity binder HPA than for the CD47 antibody. Thus, by the analysis of binding forces, the MFA on cells provides access to the force threshold that is e.g. necessary for a specific delivery of molecules on vital cells.

Additionally, on M21 melanoma cells the force equivalent for the CD47 receptor and its antibody is determined. This demonstrates that the described assay can also be applied on living cells of cultured cell lines and is not restricted to RBCs.

Altogether, the MFA applied on cells is a very sensitive and widly applicable method that yields highly valuable information about receptor profiles on cells and binding characteristics of live-cell receptors. Therefore, it supports the discovery and evaluation of possible ligands in medical research and drug design.

1. Introduction

Cells are the smallest living units. They are able to reproduce, metabolize, move, and communicate. For these fundamental tasks proteins play an important role. According to their variety of functions, there are many different types of proteins each exhibiting a specific and highly complex structure and conformation. Proteins consist of a specific sequence of amino acids that encodes their conformation and thus, determines their function [1]. Proteins can also be distinguished due to their localization in the cell. On the one hand, many proteins are dissolved in the cytoplasm, on the other hand, an important part of the proteins are associated with the cell membrane.

These membrane proteins are crucial for cell adhesion, communication, and signalling. Basically two types of membrane proteins can be distinguished. Peripheral membrane proteins are attached to the membrane whereas integral or transmembrane proteins interfuse the membrane [2].

Some transmembrane proteins provide hydrophilic channels for specific ions. Another type of membrane proteins actively pumps ions in the inner cell or vice versa consuming ATP. Many integral proteins work as receptors on the cell surface. The reaction of a specific ligand with such a receptor at the extracellular side of the membrane results in a conformational change exposing or blocking a second intracellular reaction site. This way, an extracellular signal is transmitted to the inner of the cell, where a whole signal cascade can finally take place, e.g during gene expression [2].

Since such receptors play a fundamental role in signal transduction [3], cell adhesion [4-6] and are involved in cancer development and progression [7], the investigation of cells and their membrane receptors is of crucial importance for stem cell and cancer research as well as drug development. Gaining information about receptor profiles on cells and subsequently finding the most efficient ligands for these signalling receptors, remain especially challenging tasks. But for the regulation of cells and cell signalling not only biochemical aspects have to be considered, also mechanical aspects play an important role [8-17]. Still, the analysis

of the mechanical binding behaviour of membrane proteins remains challenging [18]. In recent years, biochip technologies have steadily gained importance not only as a research tool for detecting protein-protein interactions in general, but also as a diagnostic device. Offering the possibility of screening for a vast amount of specific marker proteins in parallel, many different protein biochip formats have been developed [18, 19]. Though fast and cost-saving, the principle of microarrays is unfortunately afflicted with certain restrictions. To probe protein-protein interactions in a highly parallel format, proteins have to be immobilized on a surface. Such non-physiological conditions hold the possibility of denaturalization of the protein. Considering the influence of conformational changes on protein-protein interactions, this method might easily lead to wrong results, such as unspecific binding of non-target molecules or non-binding of the natural target [20]. An assay with such proteins seems highly demanding, because the proteins' hydrophobic transmembrane regions restrain an extraction from the membrane and their separate immobilization on surfaces. Consequently, membrane receptors only can be probed separately, if it is possible to do protein expression with the extracellular or intracellular domain or to analyse single domains [21]. This aggravates an approach with biochip assays.

Another possibility to get access to transmembrane proteins is to study them in the cell membrane. One approach is the application of flow cytometry, a method staining living or fixed cells with specific fluorescently labelled ligands. For the staining process, cells are incubated with the ligand for a certain time and washed to get rid of the excess ligand [22]. Afterwards, cells can be analysed. Nonetheless, in the absence of the target it seems possible that the ligand binds unspecifically and with lower affinity to another molecule on the cell surface thereby leading to a false positive result. A higher throughput is achieved by using stains with different emission wavelengths that enable the detection of a few different types of surface molecules at the same time. Yet, this method does not yield any information about the binding properties of the receptor under investigation.

Employing the AFM, the mechanical properties of receptor-ligand complexes on cells can be analysed in detail, and rupture forces can be measured very accurately on a single molecule level [23-27]. On the other hand, this technique is very time

consuming and, thereby, not suitable for a high throughput screening or fast force analysis of membrane receptors and their ligands on cells.

Considering these aspects, there is a high demand for new assays that aim at membrane proteins and their biochemical and mechanical binding behaviour providing a high throughput and that at the same time stick to physiological conditions.

In this thesis a live-cell method is advanced and tested with regard to its ability to study membrane receptors. It is shown that membrane proteins can be analysed in a parallel format and, furthermore, that it is possible to access both biochemical and mechanical binding information.

2. Molecular Force Assay

The Molecular Force Assay (MFA) is a comparative force assay that allows for a highly sensitive detection of binding force shifts of receptor-ligand interactions. Therefore, the method is of high interest for basic research as well as pharmaceutical industry. In the following chapter the principle of the MFA is presented and an overview of current applications is given.

2.1. Principle

The MFA analyses shifts in binding forces of receptor-ligand interactions on a single molecule level, e.g. the difference in the rupture force of a perfect match DNA compared to a single mismatch, which is only about 1 pN [28]. Thereby single molecules are used as force sensors. The Brownian motion of a force sensor limits the measurement of such small forces. The smallest measurable force is described by the fluctuation-dissipation-theorem:

$$F_{\min} = \sqrt{k_B \cdot T \cdot R \cdot B} \quad (1).$$

Here, k_B is the Boltzmann constant, T the temperature, R the coefficient of viscose damping, and B the measurable bandwidth of the force. For a given bandwidth and temperature the viscose damping determines F_{min}. Since the damping increases with the size of the force sensor, the smaller the force sensor the smaller is the measurable force. Consequently, with a force sensor on the molecular level, like in MFA experiments, very small forces are accessible.

In MFA experiments, a molecular reference complex with known binding force is compared to the binding force of the molecular complex analysed. Like indicated in Figure 1 A, both complexes are clamped in series between two surfaces. When separated, the molecular complex with the weaker bond is more likely to rupture (Figure 1, B and C). Fluorescent labels indicate the outcome of the experiment [29]. Since many of these molecular force balances are measured simultaneously, the MFA is a highly effective ensemble measurement.

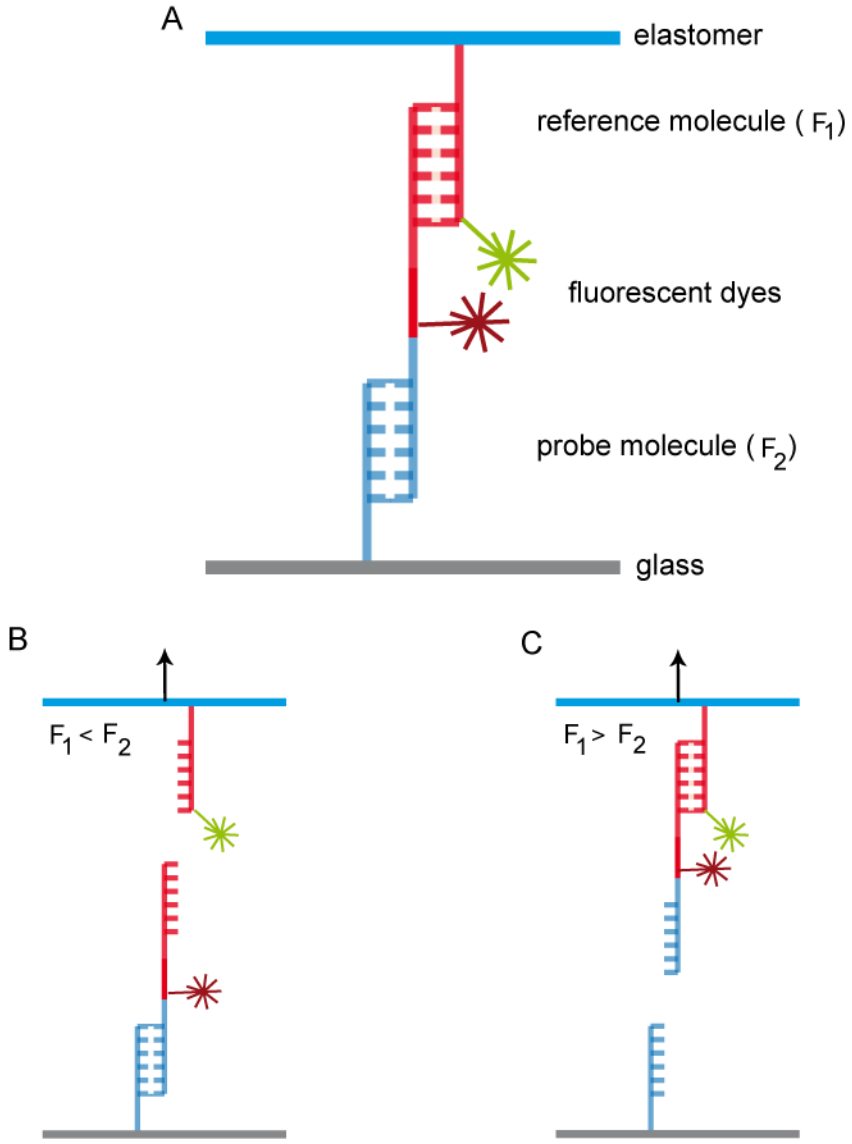

Figure 1 Schematic description of the Molecular Force Assay. A Two DNA molecules, referred to as reference (red) and probe (blue), are clamped in series between two surfaces. Upon separation of the two surfaces, the weaker bond is more likely to rupture. Two fluorophores, one at the reference DNA and one at the linker between reference and probe, form a FRET pair and indicate the outcome of the experiment. **B** If the binding force of the reference is weaker (F1 < F2), the fluorescent dye is more likely to be found at the lower surface. **C** In the inverse case the fluorophore stays at the upper surface.

In conventional MFA experiments reference and probe consist of DNA or RNA duplexes. One sequence is coupled covalently to the glass surface. The complementary sequence is part of a long strand with an overhang that forms the

reference sequence. The complementary reference strand completes the force balance. It is modified with a biotin at its end. That way, the whole force balance can couple to a streptavidin functionalised silicone elastomer surface. For fluorescence readout, usually, one fluorophore is attached at the linker between reference and probe sequence at the long strand. A second fluorophore is coupled to the biotinylated reference strand such that both dyes are close enough to form a FRET pair [30]. Typically, reference and probe bond are equally likely to rupture. Thus, the balance is very sensitive to small shifts in the binding force of the probe duplex, and the small shift in bond stability corresponds to a shift in the ratio of fluorescence on the two surfaces. The FRET pair corrects for force balances that did not couple to the elastomer surface at all.

2.2. Applications

The conventional setup allows for highly sensitive force measurements implicating a wide range of applications, which are discussed in this section.

Albrecht et al. first introduced the MFA and demonstrated the resolution of single base pair mismatches in DNA duplexes with this method [28]. Thereupon, Dose et al. analysed the influence of polyamides binding to DNA structures. They found that polyamides are suitable for tuning the reference force, since small structural changes result in shifts of the stabilizing effect and hence, increase the already high sensitivity of the MFA [31]. Further applications are the investigation of protein-DNA interactions and DNA methylation. Both interactions take part in gene regulation and therefore, are of high interest for biological and clinical research. Severin et al. showed that with the MFA it is possible to determine the affinities of the interactions he studied and implicated that gene regulation might not only be biochemically influenced, but is also mechanically induced [30, 32].

But also RNA structures were analysed. Ho et al. proved the detection of the small molecule adenosin binding to its aptamer sequence and thereby, stabilizing the structure [33]. The binding of small molecules is also a promising approach to precisely regulate protein translation. In MFA experiments, Limmer et al.

demonstrated the specific inhibition of Dicer – a molecule that cuts RNA duplexes sequence-independent into pieces of 19-22 base pairs – by the small molecule binder paromomycin [34].

Earlier, the MFA was used to study antibody-antigen interactions with respect to their specificity. Applying a certain reference force eliminates cross-reactions and unspecific binding [28, 35]. The obviation of such false-positive results is an immense advantage compared to other protein-biochip technologies, since there unspecific binding restricts high throughput measurements.

2.3. The MFA on cells

So far, the MFA was only applied to probe molecules immobilized on glass surfaces. Within this thesis a new approach is presented that offers the analysis of receptor-ligand complexes directly on vital cells assuring physiological conditions.

The setup for the in vitro analysis of membrane proteins differs in some aspects. The reference still consists of DNA, but the probe is made up of a cell surface receptor and its ligand. The glass surface is exchanged for a layer of living cells exposing certain receptors. The remaining part of the force balance is composed on the elastomer surface like shown in Figure 2.

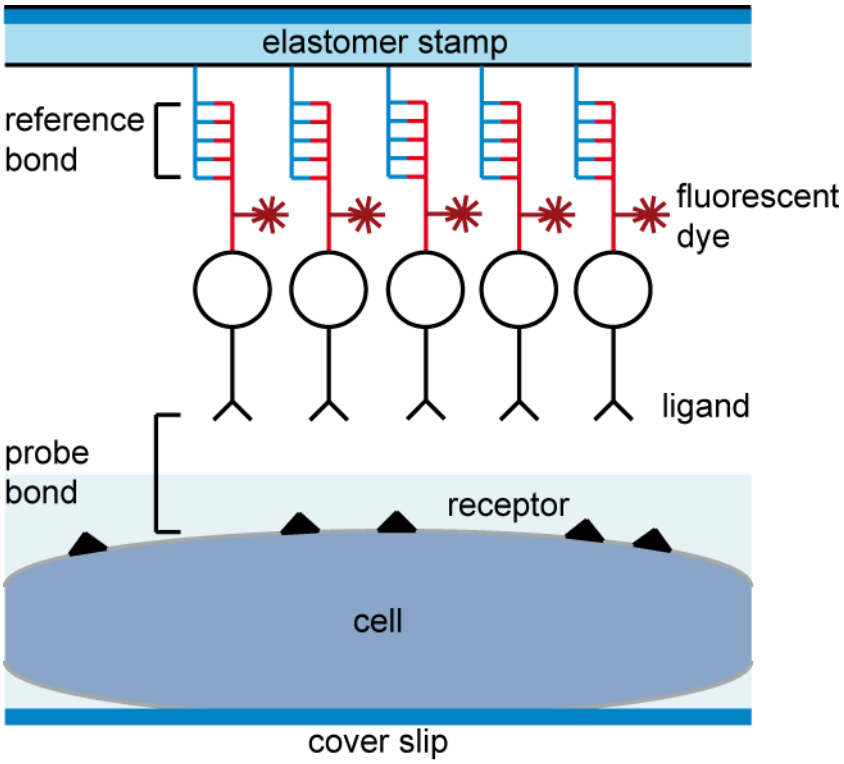

Figure 2 Biochemical setup of MFA on cells. The elastomer stamp is functionalised with covalently bound DNA. To this strand the complementary biotin modified DNA is hybridized forming the reference. The biotin end of the DNA is attached to the ligand via biotin-avidin chemistry. Functionalised with this complex, the elastomer stamp is carefully lowered until contact to the cells is made.

At the elastomer surface, the reference complex, a DNA duplex, is covalently immobilized, and a specific ligand for a cell surface receptor is linked to the reference bond via biotin-avidin chemistry. During the contact phase, reference and probe are clamped in series between elastomer and cell surface. When separating the surfaces, the molecular complex with the weaker bond is more likely to rupture. A fluorescent label at the reference complex indicates the outcome of the experiment. Compared to conventional MFA experiments, the number of force balances on the elastomer surface is much higher than the number of receptors at the cell surface. Consequently, with this setup there are many more incomplete than complete force balances, and thus, the ratio of the fluorescence intensity of the two surfaces bares no direct information about the strength of binding forces. For that reason, also the use of FRET pairs is abandoned. Still, the parameter relevant for this experiment is the relative fluorescence transfer on the cells, but from the

experiments, no absolute information about interaction strength is derived. Nevertheless, the relative fluorescence transfer obtained with the MFA on cells can be used to compare different forces within one measurement.

3. Molecular Bonds

The MFA is a single molecule experiment. The rupture force of every single receptor-ligand complex is tested individually against a certain reference force. The statistics is given by measuring many of these force balances in parallel. Thus, the theoretical approach for the MFA is the Bell-Evans model, which describes molecular bonds under force. It is based on the two-state model, a simplified model of molecular bonds in equilibrium. In the following chapter, the two-state model and the Bell-Evens model are explained in some detail.

3.1. Two-state model

The two-state model is a strongly simplified approach that assumes a bound state (RL) and an unbound state (R+L) that are separated by an energy gap ΔG. Both states are subjected to statistical fluctuations leading to transitions from one state into the other. This behavior is described by the rates k_{on} and k_{off} that are derived from the Van't Hoff-Arrhenius law and depend on the energy barriers ΔG_{off} and ΔG_{on} as well as on the testing frequency ν_{off} and ν_{on}:

$$k_{off} = \nu_{off} \cdot e^{\frac{-\Delta G_{off}}{k_B \cdot T}} \quad (2) \text{ and}$$

$$k_{on} = \nu_{on} \cdot e^{\frac{-\Delta G_{on}}{k_B \cdot T}} \quad (3),$$

where k_B refers to the Boltzmann constant and T is the temperature. Figure 3 illustrates the energy landscape of a molecule in the two-state model.

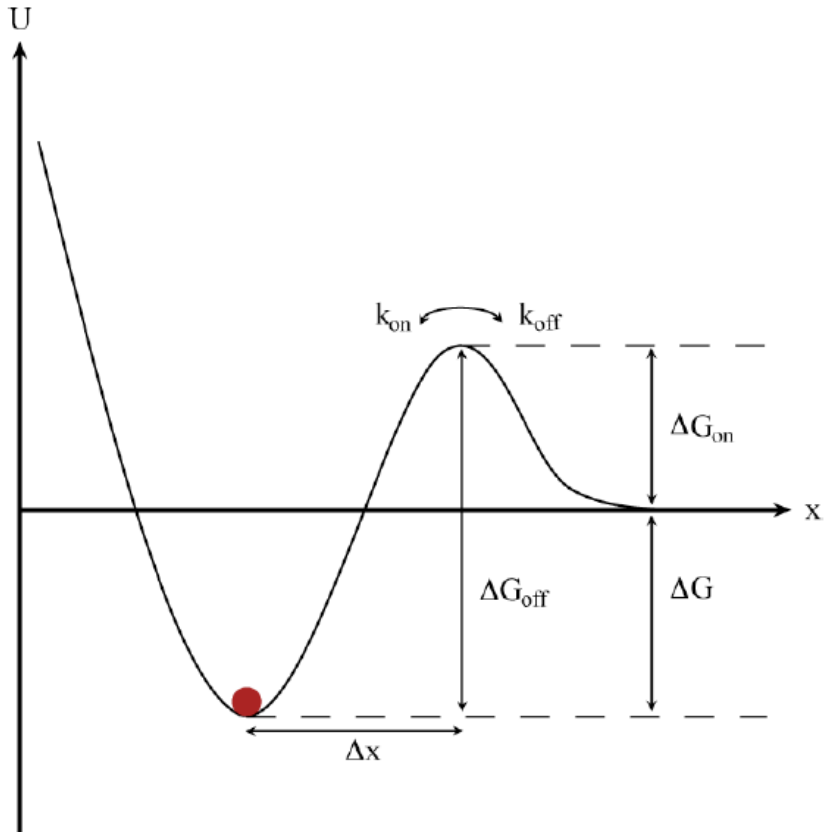

Figure 3 Energy landscape of a receptor-ligand system. The energy ΔG_{off}, which is necessary for a transition to the unbound state, consists of the free energy ΔG and the energy ΔG_{on}. The transitions from one state to the other happen statistically with the rates k_{off} and k_{on}.

The law of mass action describes the strength of a molecular bond with the equilibrium constant K_D that mirrors the ratio of k_{on} and k_{off}:

$$K_D = \frac{k_{off}}{k_{on}} = \frac{[R]\cdot[L]}{[RL]} \qquad (4).$$

The two-state model applies to the molecular bond at equilibrium. If a force is exerted on the bond, this description is insufficient and is replaced by the Bell-Evans model that is presented in the next chapter.

3.2. Molecular bond under force – the Bell-Evans model

The Bell-Evans model [36, 37] takes into account that a force exerted on a molecular bond influences the energy landscape. It reduces the energy gap by F · x and consequently changes the testing frequencies such that the association frequency is assumed to be neglectable. The dissociation rate under force k_F is given by:

$$k_F = \nu_{off} \cdot e^{-\frac{\Delta G_{off} - F \cdot \Delta x}{k_B \cdot T}} \quad (5).$$

In Figure 4 the influence of an external force on the energy landscape is depicted.

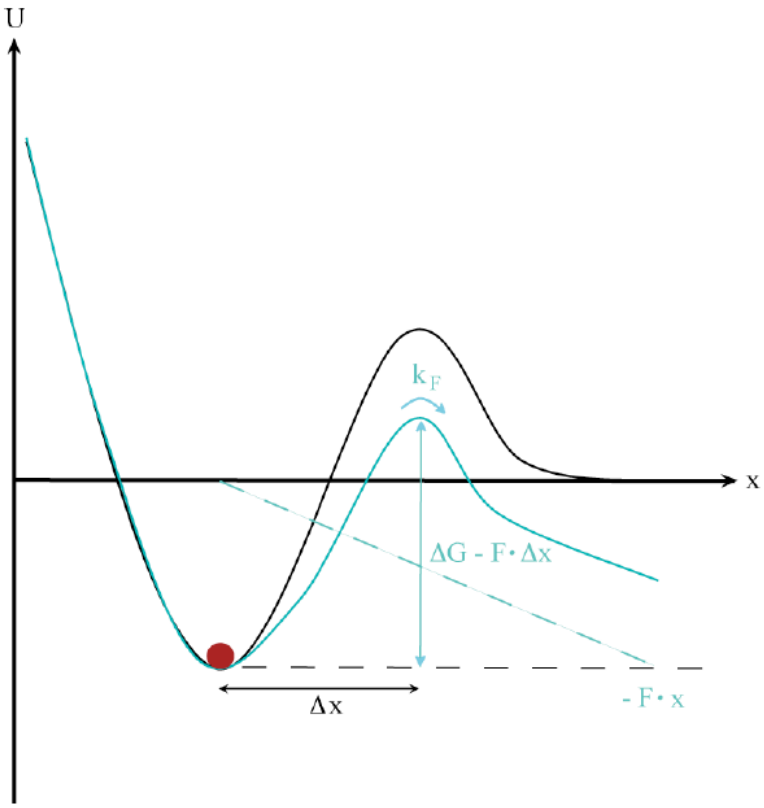

Figure 4 Influence of external force. The energy landscape of a molecule is illustrated without (black) and with (blue) external force. Applying an external force in x-direction, leads to a flattening of the energy landscape by -F · x.

Using the approximation of a harmonic oscillator, we obtain for an over-damped system:

$$k_F = \frac{\omega_{\min} \cdot \omega_{\max}}{2 \cdot \pi \cdot \gamma} \cdot e^{-\frac{\Delta G_{off} - F \cdot \Delta x}{k_B \cdot T}} \quad (6).$$

At zero force we get:

$$k_{off} = \frac{\omega_{\min} \cdot \omega_{\max}}{2 \cdot \pi \cdot \gamma} \cdot e^{-\frac{\Delta G_{off}}{k_B \cdot T}} \quad (7),$$

ω_{min} and ω_{max} describe the curvature of the potential at the minimum and maximum, respectively. Assuming that the force is a function of time, we obtain the following expression for the time dependent change in the number of bound receptor-ligand complexes:

$$\frac{dN_b(t)}{dt} = -k_t \cdot N_b \quad (8).$$

Normalization reveals the number of unbound molecules:

$$N_u(t) = 1 - N_b(t) = 1 - e^{-\int_0^t dt' \cdot k_{t'}} \quad (9).$$

Replacing time by force, we get a description for the force dependent number of unbound molecules:

$$N_u(f) = 1 - e^{-\int_0^F df \cdot k_f \cdot \frac{1}{\dot{f}}} \quad (10).$$

Here, $\dot{f}$ is the loading rate.

Hence, the probability for a force dependent bond rupture is:

$$p_F = \frac{dN_u}{dF}(F) = k_F \cdot \frac{1}{\dot{f}} \cdot e^{-\int_0^F df \cdot k_f \cdot \frac{1}{\dot{f}}} \quad (11).$$

With $k_F = k_{off} \cdot e^{\frac{F \cdot \Delta x}{k_B \cdot T}}$ (12) we obtain:

$$p_F = k_{off} \cdot e^{\frac{F \cdot \Delta x}{k_B \cdot T}} \cdot \frac{1}{\dot{F}} \cdot e^{-k_{off} \int_0^F e^{\frac{f \cdot \Delta x}{k_B \cdot T}} \cdot \frac{1}{\dot{f}} df} \quad (13).$$

Eventually, by differentiation, we get an expression for the most probable rupture force:

$$F'(\dot{F}) = \frac{k_B \cdot T}{\Delta x} \cdot \ln\left(\frac{\dot{F}}{k_{off}} \cdot \frac{\Delta x}{k_B \cdot T}\right) \quad (14),$$

which depends on the potential width Δx and on the loading rate $\dot{F}$ [36, 37].

4. Components of the force balance

The force balance consists of two main parts, a DNA duplex that works as the reference complex, and a ligand that specifically binds to a receptor on the cell surface. Both components are connected with biotin-avidin chemistry. In the following chapter, these parts are described in more detail.

4.1. DNA as reference complex

Deoxyribonucleic acid (DNA) provides the genetic information in cells and is therefore essential for life. Furthermore, DNA is a popular molecule for biotechnological applications, since it is easy to handle, thermodynamically stable, and already extensively analysed e.g. with AFM measurements [38]. Biotech companies offer the assembly of an individual sequence and length of DNA strands and additional modifications, e.g. fluorescent dyes or linkers for the attachment at other molecules are available. Because of these properties, in MFA experiments DNA molecules are used as a molecular force sensor.

DNA consists of four different bases adenine (A) and guanine (G), which are purines, and thymine (T) and cytosine (C) called pyrimidines (Figure 5).

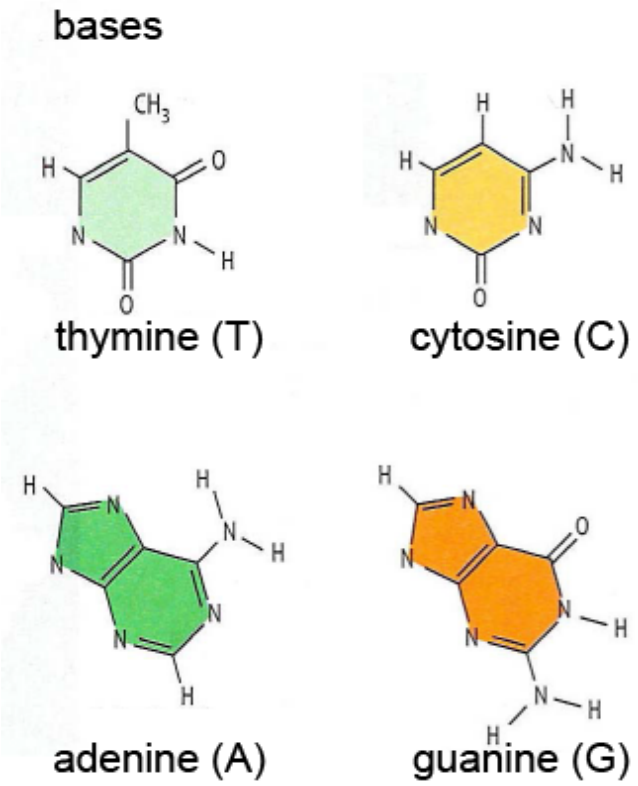

Figure 5 Chemical structure of DNA bases. DNA consists of four different nucleic acid bases. thymine (T) and adenine (A) as well as cytosine (C) and guanine (G) hybridize via two and three hydrogen bonds, respectively. The structurally similar bases T and C are pyrimidines, A and G are purines. Picture adapted from Campbell [39].

The bases are connected via a sugar-phosphate backbone consisting of deoxyribose. The sequence of the bases encodes the sequence of amino acids in proteins and is responsible for their correct structure and function. The DNA single strand is directional: dependent on which carbon atom of the sugar backbone constitutes the end of the strand, the third or the fourth, it is call 3'- or 5'-end, respectively. When two DNA molecules hybridize, the 5'-end of one strand is connected to the 3'-end of the other. The complementary bases A and T and the complementary bases G and C form two and three hydrogen bonds, respectively. Together with the sugar-phosphate backbone, this results in a helical structure of the DNA duplex [40].

There are different ways to exert force at a DNA duplex that are discussed in the following.

In unzipping geometry, the DNA is attached at the 3'-end of one strand and the force is applied at the 5'-end of the other strand. Here, for bond rupture only small forces of 12 to 15 pN are necessary [38, 41], since the double strand opens base pair wise. Higher rupture forces are achieved in shear geometry, in which the force affects the 3'-end of the other strand. This way, the rupture forces of single base pairs sum up and result in a higher force compared to the unzipping geometry. In shear geometry the total rupture force not only depends on the length of the DNA, but also on the sequence. A high G-C content results in a higher rupture force than a high A-T content, since G-C base pairs provide more hydrogen bonds. Moreover, the rupture force differs with the velocity the force is applied. Equation (14) displays the dependence of the most probable rupture force on the force-loading rate. Strunz et al. measured rupture forces of 10 bp, 20 bp and 30 bp DNA for different retraction velocities with the AFM (Figure 6).

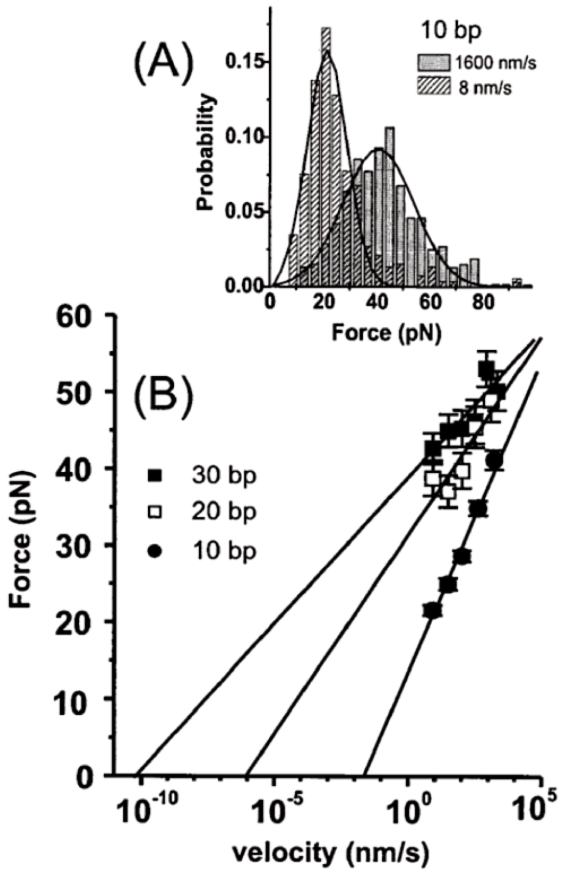

Figure 6 Measurement of DNA rupture forces by AFM. A Rupture force distribution of a 10 bp DNA strand measured with two different retraction velocities. A fast retraction leads to a broad distribution that is shifted to higher forces compared to a small velocity. **B** Velocity dependence of DNA rupture forces for three different lengths. For the retraction velocity of 50 nm/s (as used in MFA experiments), clearly distinct rupture forces of the different DNA lengths are shown in the graph. Picture adapted from Strunz et al. [42].

In Figure 6 A, the rupture force distribution is displayed for a 10 bp DNA and two different retraction velocities. For a fast retraction of 1600 nm/s, they obtained a broad distribution of rupture forces, and the most probable rupture force is shifted to higher forces compared to the small retraction velocity. The fact that DNA rupture is highly statistical process leading to a rupture force distribution with a distinct width also has an influence on MFA experiments. If one distinct rupture force would be attributed to one DNA length, we would expect no fluorescence transfer once the DNA interaction is stronger than the ligand receptor interaction. But in a statistical process with a force distribution, we expect to obtain a specific

fluorescence transfer also for such DNA lengths with an actual stronger interaction than the receptor ligand interaction.

The graph in Figure 6 B shows the velocity dependence of rupture forces for different DNA lengths. For a constant velocity of 50 nm/s, the graph shows distinctly different rupture forces for the measured DNA lengths [38].

Concluding, DNA is a valuable molecule for the reference in MFA experiments, as it offers the possibility to easily vary the force exerted on the receptor ligand complex depending on length and geometry.

4.2. Biotin and avidins

Avidin is a glycoprotein found in egg white. It consists of four identical subunits with an overall molecular mass of 67 kDa and an isoelectric point of 10.5. Each of the subunits contains one binding site for the vitamin biotin (Figure 7).

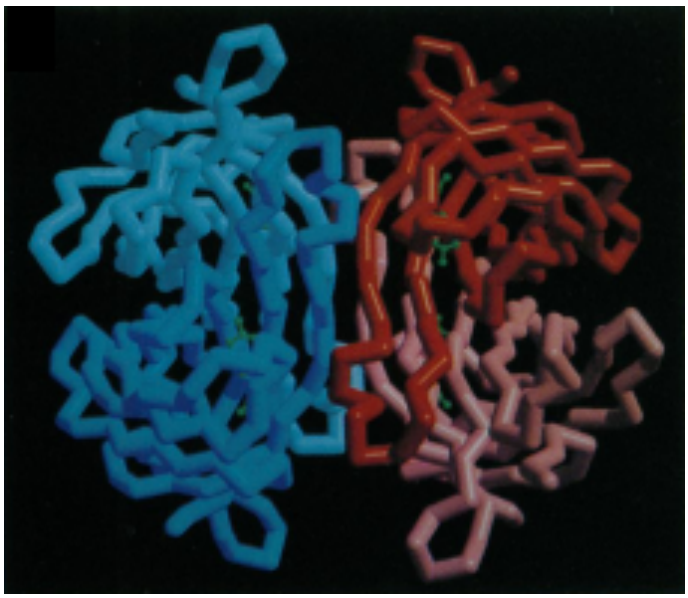

Figure 7 Structure of avidin. Avidin is a tetrameric glycoprotein form chicken egg white. It consists of four identical subunits each of which exposes a biotin-binding site. Picture adapted from Livnah et al. [43].

The biotin-avidin interaction is unusually strong with a dissociation constant $K_D \sim 10^{-15}$ M [44], which is one of the strongest non-covalent interactions and is, therefore, of high interest considering biotechnological applications. But the sugar rests of avidin also result in an affinity especially for sugar binding proteins, the lectins and its positive charge can lead to undesired surface adhesion. Thus, NeutrAvidin, the deglycosylated form of avidin, was designed. It provides high specificity and a lower isoelectric point of 6.3.

Another tetrameric molecule comparable to NeutrAvidin is StreptAvidin with a molecular weight of 53 kDa and an isoelectric point of 7. Its affinity is with $K_D \sim 10^{-14}$ M lower than the affinity of avidin but still high (Figure 8) [45].

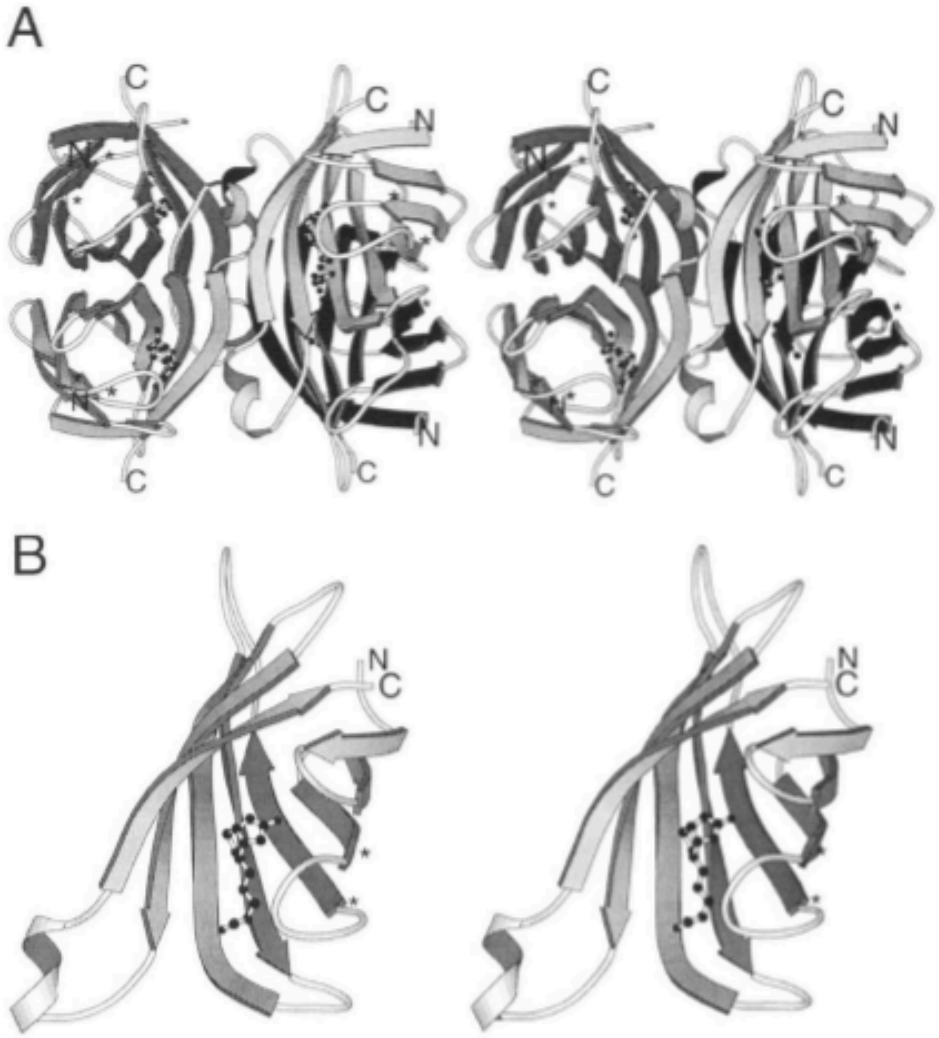

Figure 8. Structure of Streptavidin. A Tetrameric structure of Streptavidin. **B** Substructure showing the biotin binding site. Picture adapted from Freitag et al. [46].

NeutrAvidin is used for experiments without microplotting, because of its high specificity. In these experiments, the force balance consists of a biotin modified DNA duplex attached to NeutrAvidin. The ligand with a biotin modification also binds to NeutrAvidin. Using the microplotting technique with very small volumes, this force balance construct precipitates. Hence, a labeling kit is used instead covalently coupling StreptAvidin directly to the ligand. This way, the whole force balance is stable also when falling dry.

4.3. Cells

Cells are the smallest living units. They contain DNA that provides the genetic information. In prokaryotic cells, like bacteria, the DNA is moving freely and lacks a nucleus. In eukaryotic cells, a nuclear membrane encloses the DNA and separates the nucleus from the rest of the cells' organelles. The plasma membrane separates the cell from the extracellular space [47]. But its function is not restricted to separation; it also accumulates many different kinds of proteins that are crucial for transport, adhesion, and signalling. In the following section, the plasma membrane and its proteins are described in more detail.

4.3.1. Plasma membrane

Cells that are organized in tissue or organs are not individually viable, but they are the smallest structural and functional unit of the according organ. For the function of such a united cell structure, the cells must be capable of communicating and signalling. This takes place at the plasma membrane [48].

The plasma membrane of a cell encloses its organelles and the cytosol. It provides the surface for biochemical reactions and signalling. Moreover, being selectively permeable, it ensures the exchange of products and educts of the cells' metabolism [49].

The plasma membrane consists of amphipatic phospholipids and steroides that are collocated in a bilayer. The hydrophilic head groups of the lipids are directed to the outside and the inner part of the bilayer consists of the hydrophobic tail region of the phospholipids. Since the bilayer is only stabilized by hydrophobic interactions, the membrane is steadily subjected to fluctuations resulting in a movement of lipids with a mean velocity of 2 μm/s [50].

Some peripheral proteins on the interior membrane are additionally attached to integral proteins that are anchored at the cytoskeleton. Moreover, on the exterior membrane several transmembrane proteins, e.g. integrins, are connected to the extracellular matrix. These bonds lead to more stability and structure for the cell.

The liquid bilayer is interspersed with membrane proteins consisting of two main classes. Integral membrane proteins have a hydrophobic transmembrane domain that is anchored at the nonpolar region of the bilayer by hydrophobic interactions. Additionally, they have an extracellular and cytosolic domain resulting in a directed, asymmetric orientation. Peripheral proteins make up the second class of membrane proteins. They are associated with the membrane surface only. In contrast to integral proteins, they are only temporarily attached. Both types of membrane proteins can diffuse freely in the membrane and form a liquid mosaic together with the lipids [2]. The liquid mosaic model is illustrated in Figure 9.

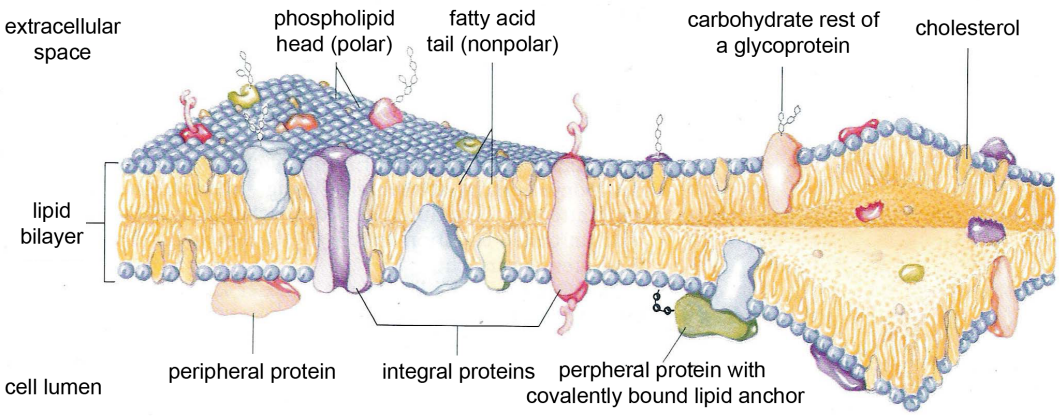

Figure 9 Liquid mosaic model of the membrane. The membrane consists of a lipid bilayer with fatty acid rests that are embedded in the inner part where as the polar heads are on the outside. The membrane contains different types of proteins, some of which are attached the bilayer (peripheral proteins) and some pervade it (integral proteins). Lipids and proteins can freely diffuse in lateral direction forming a highly dynamic structure also called a liquid mosaic. Picture adapted from Lehninger [51].

4.4. Receptor ligand systems

The following section is addressed to the receptor-ligand complexes relevant for this thesis. The cell surface receptors and their according ligands are depicted with respect to their structural and functional characteristics.

4.4.1. GalNAc and HPA

On the exterior membrane, a network of oligosaccharides, the glycocalix, is exposed. It consists of the sugar rests of glycolipids and glycoproteins. Since the exact composition is highly specific for each individual person and cell type, the glycocalix plays an important role in immune defence and the discrimination of the body's own and foreign cells [2].

In erythrocytes, the glycocalix prevents the adhesion to other cells by sterical repulsion. Apart from that, in RBCs the glycocalix ensures the recognition as self-cells [52]. For example in RBCs of blood group A, the membrane exposes the N-acetylgalactosamine (galNAc) terminated glycolipid, while it is absent in other blood groups.

The lectin *helix pomatia* agglutinin (HPA) specifically binds galNAc. HPA consists of six identical subunits each containing a galNAc binding site [53, 54] (Figure 10).

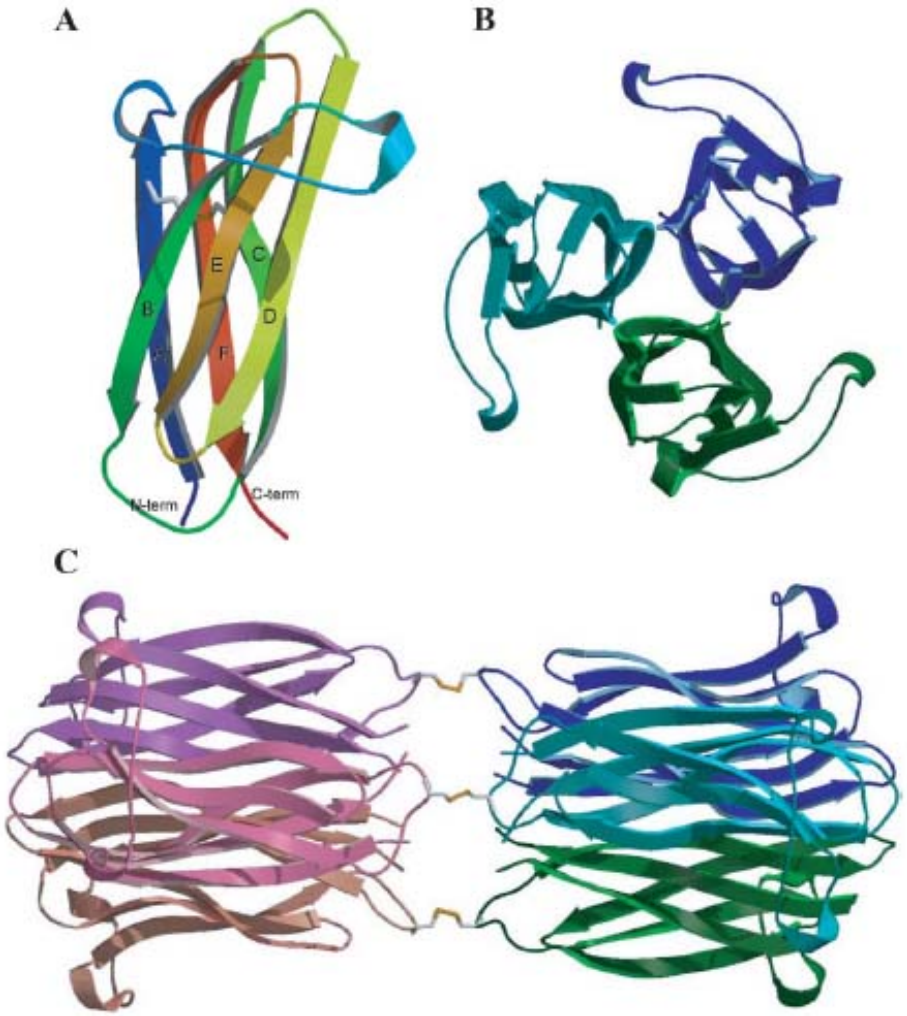

Figure 10 Structure of HPA. In **A,** a monomer consisting of two β-sheets is shown. Three of such monomers form a trimer. Two trimers are linked together over disulfide bonds forming the hexamer HPA. Overall, it has six binding sites for ligands. Picture adapted from Sanchez et al. [55].

The total weight of HPA is 79 kDA. Titration microcalorimetry measurements yield a low affinity for galNAc of 0.1 mM [53, 54].

Due to the high density of galNAc on the surface of RBCs with blood group A, this receptor-ligand complex is well suitable for the analysis with the MFA.

4.4.2. CD47 receptor and antibody

The CD47 receptor or integrin associated protein is a highly glycosylated protein with a total weight of 50 kDa. It is a widely distributed receptor that is exposed on many cell lines and in different tissue in a considerable density. One RBC exhibits approximately 25.000 molecules [56].

The CD47 receptor is an immunoglobulin consisting of an extracellular IgV domain, five transmembrane segments, and a cytoplasmic tail region with four different isoforms (Figure 11) [57].

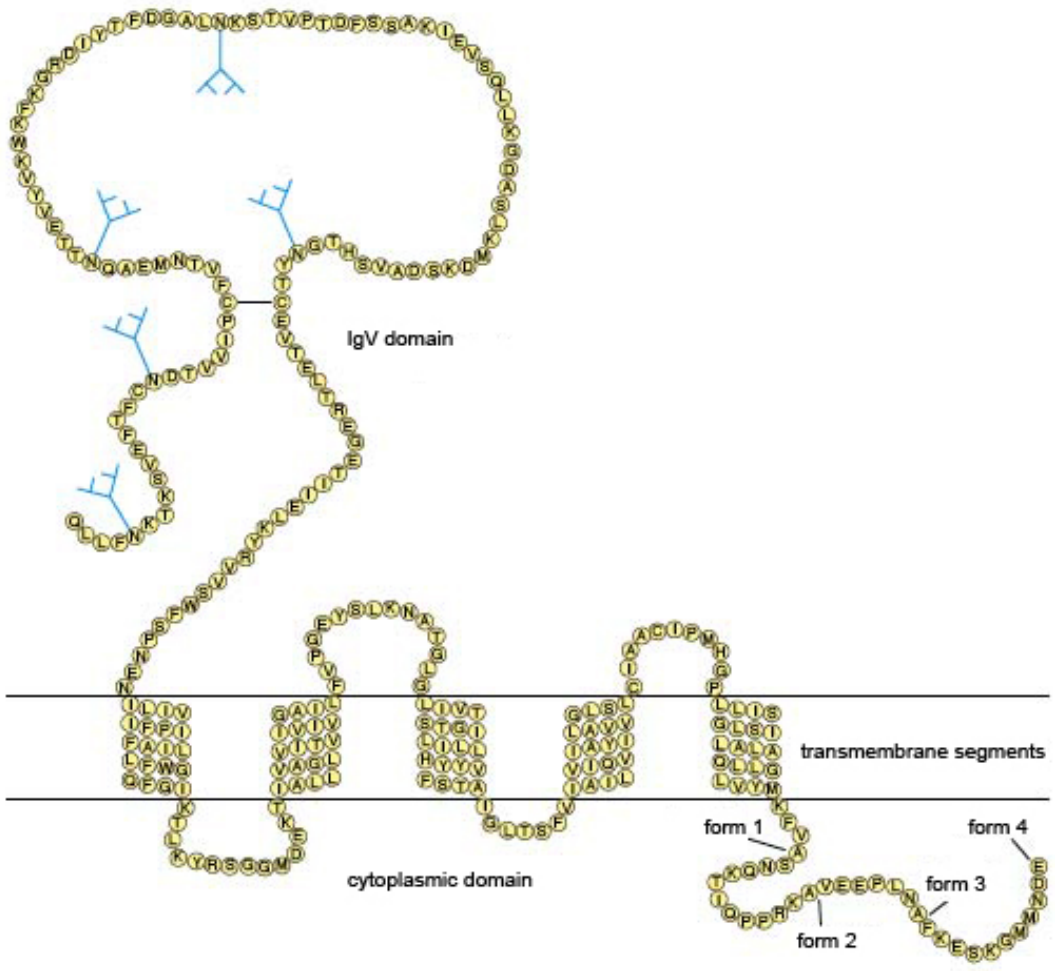

Figure 11 Structure of a CD47 receptor. The receptor consists of an extracellular Ig V domain, five transmembrane segments, and a cytoplasmic domain with four isoforms. Picture adapted from Brown et al. [58].

The IgV domain binds the intrgins $\alpha_v\beta_3$ and $\alpha_2\beta_1$, as well as thrombospondin and SIRPα. The cytoplasmic tail region is associated to the cytoskeleton via a second protein [59]. Indeed, the connectivity of membrane proteins to the cytoskeleton is usually only fractional. In RBCs, Dahl et al. found that only 62% of the CD47 receptors are attached to the cytoskeleton. The rest freely diffuses in the membrane [60].

Together with the integrin $\alpha_v\beta_3$, the CD47 receptors form dimers that take part in cell signaling. Brown and Frazier found that an antibody against the CD47 receptor influences the cell functions regulated by the integrin $\alpha_v\beta_3$ and blocks the endothelial Ca^{2+} influx during the adhesion to surfaces coated with fibronectin or vitronectin [59].

Upon binding to thrombospondin-1, it takes part in thrombocyte and T lymphocyte activation and the apoptosis of T and B lymphocytes [59]. Additionally, it contributes to the transmigration of neutophil granulocytes to injured tissue.

The association of the CD47 receptor with SIRPα leads to cell-cell adhesion and supports the aggregation of B lymphocytes as well as the creation of memory B cells. Moreover, in RBCs, it is essential for the recognition as self-cells [61].

With respect to these manifold regulatory functions and since its wide distribution and considerable density, the CD47 receptor is an interesting molecule for MFA experiments on different cell types.

A specific antibody against the CD47 receptor is used as ligand. Antibodies are immunoglobulins consisting of four polypeptide chains. Two identical heavy chains couple to two identical light chains via a disulfide bond forming a Y-shape. The arms of the Y each contain a variable region in their ends. They represent the two binding sites, where the specific antigen is recognized. The sequence of amino acids determines the affinity of the binding site. The tail of the Y contains the ends of both heavy chains. Their amino acid sequence is identical for a class of antibodies [62]. Figure 12, A and B depict the structure of an antibody.

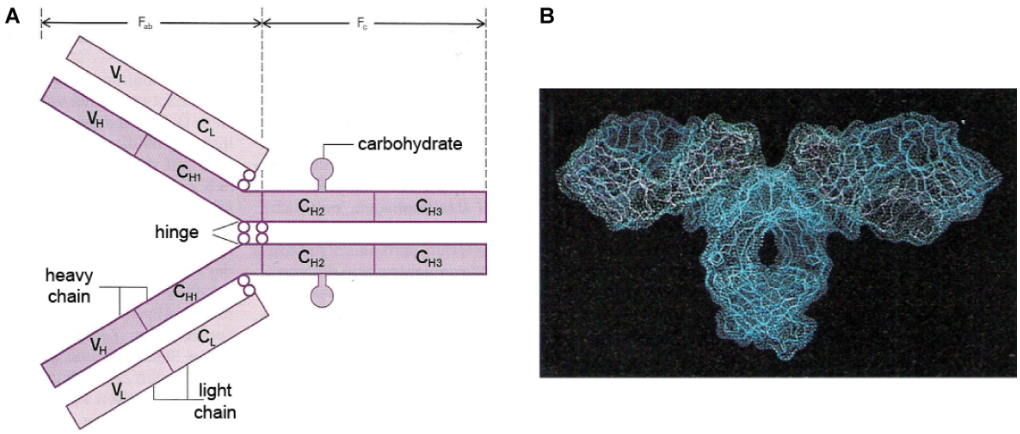

Figure 12 Structure of an antibody. A An antibody has a symmetric Y-structure consisting of two identical heavy and light chains, respectively. The arms of the Y contain a variable region exposing the binding site a specific antigen. The tail region of the antibody determines its class. Picture adapted from Klinke [63]. **B** Computational model of an antibody based on x-ray data. Picture adapted from Campbell [64].

In the experiments described in this thesis, a monoclonal antibody against the CD47 receptor is applied. In contrast to polyclonal antibodies that are the result of many different antibody-producing cells in an animal, monoclonal antibodies follow from clones, a population of identical cells. These antibodies are homogenous and bind only one specific epitop of the antigen [62].

Thus, monoclonal antibodies are preferred for biotechnological applications like the MFA, in which binding forces of receptor ligand complexes are analysed.

4.5. Cell types

The measurements presented in this thesis are conducted on erythrocytes, on M21 melanoma cells, on SW 480 colon cancer cells, and MBA MD 231 cells. The next paragraph depicts their characteristics.

4.5.1. Erythrocytes

Erythrocytes or RBCs emerge from pluripotent stem cells in the spinal marrow that subsequently differentiate into erythroid progenitor cells. The mature erythrocytes lack a nucleus. They are in the blood circulation for 120 days before degraded by liver and melt. RBCs have a mean diameter of 7.5 μm and a mean thickness of 1.5 μm. Their structure is biconcave discoidal providing a high surface-volume ratio, which is important for their main function - gas exchange (Figure 13) [52].

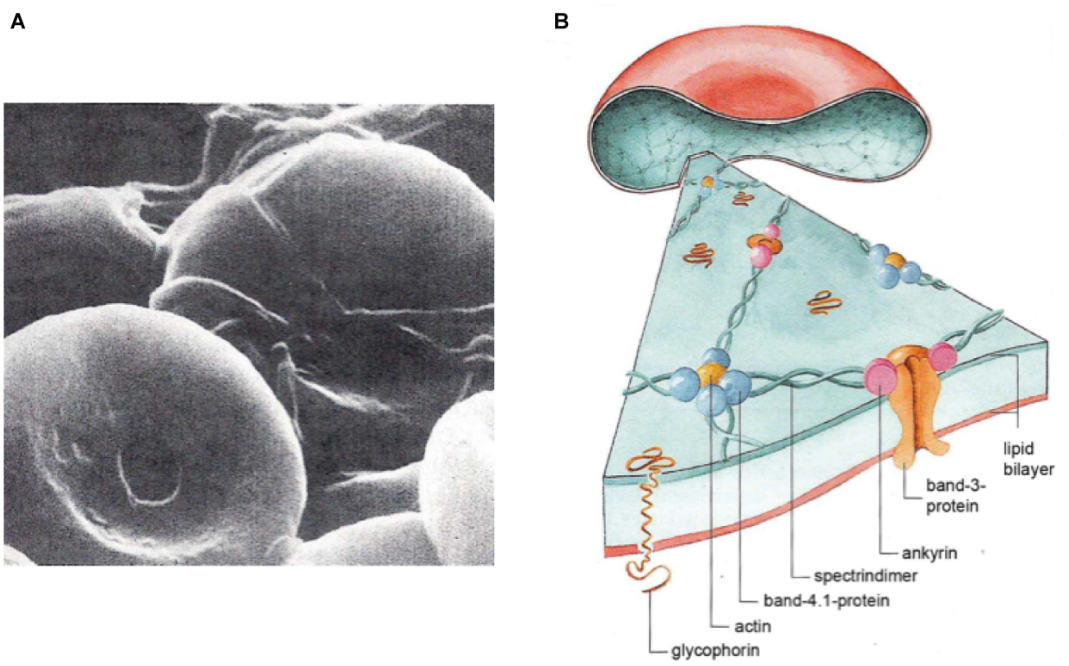

Figure 13 Erythrocytes. A Electron microscope image of an erythrocyte. The discoidal shape is clearly visible. Picture adapted from Lehninger [65]. **B** The membrane of erythrocytes lacks the cross-linking by typical cytosceletal fibres. Instead, a spectrin network cross-linked with ankyrin provides the form of erythrocytes. Picture adapted from Klinke [66].

To pass the small capillaries of the lung, RBCs need to be able to deform easily. This is possible, because RBCs lack the usual cytoskeleton filaments like microtubules, intermediate and actin filaments, but possess a meshwork of thread-like spectrin molecules cross-linked with actin and ankyrin providing a highly flexible structure [52].

The glycocalix of RBCs consists of glycolipids and glycoproteins. Their carbohydrate groups act as blood group-specific antigens [52].

4.5.2. Cultured cells

4.5.2.1. M21 cells

The human melanoma cell line M21 is provided by D. L. Morton (University of California, Los Angeles, CA) and is cultured in RPIM 1640 medium (GIBCO, Life Technologies, Paisley, UK) supplemented with 10% fetal bovine serum and 5 mM glutamine at 37 °C in 5% CO_2 atmosphere. M21 cells exhibit a spindle shaped form (Figure 14).

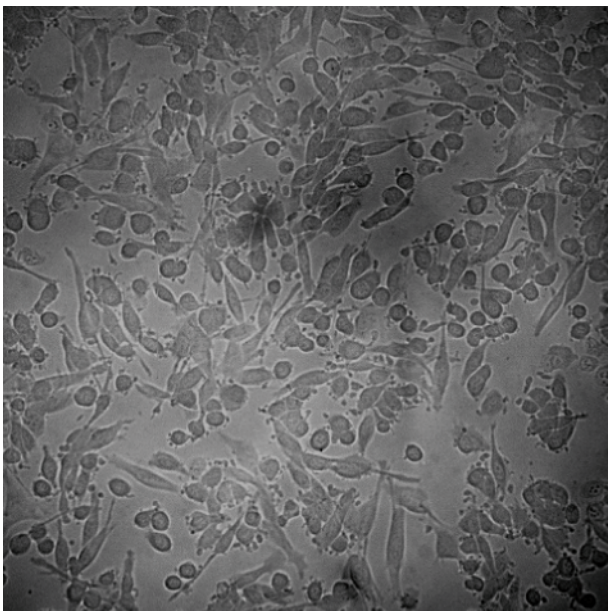

Figure 14 Spindle shaped M21 cells. Rounding-up of cells could mean that they are just before cell division or cell death.

4.5.2.2. SW480 and MDA MB231

The cell lines SW480 and MDA MB231 are derived from human breast cancer and colon cancer tissue, respectively. They were purchased from ATCC (LGC Standards, Teddington, UK). For culturing, they are kept in Leibovitz's L-15 Medium with fetal bovine serum at a concentration of 10% and kept at 37 °C without CO_2. In structure and form, both cell types are similar to the M21 cells.

5. Experimental Section

5.1. Biochemical setup

In the subsequent paragraphs, the single steps of the biochemical preparation of an MFA experiment are explained.

5.1.1. Production of elastomer stamps

Elastomer stamps consisting of the silicone elastomer Sylgard (Dow Corning, Midland, MI) are the contact devices for MFA experiments. For the success of such experiments, it is crucial to provide an even and uniform surface.

The uncured polymer is mixed with curing agent in a 10 : 1 ratio and filled in a special mould. The mould consists of a glass plate and a silicon waver that are arranged parallel with a distance of 2 mm. The silicon waver exhibits cylindrical cavities that are 1 mm in diameter and 1 mm deep. The moulds show a microstructure etched into the silicone in a photolithographical process. The microstructure represents 5 μm deep, square pits with an area of 100x100 μm and a 41 μm distance between each other. In Figure 15, the detailed microstructure of a stamp is illustrated.

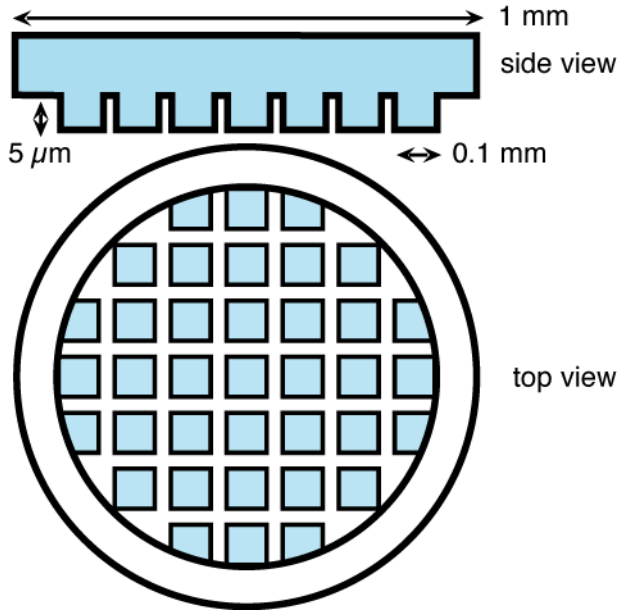

Figure 15 Microstructure of the elastomer stamp in side view and top view. The elastomer stamps used in the MFA experiments have a diameter of 1 mm and their microstructure consists of elevated pads of 100 x 100 μm.

Curing of the elastomer results in a sheet of stamps exhibiting a microstructure and a very even surface.

The sheet is cut into appropriate pieces and subsequently, is washed with toluene to extract uncured elastomer. After evaporation of the toluene, stamps are ready to be functionalised [67].

5.1.2. Chemical functionalisation

The elastomer surface is chemically functionalised in several steps that are presented in this section. Usually, a batch of four of the former described stamps is prepared for experiments on cells.

5.1.2.1. Surface activation

Before functionalisation, the elastomer surface is chemically inert and hydrophobic and thus, has to be chemically activated. Previously, the stamps are ultrasonically cleaned in 50% aqueous isopropanol solution for ten minutes and irradiated for another ten minutes in an UV cleaner. Afterwards, the stamp is kept in 12.5% hydrochloric acid overnight resulting in highly reactive hydroxyl groups on the stamp surface.

5.1.2.2. Silanization

In the next step, the stamps are incubated for 30 minutes in (3-glycidoxypropyl)-trimethoxysilane (ABCR, Karlsruhe, Germany) to generate epoxide groups on the surface. Therefore, 0.75 ml of pure silane is mixed with 0.32 ml of a 0.015 % solution of sulfuric acid and incubated for one hour while stirring. Subsequently, 20 ml isopropanol are added to this mixture, and the batch of stamps is inserted. After rinsing excess silane with isopropanol and ddH_2O, the stamps are heated up to 80 °C in argon atmosphere for half an hour and are then stored in argon atmosphere at 6 °C until usage.

5.1.2.3. Covalent attachment of amino-DNA

For DNA functionalisation, the amino-DNA strand is mixed 1:4 with borate buffer resulting in a concentration of 20 μM. On each stamp, 1.25 μl of this solution is spread. Then the stamps are kept at room temperature in a saturated salt atmosphere over night. This way, the formation of a covalent bond between the epoxide group on the stamp surface and the amino group at the DNA is promoted. To guarantee a uniform attachment of DNA, it is crucial that the stamps do not dry out building salt crystals. For further treatment, excess DNA is washed away with water and with a 1 % solution of sodium dodecyl sufate. Subsequently, the stamps are passivated with a 4% bovine serum albumin (Carl Roth, Karlsruhe, Germany)

solution for 10 min and are finally rinsed with water and dried with N_2. The passivation is important to prevent unspecific adhesion of other parts of the force balance to the surface. Next, the dried batch of stamps is cut and single stamps are adhered to small cover glasses with a diameter of 12 mm. During the following steps, the stamps must be kept in solution to prevent bond break.

5.1.2.4. Composition of the force balance

The complementary biotin-modified DNA strands with a Cy5 fluorescence dye marker and streptavidin-modified antibody (Lightning Link, Innova Bioscience, Cambridge, UK) are mixed in a 1:1 stoichiometry in 3x phosphate buffered saline (PBS) solution, which is deposited on the stamps (Figure 16, A and B).

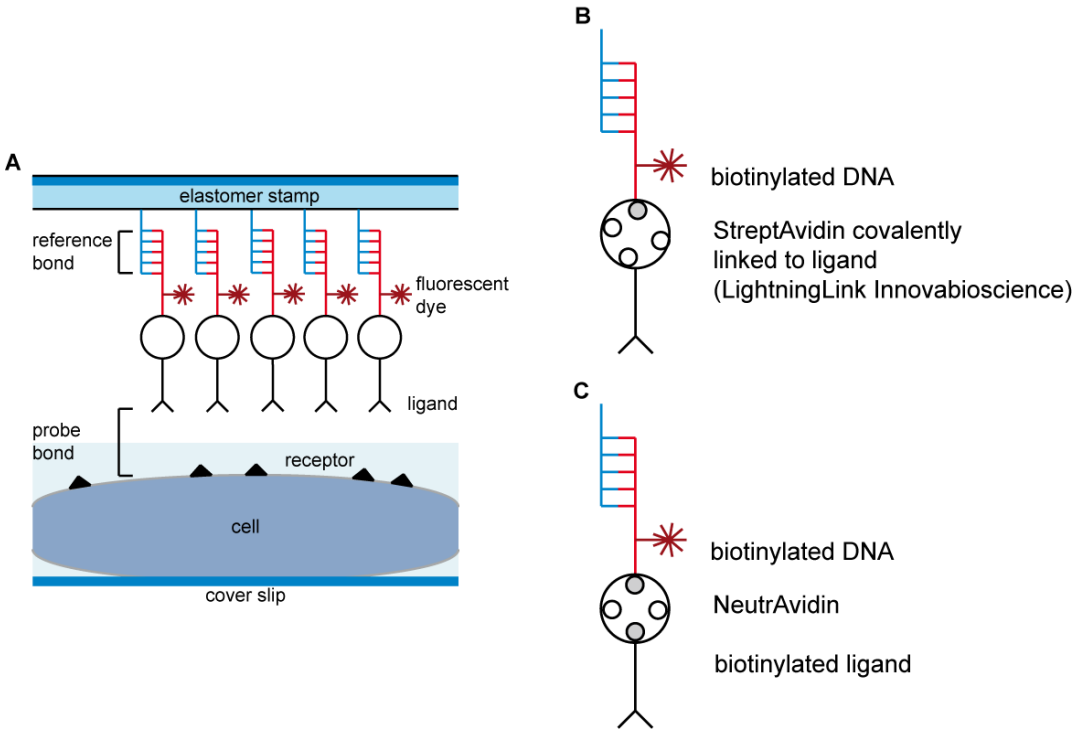

Figure 16 Detailed composition of force balance. A Biochemical setup of the MFA on cells. **B** One possibility to attach the biotin end of the DNA to the ligand is to covalently attach StreptAvidin to the ligand and then couple the complex to the biotin end of the DNA. **C** The other way to couple the DNA to the ligand is to use NeutrAvidin. Therefore, the ligand has to be biotin modified.

Alternatively, a 3x PBS solution with the complementary biotin-modified DNA, a biotinylated antibody and NeutrAvidin in a 1:1:1 stoichiometry can be used (Figure 16 C). After one hour in a humidity chamber, stamps are washed in 1x PBS, 1x PBS with 0.1% tween and again 1x PBS for five minutes each. Then they are blocked with 4% bovine serum albumin for ten minutes. Finally, the stamps are rinsed and kept in 1x PBS till usage. The ligand concentrations in the solution depend on antibody stock concentrations and range from 0.56 to 1.12 µM.

5.1.2.5. Preparation of the stamps for high throughput microspotting

The use of a microplotter for stamp functionalisation offers the perspective of simultaneous measurements with high throughput, since it deposits very small volumes of the above described ligand solutions at accurately defined positions on the microstructure of the stamp surface. On the other hand, such small volumes accompany certain problems. The ligands in the spotting solution are often proteins or other complex molecules that, when falling dry, precipitate and lose their function. To prevent this, the microplotter was additionally equipped with a humidity tent enclosing the whole apparatus. Unfortunately, using the humidity function leads to frequent crashes of the system and is therefore not feasible.

Crowe et al. studied the effect of different sugars on the recovery of freeze-dried proteins and phospholipid bilayers and could show that e.g. trehalose has a remarkable effect on the recovery [68]. Dráber et al. could show the protecting effect of trehalose on freeze-dried monoclonal antibodies [69]. Trehalose is a disaccharide consisting of two glucose molecules. Allison et al. investigated the mechanism of the protecting effect. They found that the stabilization is not due to the sugar capturing water, but it is caused by hydrogen bonding of the sugar to the proteins [70]. Dráber et al. proposed a concentration of 250 mM for antibody protection. This concentration proved too high for the use of the microplotter, since the small capillary is choked by the sugar solution. But a concentration of 30 mM trehalose also yields good results.

Still, when using the microplotter spotting a solution of NeutrAvidin and a biotinylated ligand as described above, often a brightly fluorescent precipitate occurs on the stamp and the fuctionalization is destroyed. Employing the Lightning Link kit to directly label StreptAvidin to the ligand and subsequently, spotting this complex together with the biotinylated DNA like mentioned above, circumvents this problem.

5.1.3. DNA sequences

In this section, the DNA strands used in the experiments are introduced.

The covalently attached amino-DNA is used in all experiments. Its 45 bp binding sequence is marked gray:

NH2-5xHEGL-5'-T TTT TTT TTT CGA ACG ACC TCG AGA GAC ACG TGA GTG CAG ACT GAG CAG CGA CTG-3'.

The amino group at the 5'-end reacts with the epoxide group at the stamp surface and forms a covalent bond. To prevent interactions of the force balance with the stamp surface, five hexa-ethylene glycol (HEGL) molecules and ten thymine bases serve as spacer.

Depending on the experiment, different complementary sequences are hybridized to the binding sequence described above.

For measurements in shear geometry, the complementary 45 bp sequence is marked gray.

Bio-5'-TTT TTT TTT TTT TTT TTT TT(Cy5)T CAG TCG CTG CTC AGT CTG CAC TCA CGT GTC TCT CGA GGT CGT TCG-3'.

At its 5'-end, the fluorescence dye cyanine 5 (Cy5) is coupled to a thymine base. The thymine spacer should prevent quenching effects that might be caused by the ligands attached to the biotin molecule at the 5'-end. The absorption and emission spectra of Cy5 are shown in Figure 17.

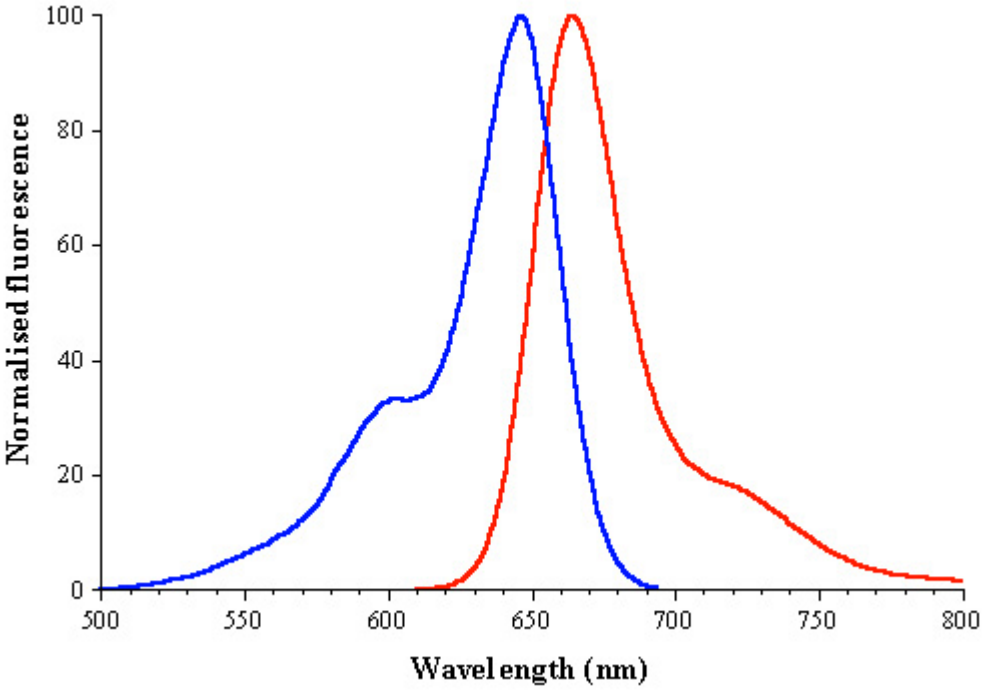

Figure 17 Absorption and emission spectra of cyanine 5. The maximum absorption occurs at a wavelength of approx. 649 nm and the maximum emission is found around 670 nm Picture adapted from bio-ope [71].

The 45 bp sequence corresponds to the highest reference force in the presented experiments. For the reference force variation, complementary strands with a shortened binding sequence (30, 15, 13, 11, 9, 8 bp) are used.

DNA opening in zip geometry represents the lowest measurable reference force, since it opens one base pair after the other. The 20 bp zip DNA (binding sequence marked gray) offers the advantage of a thermodynamically stable strand that mirrors the rupture force of a single base pair. Zip DNA, therefore, defines the maximum fluorescence transfer.

5'-CAG TCG CTG CTC AGT CTG CAT(Cy5)TTT TTT TTT TTT TTT TTT TT-3'-Bio.

The biotin at its 3'-end is couples the ligand via avidins.

5.1.4. DNA stability

The thermodynamic stability of DNA increases with its length. Conversely, measurements with DNA duplexes are restricted to thermodynamically stable duplexes. For short DNAs like 8 and 9 bp DNA, the salt adjusted melting temperature is below 40 °C. Table 1 shows the salt adjusted melting temperatures of the different shear strands.

DNA	8 bp	9 bp	11 bp	13 bp	15 bp	30 bp	45 bp
$T_{M\text{-}salt}$	34.7 °C	38.7 °C	44.7 °C	50.7 °C	57.5 °C	84.9 °C	94 °C

Table 1 Salt adjusted melting temperatures of DNA strands used in the MFA experiments.

Since the experiments are conducted at temperatures between 24-26 °C, most of the strands are still hybridized. Yet, it is not reasonable to use shorter strands to further decrease the reference force. The minimum reference force is measured with a 20 bp DNA in zip geometry, which is thermodynamically stable and represents the force required to open one base pair.

5.1.5. Cell preparation

For all experiments, cells are seeded in self-made petri dishes consisting of a frame of high-grade steel and a bottom made of a glass cover slip. Both parts are glued with a heat resistant silicone rubber to ensure the petri dish still can be autoclaved. The cover slip provides an even surface that is necessary for a successful contact process of the stamps with the cells.

5.1.6. Erythrocytes

The autoclaved petri dish is coated with poly-L-lysine (Biochrom, Berlin, Germany) in the incubator overnight. Uncured poly-L-lysine is washed away with 1x PBS. Human red blood cells are taken freshly from the finger pad of healthy volunteers, washed with 1x PBS and centrifuged five times at 3.7 rpm for one minute to separate the cells from the blood plasma. RBCs in 1x PBS suspension are then seeded on the coated glass cover slip and incubated for 30 min at 37°C in the incubator. During this time, cells settle down and adhere forming a homogeneous single cell layer. Afterwards, RBCs are rinsed three times with 1x PBS to remove non-adherent cells. The measurements are performed in 1x PBS.

5.1.7. Cell lines

Cell lines are kept in cell culture. At least 24h prior to experiments, cells are harvested with 0.01% EDTA and seeded on a glass cover slip. Directly before measurement, the culture medium is removed and cells are rinsed three times with 1x PBS. The measurements are performed in CO_2-independent L-15 Leibovitz medium without phenol red (GIBCO, Paisley, UK) to eliminate background fluorescence.

5.2. Technical setup

5.2.1. Microplotter

The MFA offers the possibility of a high throughput screening. Therefore, each of the pads of one stamp can be functionalised with different force balances using a GIX I microplotter (SonoPlot, Middleton, WI) that is described in the following paragraph.

The microplotter uses ultrasonic to deposit small liquid spots on surfaces. It consists of a micropipette made up of a hollow glass needle, which is attached to a piezo electric device. A scheme is shown in Figure 18.

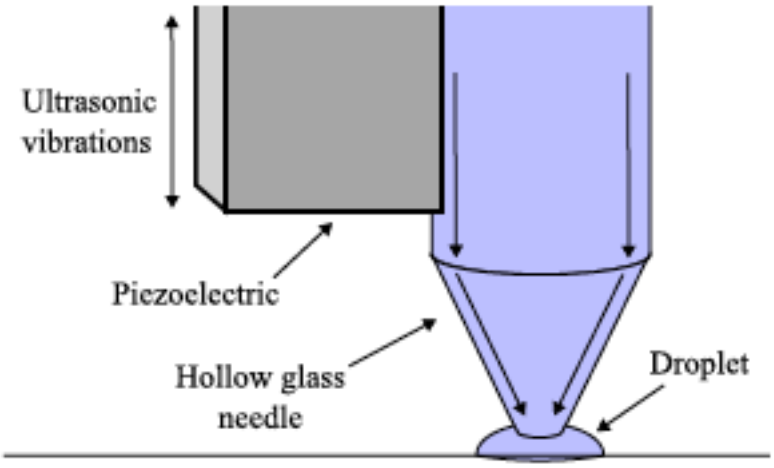

Figure 18 Schematic view of microplotter dispenser. A piezo-electric device applies ultrasonic vibrations to a glass capillary resulting in the delivery of liquid spots. Picture adapted from Sonoplot, Inc. manual for GIX mikroplotter [72].

An alternating current results in vibrations of the needle and at its resonant frequency pumping action can be observed. Thus, the liquid can be dispensed on a surface or at higher amplitudes is sprayed out. The spraying is also used to empty the needle. For refilling, the needle is dipped in the liquid depot and capillary forces lead to the intake. The amount of liquid in the capillary is controlled by the time the needle is dipped. A robotic precision positioning system ensures the exact delivery

of liquid spots. It can move the dispenser in a volume of 31 x 30 x 9.6 cm with a 5 μm resolution on each axis.

With the SonoGuide software, the automatic positioning and the applied currents at the dispenser can be controlled. The SonoDraw software offers the possibility to design individual patterns for liquid dispensing. After determining the starting point, the microplotter can automatically dispense the pattern also using different solutions (Figure 19, A and B) [73, 74].

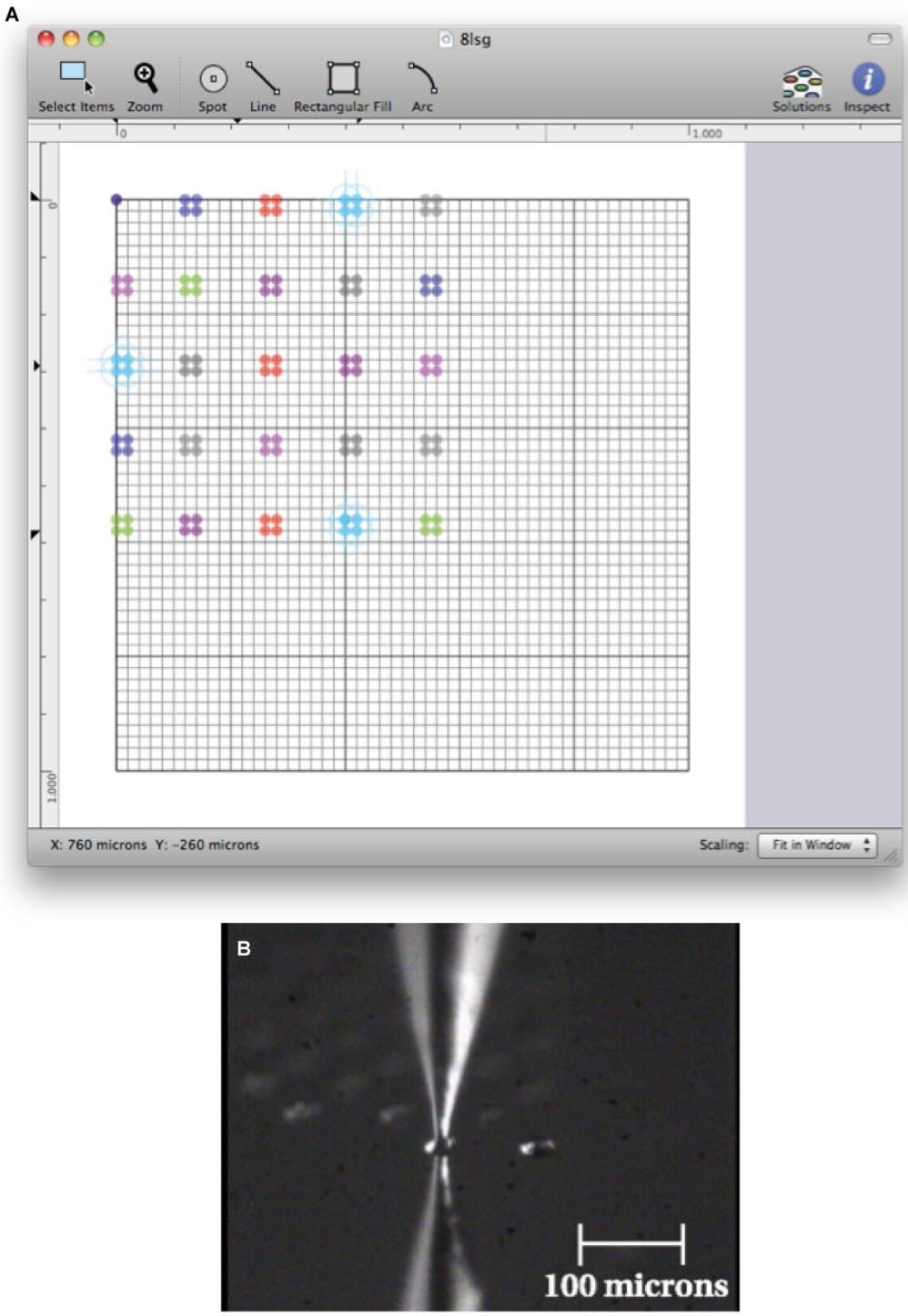

Figure 19 Pattern design and delivery of liquid spots. A With the software Sonodraw individual spotting patterns can be designed. **B** Image of the glass capillary delivering liquid spots to a surface. Picture adapted from microplotter manual [72].

5.2.2. Microscope

The experimental setup used for this thesis consists of an inverted epi-fluorescence microscope with LED illumination and a contact device, which allows contacting cells with a functionalised surface. Fluorescence pictures of the cells are recorded with an Andor iXon camera (Andor Technology, Belfast, UK). The following section presents these components in more detail.

5.2.2.1. Inverted epi-fluorescence microscope

A scheme of the inverted epi-fluorescence microscope (Observer. Z1, Zeiss, Oberkochen, Germany) is shown in Figure 20.

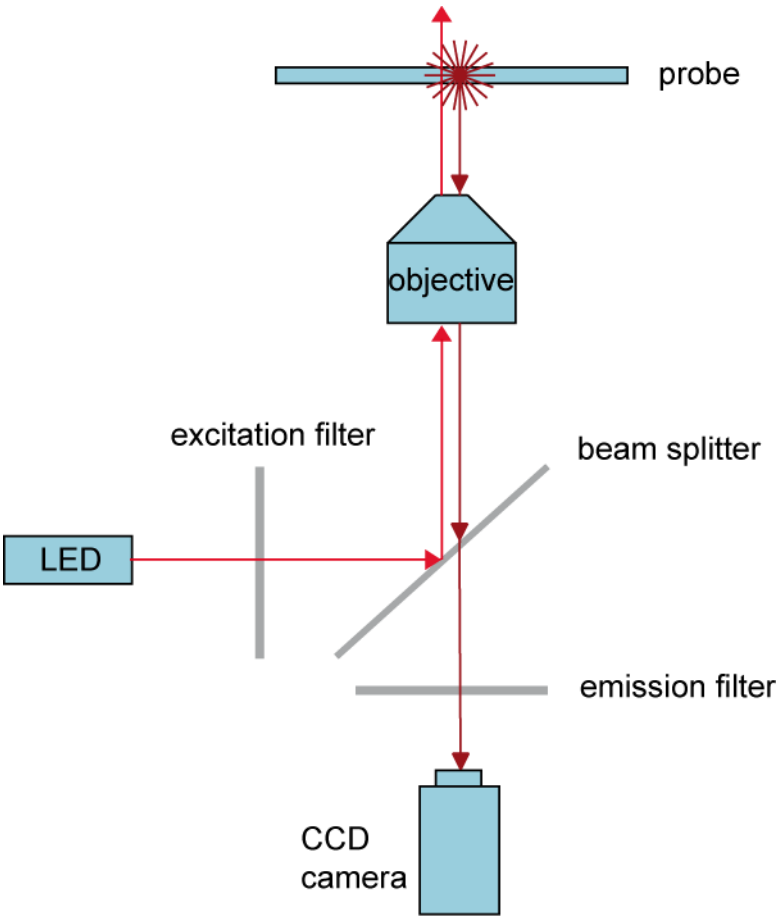

Figure 20 Scheme of the inverted epi-fluorescence microscope used in the experiments. The path of the exciting light is marked in light red, the emission light is dark red.

The excitation filter selects the appropriate wavelength for fluorescence excitation. Subsequently, the light is reflected by a beam splitter, which is selectively reflecting for light of this wavelength. Then it passes the objective and hits the sample exciting fluorescence. The fluorescence light passes the objective and hits the beam splitter, which is translucent for light of that wavelength. Finally, an emission filter blocks the undesirable excitation light.

In an epi-fluorescence microscope, characteristically, the objective works as a condensor for the exciting light at the same time. Since both light paths for excitation and emission are the same, the system is always ideally adjusted.

In the described experiments, an LED illumination (627 nm peak wavelength, Thorlabs, Dachau, Germany) is used for fluorescence imaging of the Cy5 dye, and a mercury arc lamp (Osram, Munich, Germany) is applied for interference contrast microscopy.

5.2.2.2. Contact device

The contact device consists of a micrometer stage with the cell samples and a z-stage moving the elastomer stamp towards the cells. The x-y- stage uses high precision stepper motors (PI, Karlsruhe, Germany). For the z-stage, another high precision stepper motor, offering a travelling distance of 15 cm, is combined with a piezo actuator (piezosystem, Jena, Germany) with a travelling distance of 320 μm. Below the piezo, a glass block coated against refelction is mounted for fixation of the elastomer stamps. Figure 21 shows a schematic picture of the contact device.

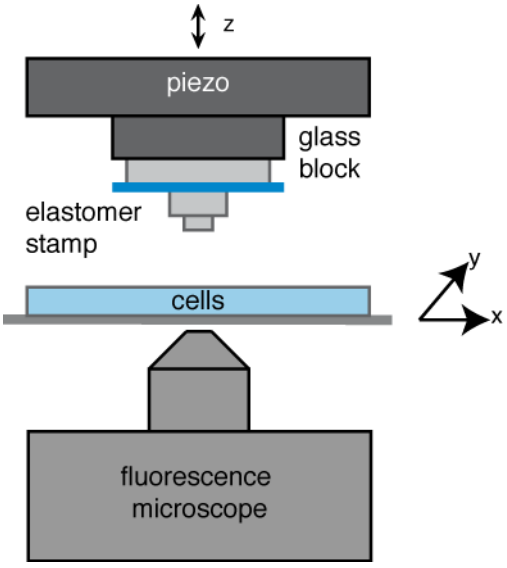

Figure 21 Contact device. In z-direction, the glass block with elastomer stamp is roughly positioned with stepper motors and fine adjusted via a piezo actuator. An x-y-stage positions the probe.

Previous to the contact process, the elastomer stamp, which is adhered to a small 12 mm glass cover slip, is kept in buffered solution to maintain an intact functionalisation. For attachment to the glass block, the cover slip with the stamp on it is removed from the buffer. The bottom side is dried with a filter paper and then adhered to the glass block by an elastomer connecting-piece. The stamp surface stays wet during this procedure and afterwards, is dipped into the sample buffer as soon as possible lowering the glass block to the sample. The parallel alignment of the stamp to the cell surface is done by micrometer screws (OWIS, Staufen, Germany) and monitored by reflection-interference-contrast-microscopy.

5.2.2.3. Reflection-interference-contrast-microscopy

The exact parallel alignment of stamp and sample is challenging but crucial for a reasonable outcome of the experiment. Basically, the tilt of the stamp and the contact process can be observed with reflection-interference-contrast-microscopy (RICM), which is presented in the following paragraph.

Light is reflected and refracted, when passing the interface of optical media with different refractivity. The reflected light fractions exhibit optical path differences that interfere constructively and destructively. In the image plane, an interference pattern depending on the angle of the two surfaces is visible. This is illustrated in Figure 22.

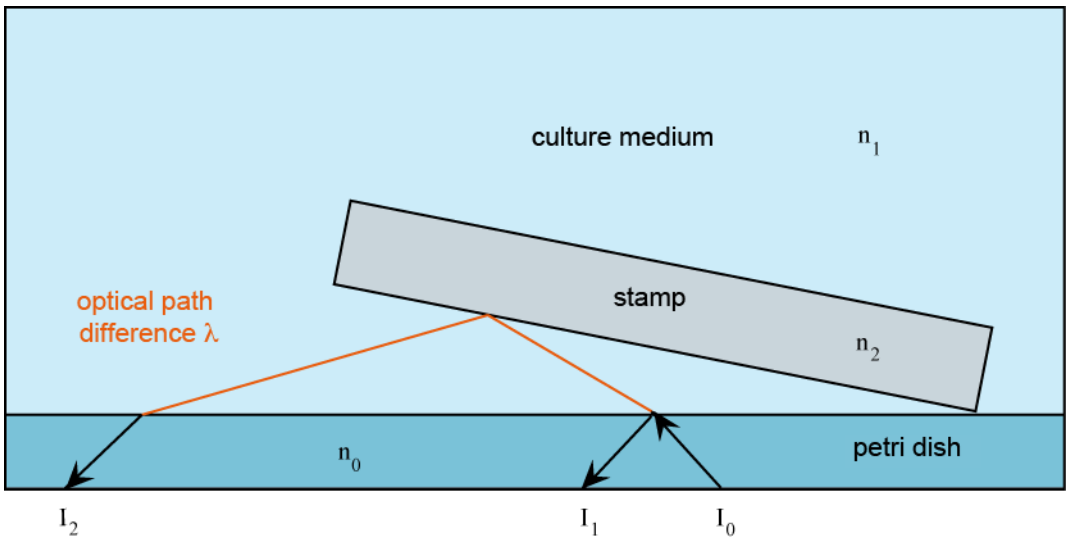

Figure 22 RICM method. If light passes from one optical medium to another, reflexion at approaching surfaces results in an optical path difference that leads to interference patterns.

If the two surfaces are aligned perfectly parallel, no optical path differences occur, and thus, the interference pattern vanishes [75].

The proximity of two surfaces that is necessary to create interferences depends on the coherence length of the light. During the alignment process, the particular challenge is to absolutely avoid contact with the cells though being in close proximity. Since the LED exhibits only a small coherence length, interferences occur only in close proximity of the two surfaces. This works only for the alignment of the stamp in presence of RBCs, which are extremely uniform considering their height and structure. But for experiments with cultured cells that are bigger and less uniform, the alignment of the stamp using LED light is not possible anymore. Instead, a mercury arc lamp (Osram, Munich, Germany) with a

longer coherence length is used for these experiments. Its maximum intensity at 546 nm is selected with a Cy 3 excitation filter (550 nm).

Still, another problem is the low contrast between maximum and minimum intensity making the exact supervision during alignment difficult. Using the anti-flex technique (Figure 23), much of the scattered light is eliminated by polarisation, and thus, the contrast can be enhanced.

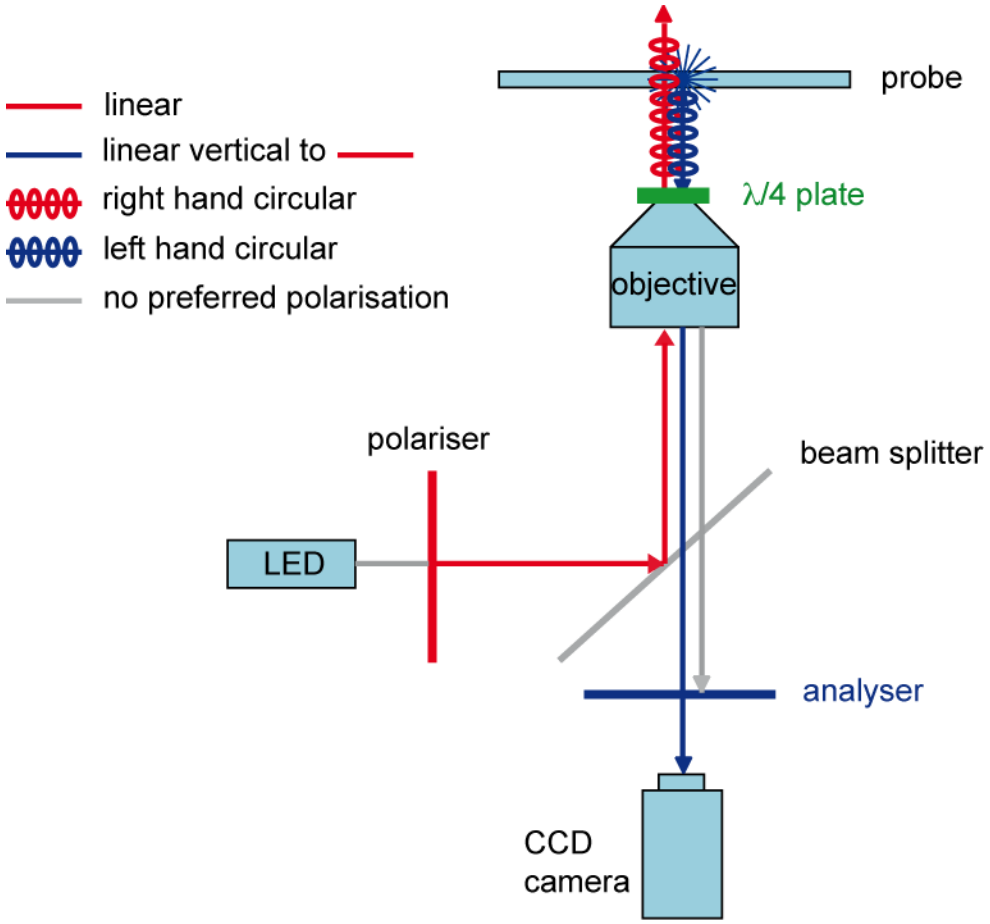

Figure 23 Principle of anti-flex technique. With this method scattered light can be reduced effectively.

First, the light is polarised linearly and after passing a λ/4 disc it is polarised circularly. When hitting the sample the polarisation changes such that passing the λ/4 disk again yields linearly polarised light, of which the polarisation is vertical to the original light. This offers the possibility to select the light making up the signal

and to reduce the scattered light [75]. Altogether, these arrangements result in an improved parallel alignment.

5.2.3. Contact process

After parallel alignment, the stamp is lowered and brought in contact with the cells. The process is observed with an optical microscope at 40x magnitude. The approach of the stamp is stopped in the experimenter's sole discretion considering that, typically, cells change their form slightly when they start to get squeezed. After the cells have been in contact with the functionalised stamp for one minute, the stamp is retracted with a velocity of 50 nm/s. Since the described process does not allow for a reproducible contact force exerted on the cells, two experiments can hardly be compared quantitatively. But working with RBCs allows for a qualitative control of the contact pressure, because healthy cells with haemoglobin exhibit a good contrast in optical microscopy (Figure 24 A).

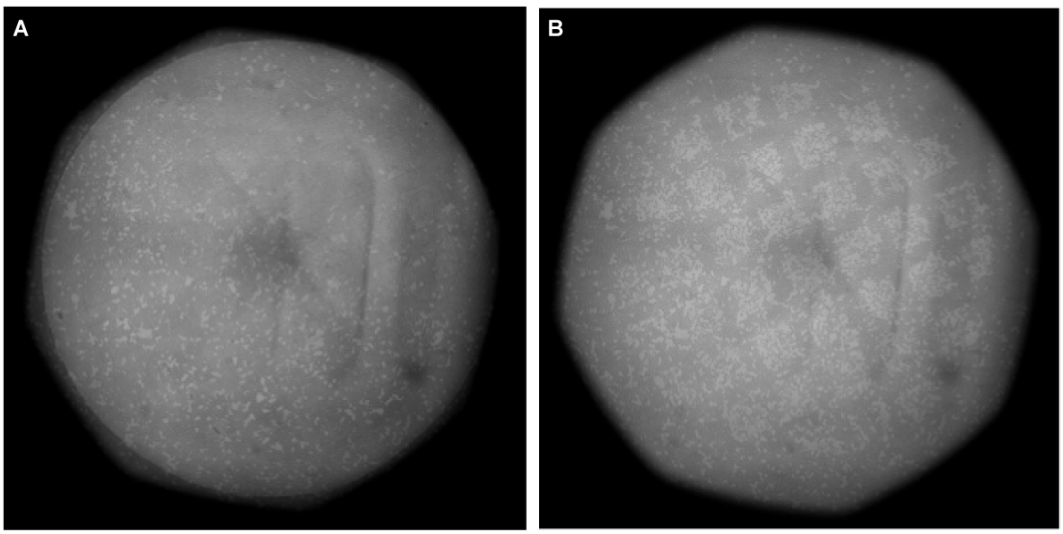

Figure 24 Transmitted light image of cells before and after contact. A Image of red blood cells before the contact process. **B** After contact with high contact force the cells burst, which lowers their contrast resulting in a pale pattern of the pads.

If squeezed too hard, the cells' membrane breaks and the haemoglobin disappears leaving a cell without contrast (Figure 24 B). This way, taking pictures of the cells after contact, represents a qualitative control estimating, if the contact pressure in two experiments is comparable or not. Additionally, after contact, fluorescence pictures with 10x and sometimes 40x and 63x magnitude are taken. In one petri dish up to three experiments are conducted.

5.3. Data analysis

For a better quantitative comparison, in all measurements the same camera adjustments, light intensities, and focal apertures are used for transmitted light images and fluorescence pictures respectively. Usually, the images for the analysis of the experiment exhibit an inhomogeneous intensity profile. Since fluorescence is proportional to the intensity of exciting light, the same fluorescence transfer yields darker spots in the border area of the aperture compared to the central part (Figure 25 A).

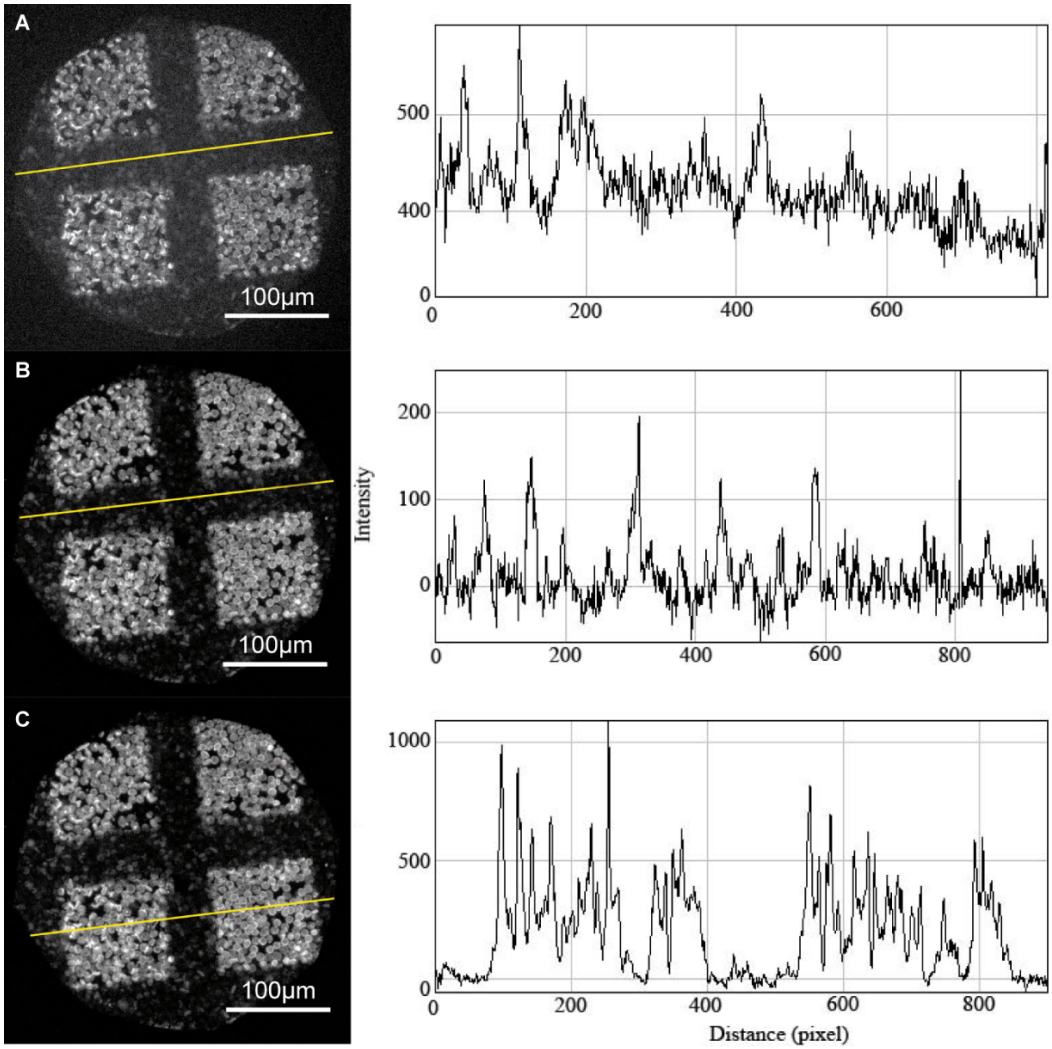

Figure 25 Data analysis. A Left side: Fluorescence image of fluorescently labelled RBCs. In an MFA experiment the interaction of the galNAc-HPA complex is detected. The yellow line marks the intensity analysis. Right side: Intensity histogram of the background. Due to the inhomogeneous illumination, no even intensity is obtained. **B** Left side: Levelled out fluorescence image after correction with a picture of the illumination and subtracted mean background. Right side: The histogram of intensity shows an even background. **C** Intensity analysis of fluorescently labelled cells. In the histogram, fluorescent cells result in intensity levels that are significantly higher than the base line.

To prevent biased results, pictures are corrected with a fluorescence picture of the illumination (Figure 25 B). In the corrected pictures the background is determined in areas between the pads, where no fluorescence transfer occurred. The background value is gained by integration over several lines of pixels in different areas of the picture and subsequent averaging. The background value is then subtracted from the picture. Thus, the background does not contribute to the signal.
The above-described normalized pictures exhibit a uniform illumination profile with an average background of zero (Figure 25 C). For the analysis of the fluorescent areas, a grid is overlaid and aligned in the pictures of the stamp and of the cells after stamping. According to the grid, the mean intensity of the areas is measured, and afterwards, the mean intensity of the fluorescent areas on the cells is divided by the mean intensity of the corresponding pads on the stamp. This yields the relative fluorescence transfer on the cells.
The data analysis is automated using a self-written LabView program (National Instruments, München, Germany) (Figure 26).

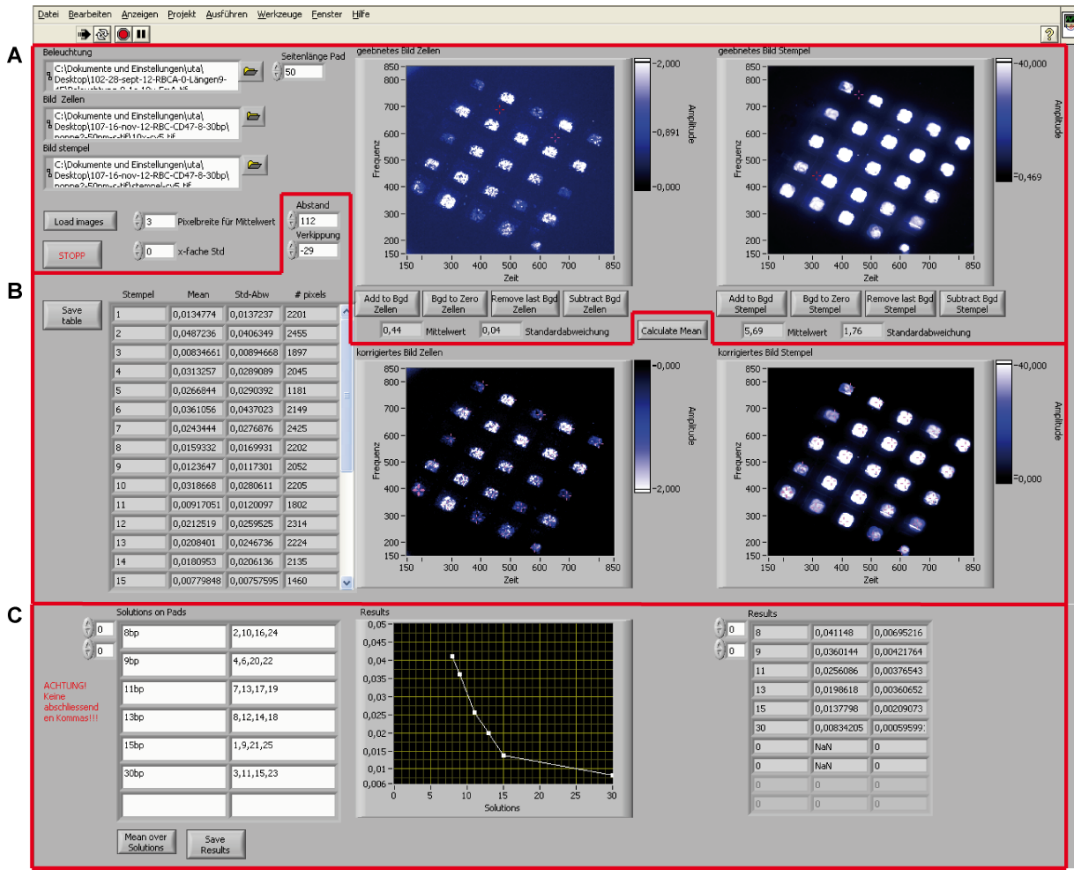

Figure 26 Screenshot displaying analysis program A On the left side, images of the illumination, the cells, and the stamp can be uploaded. In the windows on the right side, the background fluorescence is analysed in areas between the pads using cursors that determine the lines of pixels for integration. **B** Fluorescence images are overlain by a grid that marks the pads, which are the areas of intensity analysis. In these areas the mean intensity is determined and written in the table on the left side. **C** On the left side, the pads are assigned to the according DNA reference lengths. A graph and a table display the results.

5.3.1. Theoretical prediction of using the MFA on cells

To better understand the results obtained from the MFA assay, the outcome of such experiments is discussed from a theoretical point of view in the next section.

The read-out provided by using the molecular force balance on cells is the relative fluorescence transfer (*rft*) onto the cells. Hence, the signal depends on the strength of the probe interaction F_{probe} and the reference interaction $F_{reference}$. It is determined

by the ratio of the background corrected fluorescence intensities of the cells after contact ($f_{cell}\left(F_{probe},F_{reference}\right)$) and the stamp before contact (f_{stamp}):

$$rft = \frac{f_{cell}\left(F_{probe},F_{reference}\right)}{f_{stamp}} = \frac{I_{dye,cell}\cdot n_{cell,labelled}\left(F_{probe},F_{reference}\right)}{I_{dye,stamp}\cdot n_{stamp}} \quad (15).$$

$I_{dye,stamp}$ and $I_{dye,cell}$ are the intensities per dye on the stamp and the cells, while $n_{cell,labelled}\left(F_{probe},F_{reference}\right)$ and n_{stamp} are the numbers of fluorescently labelled receptors on the cell and reference molecules on the stamp, respectively.

As the intensity of the fluorescent dye was found to be approximately the same, no matter, if it is measured at a duplex DNA (found on the stamp) or at single stranded DNA (found on the cell surface), we can simplify equation (15). Introducing the probability for a transfer event $P_{transfer}\left(F_{probe},F_{reference},n_{cell},n_{stamp}\right)$ and with $n_{cell} = n_{stamp}\cdot P_{transfer}\left(F_{probe},F_{reference},n_{cell},n_{stamp}\right)$ we gain:

$$rft = \frac{n_{stamp}\cdot P_{transfer}\left(F_{probe},F_{reference},n_{cell},n_{stamp}\right)}{n_{stamp}} = P_{transfer}\left(F_{probe},F_{reference},n_{cell},n_{stamp}\right) \quad (16).$$

The probability for a transfer event $P_{transfer}\left(F_{probe},F_{reference},n_{cell},n_{stamp}\right)$ depends on the ratio between the interaction strengths of the reference and probe bond, the number of reference bonds presented on the stamp n_{stamp}, and the number of accessible receptors on the cell n_{cell}.

As in typical experiments $n_{stamp} >> n_{cell}$, the fluorescence transfer is not limited by the availability of reference bonds, i.e. for every receptor on the cell a reference bond is provided. Hence, we can assume that the probability of a transfer event $P_{transfer}(F_{probe},F_{reference},n_{cell})$ is independent of n_{stamp}.

On the other hand, the number of receptors accessible n_{cell} is a crucial parameter for the experiment. If the number of cell receptors accessible to the stamp increases, the fluorescence transfer also increases, although the strength of the probe interaction stays constant or even decreases. The number of receptors accessible n_{cell} mainly is influenced by two factors: the cell type and the contact force, i.e. the pressure used to bring the two surfaces into contact. Regarding the cell type, we can assume that within a given cell type the number of receptors exposed on its surface is comparable within their biological variance. Thus, when analyzing forces of a receptor-ligand interaction using a distinct cell type, this influence can be neglected.

The second main influence on the number of accessible receptors n_{cell}, the contact force, sets more restrictions to the experiment. In order to compare the fluorescence transfer of different measurements with varying reference interactions, the contact pressure needs to be identical. This can be achieved, for example, measuring multiple reference strengths against one probe interaction on the same stamp, which is realized using a microplotter.

Hence, the method allows measuring relative changes in the fluorescence transfer, but it is not possible to obtain absolute values for the fluorescence transfer, since the method does not provide access to information about the number of receptors on the cell surface.

Thus, if accepting that the method only provides relative values of the fluorescence transfer, the probability of a transfer event $P_{transfer}\left(F_{probe}, F_{reference}\right)$ is also independent of the number of receptors accessible and, for a give reference interaction, only depends on the strength of the probe bond.

This means that under the above assumptions the probability of a transfer event only depends on the probability that the receptor-ligand bond will survive the stamping process. If the receptor bond ruptures, no fluorescence transfer will occur, no matter if reference bond stays stable, or not.

In contrast to our everyday live, interactions on the molecular level typically do not show singular rupture forces but a rupture force distribution with a mean rupture

force and a given distribution width. Two exemplary probability distributions $D_A(F)$ and $D_B(F)$ for the rupture force of two different molecules A and B are shown in Figure 27.

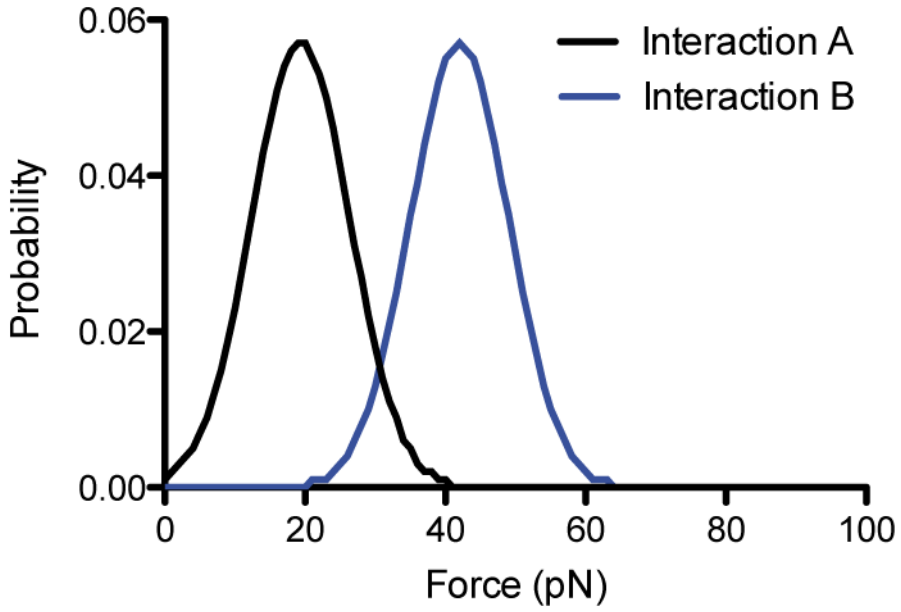

Figure 27 Force-Probability-Distributions. The Figure shows two exemplary force probability distributions, as they can be found for DNA-DNA duplexes or other molecular interactions. The distributions are typically derived from histograms measuring the most probable rupture force.

Coming from such a distribution, the probability for a rupture event $P_{rupture}(F)$ is calculated as the cumulative integral. As we want to know the probability for a fluorescence transfer, we need to calculate the probability of not-rupturing the probe bond, i.e. $1 - P_{rupture,probe}(F)$. In an MFA experiment, the forces applied to the force balance clamped between the surfaces is ramped up from zero force upon contact to the maximum force necessary to rupture all balances. This means that the forces, which are available for testing the probe, are defined by the force distribution of the reference bond.

Hence, the probability of a transfer event $P_{transfer}(F)$ for a given force value F can be written as the product of the available reference force distribution $D_{reference}(F)$ and the probability of not-rupturing the probe:

$$P_{transfer}(F) = D_{reference}(F) \cdot \left(1 - P_{rupture,probe}(F)\right) \tag{17}.$$

As the force is ramped up though the experiment, the probability of a transfer event $P_{transfer}\left(F_{probe}, F_{reference}\right)$ for a given reference interaction can be calculated as the integral over all force values:

$$P_{transfer}\left(F_{probe}, F_{reference}\right) = \int_0^\infty P_{transfer}(F)dF \tag{18}.$$

This means the fluorescence transfer only depends on the probability of not-rupturing the probe bond and the force distributions of the reference bond. Figure 28 shows the probability of not-rupturing the probe bond and three different force distributions of the reference bond.

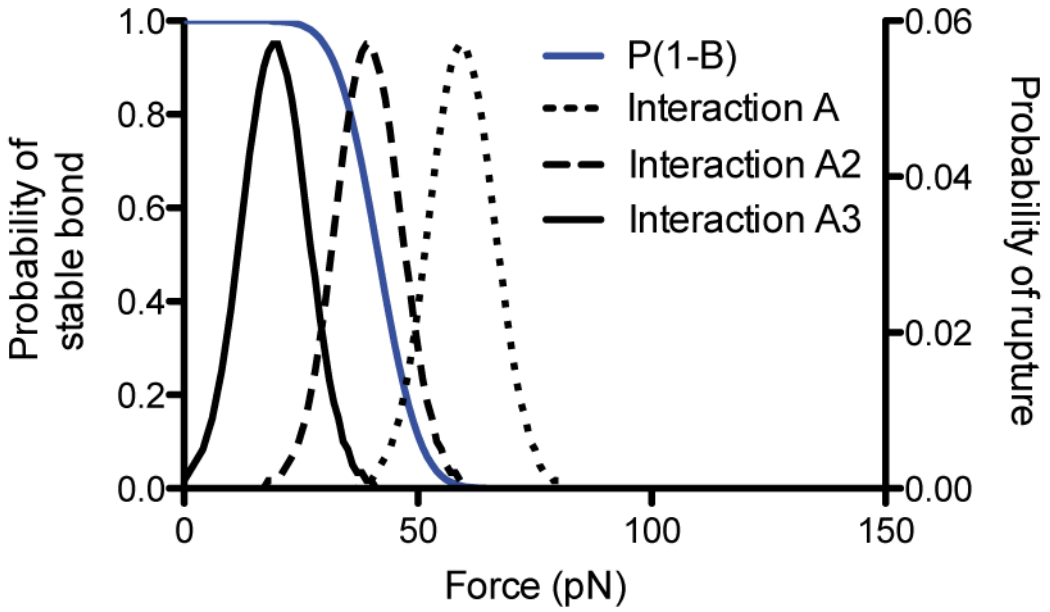

Figure 28 Example for different reference force distributions. Testing of the probe molecule ($P(1-B)$ is the probability of a not-rupturing probe bond) with reference bonds of different strengths (Interaction A-A3) leads to a decreasing fluorescence transfer. As the product of $P(1-B)\cdot A$ is decreasing, the higher the mean of the force distribution becomes.

When now varying the reference interaction with DNA strands of different lengths and calculating the probability of a transfer event $P_{transfer}\left(F_{probe},F_{reference}\right)$, the result of a detailed comparative force measurement can be predicted. Using published DNA rupture data [38, 76] and reasonable rupture forces for the surface receptor interaction $F_{receptor,mean}\approx 40\,pN$, the following behaviour (Figure 29) is predicted:

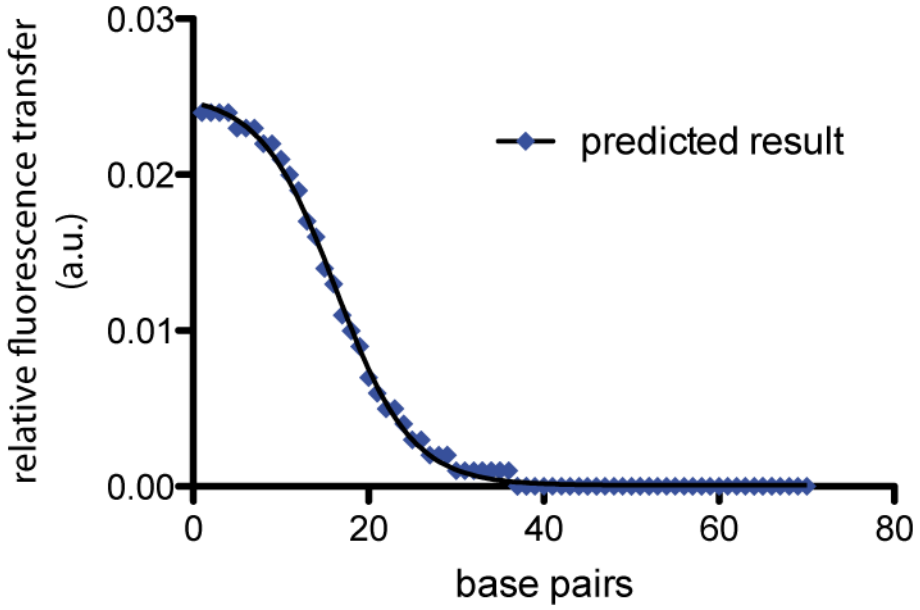

Figure 29 Predicted result for a detailed comparative force measurement. Using previously published DNA rupture data, the result of a comparative force experiment can be predicted. The DNA rupture-distributions are Gaussian distributions with their mean calculated using the formula presented by deGennes (χ^{-1}=14.1 bp, f = 4.5 pN, the values were adapted to fit measurement data from Ho et al. [77]). The mean rupture force for the probe interaction was assumed to be approx. 40 pN. A constant width of 7 pN was assumed for both interactions. The sigmoidal fit leads to a DNA force equivalent of approx. 16bp.

The theoretical prediction shows two plateaus when either the reference bond or the probe bond is more likely to rupture. In between, a transition occurs if both interactions are of comparable strength. Furthermore, the theoretical behaviour shows that even for reference bonds stronger than the probe, the fluorescence transfer is not zero. This is due to the non-zero widths of the rupture probability distributions of both interactions.

The simulated data in Figure 29 shows that the experimental behaviour can be predicted to some extend. However, as it is difficult to exactly determine the loading rate in an MFA experiment, it is not reliable to extrapolate a distinct force value for the receptor-ligand interaction based on the measurement data. Therefore, the presented force values will only represent a DNA force equivalent, which incorporates the uncertainty in the loading rate.

6. Results & Discussion

6.1. Non-comparative measurements

In this section, MFA experiments without the use of the microplotter are described, meaning that the whole stamp is functionalised with the same reference and receptor-ligand interaction. These are preliminary experiments before the application of the microplotter was introduced.

6.1.1. Screening for CD47 receptor on Rh_{null} RBCs

Human RBCs expose the CD47 receptor that plays a crucial role in the recognition of self-erythrocytes. It becomes apparent in Rh_{null} patients having strongly decreased expression level of CD47. Speculations are that this leads to a hemolytic anemia, meaning that their RBCs are destroyed by the immune system [78]. The Bavarian blood donation service provided freshly taken blood probes of an Rh_{null} patient. In MFA experiments, we specifically detected the CD47 receptor on these Rh_{null} cells and compared our measurements to normal RBCs. A biotinylated CD47 antibody and a 15 bp DNA reference strand in shear geometry were used for the experiments. The relatively low reference force of this DNA strand ensures that we on the one hand obtain a considerable transfer, but, on the other hand, only get a specific signal. The fluorescence pictures of Rh_{null} and healthy blood clearly show lower fluorescence intensities for the Rh_{null} blood sample compared to the blood cells of a healthy person (Figure 30, A and B).

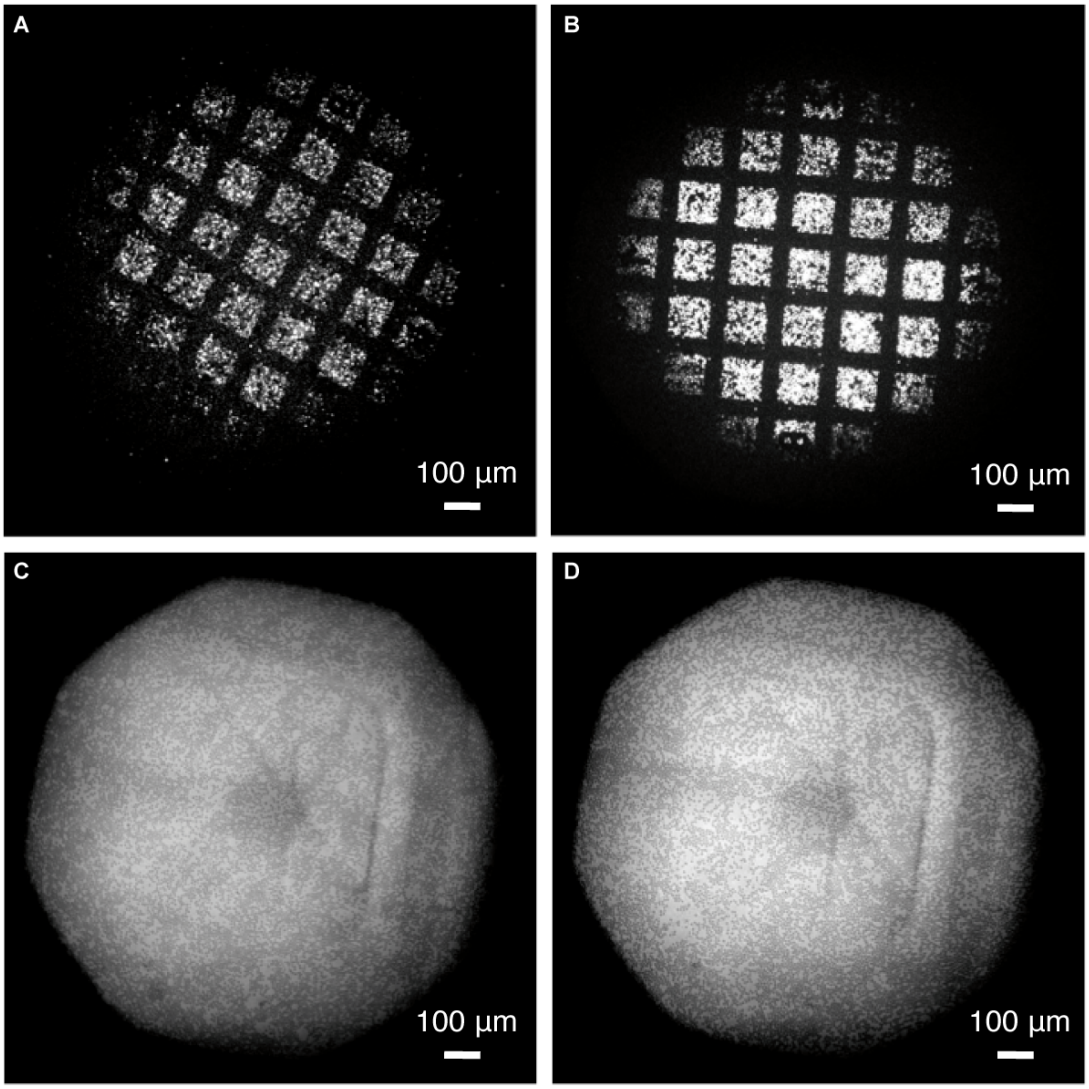

Figure 30 Detection of CD47 receptor on Rh_{null} RBCs. A Fluorescence image of Rh_{null} RBCs. The CD47 receptor is clearly detectable. **B** Healthy RBCs show a higher fluorescence transfer in the same experiment. **C** The transmitted light image of Rh_{null} RBCs after contact exhibits lighter areas in the form of the pads. This results from several burst cells proving a quite high contact force. **D** As the transmitted light image of healthy cells shows no lighter areas after the experiment, this implies a lower contact force than for the Rh_{null} cells.

Though, as discussed above, a comparison of two different experiments is suitable only to a limited extend, in this case the transmitted light pictures show that the contact pressure was slightly higher for the Rh_{null} sample compared to the healthy cells, because the membrane of some Rh_{null} cells burst and they lost their contrast

(Figure 30, C and D). Comparing similar experiments on the same cells the one with the higher contact pressure, exhibits more fluorescence transfer. But for the above-described experiment, we gain even less fluorescence transfer on the Rh_{null} cells, because of the lower expression level of the CD47 receptor on Rh_{null} cells.

6.1.2. Visualization of cancer-involved receptors on the cell surface

The composition of surface receptors often distinguishes between healthy and diseased cells. Therefore, a visualization of relevant receptors is important for a fast diagnosis. The cancer cell line SW480 is selected to demonstrate the ability to detect such cancer involved receptors on the cell surface with the MFA. Colon cancer is the second most frequent malignancy in the western world and causes many of the cancer related deaths [79]. The major problem in combating cancer progression is the fast spread of metastasis. The metastasis-associated adhesion molecules CD44 and E-cadherin are over-expressed or absent on SW480 cells, respectively. For MFA experiments, stamps are functionalised with a CD44 antibody and an E-cadherin antibody. Additionally, the CD47 receptor that is expressed in an appropriate density on many cells is detected for comparison. Expectedly, the fluorescence images after contact depict a considerable fluorescence transfer for the CD47 and CD44 receptor, respectively (Figure 31, A and B).

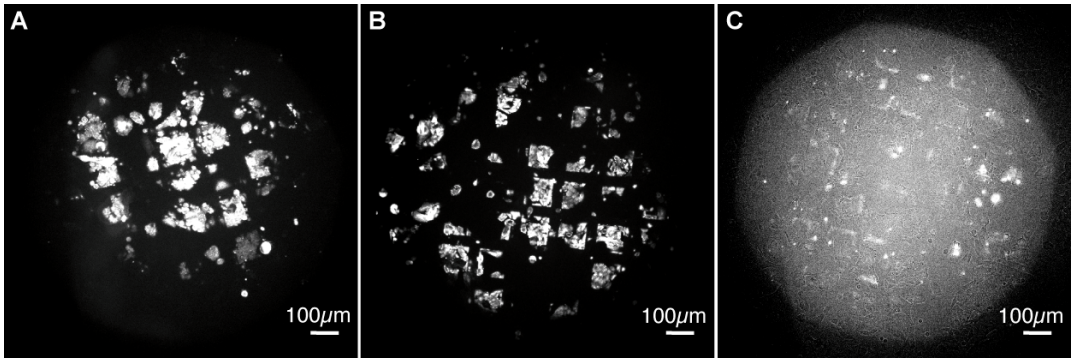

Figure 31 Detection of different cancer involved receptors on SW480 cells with MFA. A Detection of CD47 receptor. The fluorescence image reveals a considerable fluorescence transfer. **B** An antibody against the CD44 receptor results in a clear fluorescence transfer. **C** The experiment with an antibody against E-cadherin only leads to a slight nonspecific transfer.

Figure 31 C implies that the E-cadherin receptor is almost absent on SW480, which is in accordance with [80].

For a comparative screening assay it is necessary to be able to dispense different ligands on one stamp and thus, detect different receptors in one experiment. Corresponding experiments are realized with a microplotter and are described below.

6.2. Comparative measurements

In the following section, a mircoplotter is applied to dispense different ligands on one elastomer stamp. This way, a simultaneous analysis of more than one ligand is realized. The according experiments are discussed below.

6.2.1. Screening assay

In the next step, the high specificity of detection for this method is demonstrated with two different ligands. A 15 bp DNA double strand was used as a reference duplex for both molecular complexes. The first ligand is an antibody against the CD47 receptor. The second ligand is the lectin HPA that binds to galNAc [53]. This

glycolipid rest is exposed in a high density on RBCs of only blood group A. On RBCs of blood group 0 or B galNAc is absent [54]. Grandbois et al. previously analysed this receptor ligand complex with the AFM. They obtained rupture forces of about 35 pN for a single bond rupture of the galNAc-HPA complex at a retraction velocity of 6 μm/s [81]. In the MFA experiments, HPA was deposited with a microplotter on every second pad in a chessboard-like pattern, and the CD47 antibody was transferred to the remaining pads (Figure 32, A and B).

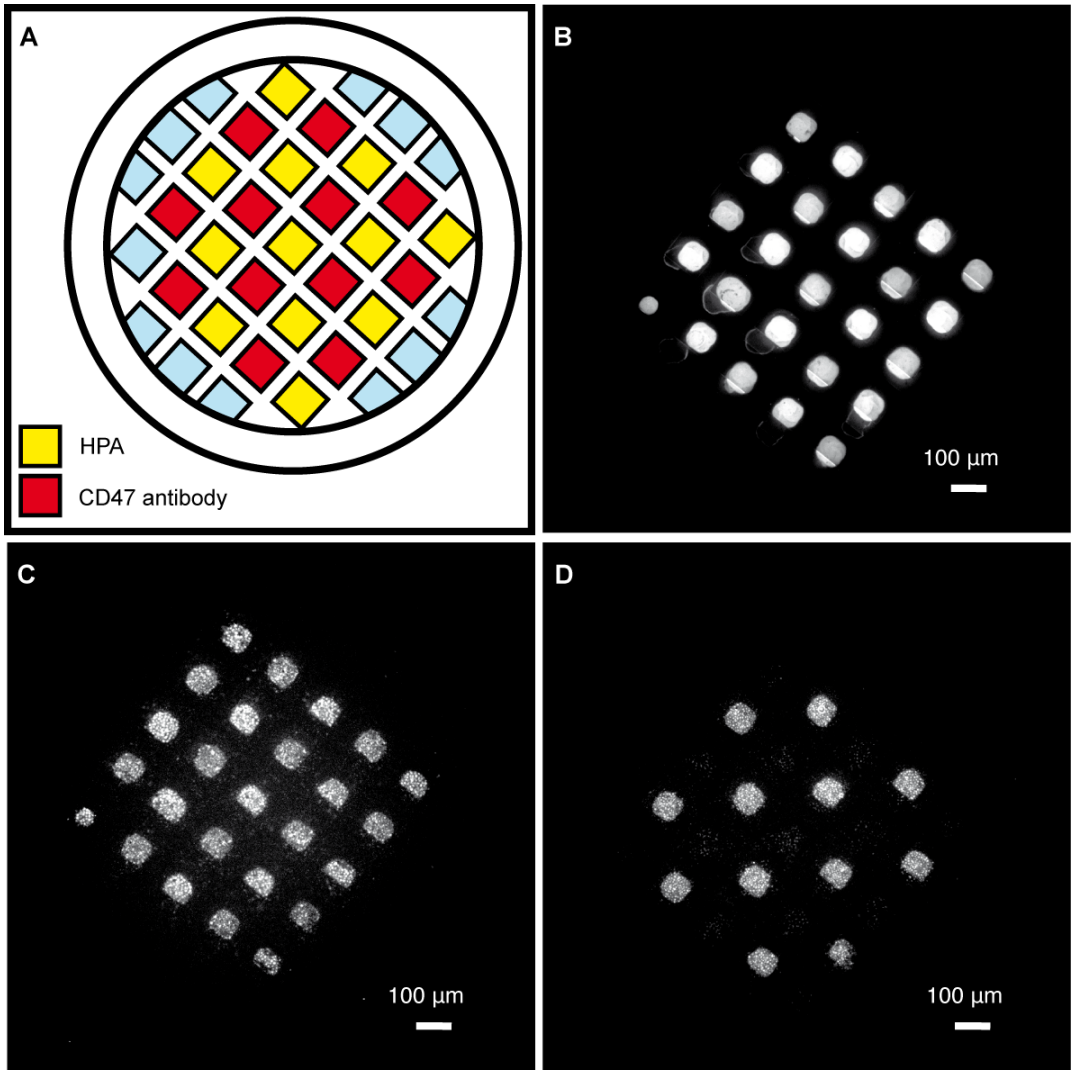

Figure 32 Detection of CD47 receptor and galNAc on human RBCs. A Force balances consisting of a 15 bp DNA duplex as reference force and the CD47 antibody or the lectin HPA, respectively, are deposited in a chessboard-like pattern. **B** The fluorescence picture shows the elastomer stamp after functionalisation. With one stamp, two different experiments are conducted. **C** A post-contact fluorescence picture demonstrates that a fluorescence signal is obtained for both the CD47 receptor and galNAc on cells of blood group A with slightly different intensities. This difference might be due to different ligand densities on the cells or a lower binding force of the receptor ligand complex. **D** In the fluorescence image of cells of blood group O after contact, no fluorescence transfer is observed for the pads functionalised with the lectin. This is due to the absence of galNAc in blood group O and clearly demonstrates the elimination of unspecific interactions with this method.

The first pad is always excluded from the measurements, because it is the starting and end point for the plotting process. Here, different solutions might accidently mix up. With only one stamp, two different experiments are conducted, first on RBCs of blood group A and second on blood group 0. This is possible, because the number of receptors on the cells is much lower than the number of ligands on the stamp. In the first experiment, the RBCs of blood group A precisely exhibit the pattern on the microstructure of the elastomer as a fluorescence transfer pattern (Figure 32 C) indicating that both galNAc and the CD47 receptor are exposed on the cells. The fluorescence transfer for HPA is higher than for CD47 antibody. One explanation could be a higher galNAc density on the cell surface. A higher binding force of galNAc to HPA, on the other hand, would lead to the same result, since the DNA duplex is more likely to rupture. Repeating the experiment with the same stamp on RBCs of blood group O, only the chessboard-like pattern of the CD47 antibody was obtained (Figure 32 D). The measurements clearly yield no fluorescence transfer for the lectin HPA on blood group O. On the one hand, this shows the absence of galNAc on blood group O. Furthermore, these results strongly suggest the elimination of unspecific interactions with this method, since the force to open the 15 bp DNA strand exceeds the strength of possible unspecific interactions. Similar experiments with shorter DNA strands (9 bp DNA) confirm the results. These experiments demonstrate that the MFA on living cells in combination with the microplotter technique is a powerful tool for the parallel screening for cell surface receptors.

6.3. Force analysis with the MFA

In this paragraph simultaneous experiments are described, in which the reference force is varied by the DNA length. This enables a comparative force analysis of receptor-ligand interactions on the cell.

6.3.1. First comparative force analyses

Since the MFA is primarily a method for highly sensitive force measurements [28], using the MFA on cells to reveal binding characteristics of the receptor-ligand bond, seems a logical direction. The comparison of binding forces of different ligands provides valuable information about the interaction parameters and hence, is of high interest for basic research and drug development. By performing a comparative force analysis, elaborate direct force measurements like AFM experiments are avoided. Instead, the binding force of the receptor-ligand complex of interest is compared to a reference molecule that in case of the DNA is easier to analyse than the receptor-ligand complex itself [38]. DNA is very well suited for those comparative force measurements, as the rupture force between duplexes may be programmed in a wide range by choosing attachment geometry, overlap length and sequence [38, 41]. In a single experiment, the pads of the elastomer stamp are functionalised with different DNA lengths linked to the ligand. The ligand binds to the receptor in contact with the cell surface, and upon retraction the reference or the probe bond ruptures in a stochastic process. The shorter the DNA duplex the weaker the reference bond is and the more readily it breaks resulting in a fluorescence transfer to the cell surface. Dependent on the length of the DNA duplexes and on the according strength of the reference bonds, three regimes are expected. For high reference forces corresponding to long DNA duplexes a minimum fluorescence transfer is anticipated. On the other hand, for short DNA duplexes with a low reference force saturation of fluorescence transfer should be obtained. In between these two regimes, a gradient is anticipated and the specific case is expectable that the probability of bond rupture is 50%. This is when the reference force equals the force of the probe bond.

The first force measurements are conducted using three different DNA lengths (15 bp, 30 bp and 45 bp) for the analysis of the CD47 receptor on M21 cells, MDA MB231 cells, and RBCs, respectively. An elastomer stamp is functionalised like shown in Figure 33, A and B using the microplotter.

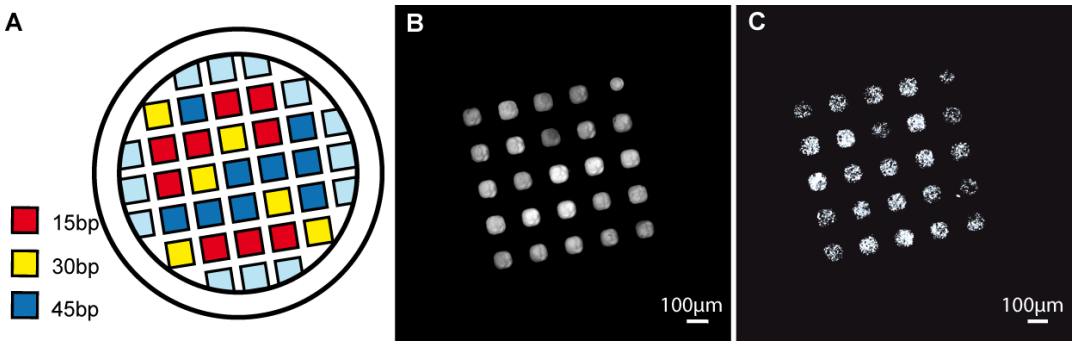

Figure 33 Comparative force analysis of CD47 receptor on RBCs. A The picture illustrates the pattern of force balances with different legths. **B** Fluorescence image of the functionalised elastomer stamp before contact. **C** The RBCs exhibit fluorescence transfer with brighter areas according to pads with shorter DNA that results in lower reference forces.

Figure 33 C shows the fluorescence image of RBCs after the experiment. The image already reveals brighter areas, where the pads with 15 bp DNA were in contact. This is the case for all used cell types.

Detailed data analysis confirms the tendency that the longer the DNA strand and the higher the corresponding reference force the smaller the fluorescence transfer (Figure 34).

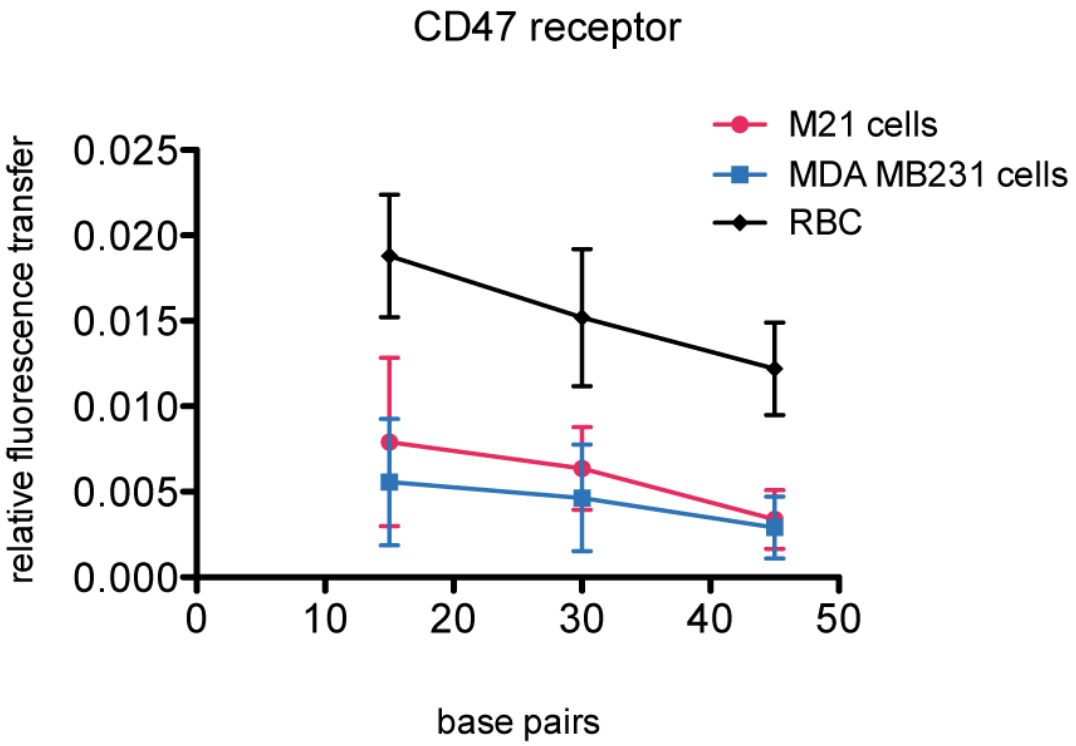

Figure 34 Graph showing force analysis of CD47 receptor on different types of cells. RBCs show the highest fluorescence signal with a decrease of fluorescence transfer for long DNA strands according to a high reference (black). Experiments with M21 melanoma cells (red) and MDA MB231 breast cancer cells (blue) yield lower signals with the same trend. For all cell types, non-zero transfer for the 45 bp DNA is obtained.

Since the obtained data does not show saturation or zero transfer, it is not obvious, if we are in a high force or low force regime compared to the binding force of the receptor ligand complex. Hence, the next approach for a more detailed force measurement is to further increase the reference force to obtain a baseline with minimum fluorescence transfer.

6.3.2. Increasing the reference force - 80% GC content

For a minimum fluorescence transfer, the reference force is further increased. To realize this, a further rise of the DNA length is not reasonable, since very long DNA tends to form loops and bubbles and this decreases the binding force. One

possibility to increase the stability of DNA is to raise the content of the bases guanine and cytosine, which exhibit three hydrogen bonds instead of two hydrogen bonds. In all the other experiments, we used a GC content of approx. 60%. To test the effect of a higher GC content, we conducted measurements with 80% GC content of the DNA and with lengths of 15 bp and 45 bp. Force balances with the two different reference forces and the anti-CD47 antibody are deposited on one stamp with the microplotter. Measurements are conducted on RBCs. For data analysis, the average of six measurements with 80% GC content and three measurements with 60% GC content was evaluated. The graph in Figure 35 shows that the shift to higher reference forces still yields fluorescence transfer for the 45 bp DNA, and also, the statistical spread of data points is still large compared to the difference in the mean values of 15 bp and 45 bp reference DNA.

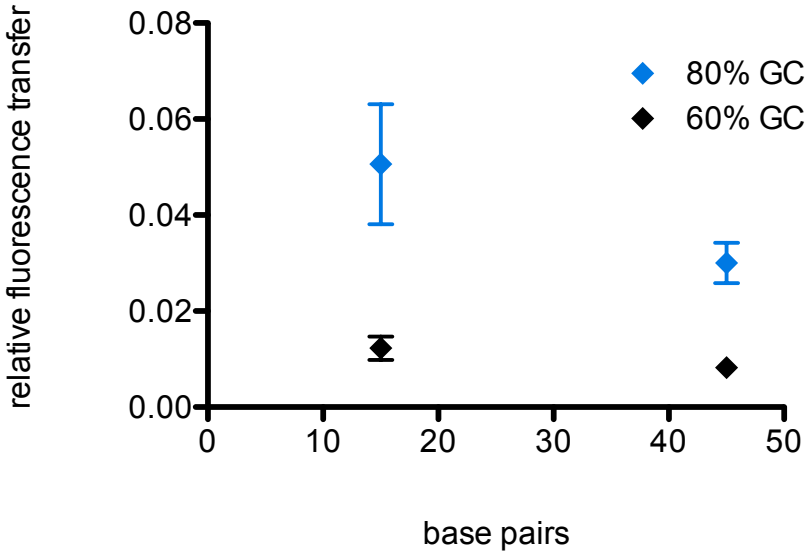

Figure 35 Graph showing measurement with DNA reference containing 80% GC. In the experiment, the interaction of the CD47 receptor and its antibody are analysed with two different DNA reference lengths. The graph represents the mean values of six measurements with 80% GC content and the mean value of three measurements with 60% GC content. Although the 80% GC content of the reference DNA should lead to higher reference forces, we still obtain a non-zero fluorescence transfer for 45 bp reference.

An interpretation of the higher fluorescence transfer in the measurement with 80% GC content is not possible, since the experiments were conducted with different contact forces.

Altogether, the enhancement of the GC content does not yield improved results.

Another possibility to enhance the reference force is the use of stabilizing polyamides or intercalators. But for the experiments on cells this approach was abandoned because of the cytotoxicity of the relevant substances.

6.3.3. Force measurements on RBCs

Subsequently, detailed force measurements are performed decreasing the reference force by using shorter DNA strands. The experiments were conducted with the CD47 antibody and the HPA on RBCs. For the analysis of the CD47 receptor, an elastomer stamp was functionalised with force balances consisting of the CD47 antibody and eight different lengths of DNA double strands (zip, 8, 9, 11,13, 15, 30 and 45 bp) corresponding to different reference forces (Figure 36 A).

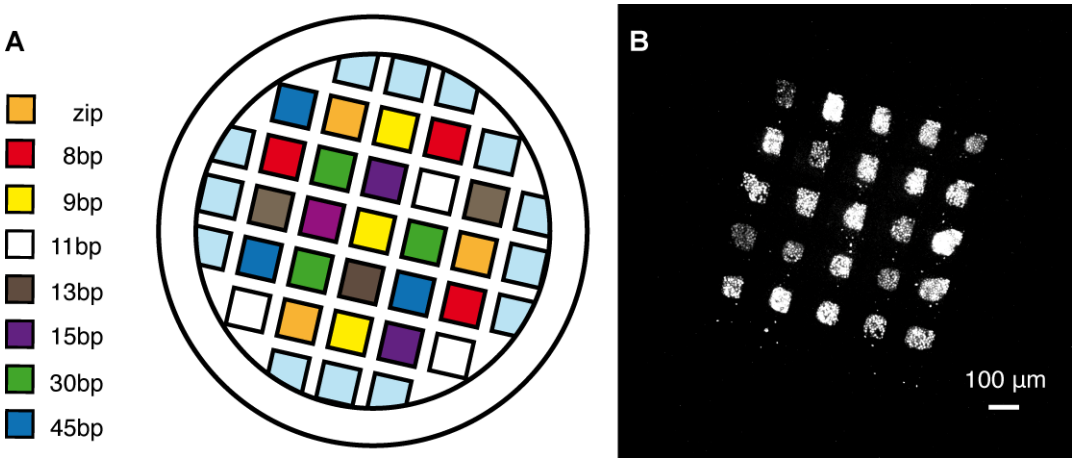

Figure 36 Detailed force analysis of CD47 receptor and its antibody on RBCs. **A** A stamp is functionalised with force balances consisting of the CD47 antibody and DNA duplexes of eight different lengths varying from 8 to 45 bp that correspond to different reference forces increasing with DNA length. The maximum fluorescence transfer is defined by a 20 bp DNA strand that opens base pair by base pair like a zipper and is named zip DNA. It is thermodynamically stable and mirrors the binding force of a single DNA base pair. **B** The fluorescence picture of the cells after contact already depicts higher fluorescence intensities for lower reference forces.

For a maximum transfer, we use a 20bp DNA, called “zip DNA”, that opens one base pair after the other. This offers the advantage of a thermodynamically stable strand that mirrors the rupture force of a single base pair. Zip DNA, therefore, defines the maximum fluorescence transfer. The geometry of the remaining duplexes is designed in a way that the force affects both 5’-ends of the double strand, resulting in a shear force. The fluorescence image of the RBCs after the contact process (Figure 36 B) already reveals that pads with short DNA duplexes (corresponding to low reference forces) lead to more fluorescence transfer onto cells than pads with long DNA as a reference force. The graph obtained by explicit data analysis of three measurements (Figure 36 C) shows the maximum fluorescence transfer for the zip DNA and the short 8 and 9 bp DNA duplexes. This indicates that the binding force between antibody and receptor exceeds the reference force in this regime.

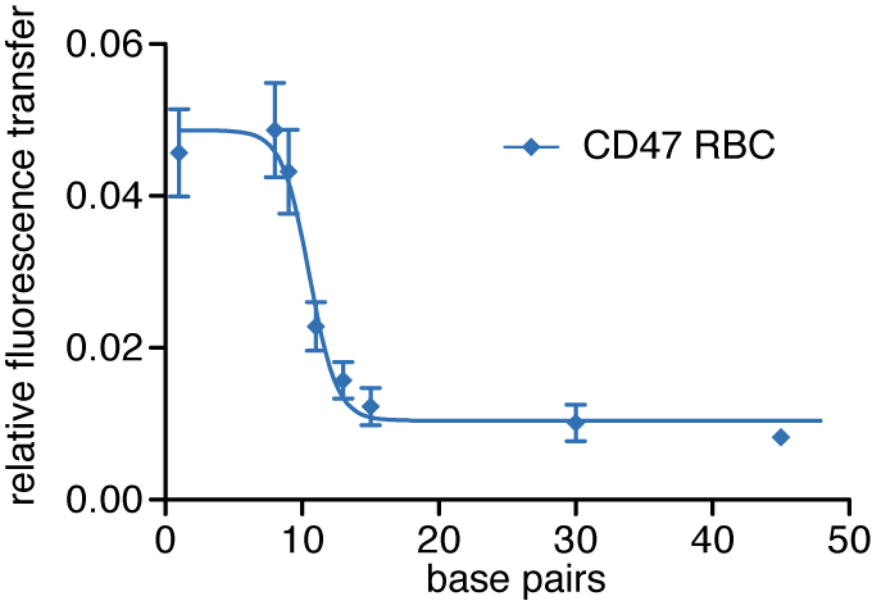

Figure 37 Graph showing detailed force analysis of CD47 receptor on RBCs. The mean fluorescence transfer of three measurements is shown in the graph. For low reference forces (8 and 9 bp duplexes), the maximum transfer is obtained, which is defined by the zip DNA. With increasing DNA length, which represents an increasing reference force, a rapid decrease in fluorescence intensity is observed. When further increasing the DNA length to 45 bp, the intensity stays nearly constant. A Boltzmann sigmoidal fit displays a 50% value of 10.5 ± 0.32 bp DNA.

A further increase in the number of base pairs corresponding to higher reference forces leads to a rapid change in fluorescence intensity. For long strands (30 and 45 bp), the fluorescence intensity hardly decreases indicating that the binding force of the DNA duplex is higher than the force of antibody and receptor. A fit with a Boltzmann sigmoidal function displays a force equivalent of 10.5 ± 0.32 bp DNA duplex for the CD47 antibody and its receptor.

In a similar experiment, a second receptor ligand complex consisting of the glycolipid rest galNAc and its ligand HPA was analysed. Since the affinity of the HPA for galNAc is only in the 10^{-4} M regime [53], a shift to lower forces is expected. For the rupture force analysis, balances with HPA and again eight different DNA lengths (zip, 8, 9, 11, 13, 15, 30, 45 bp) are attached onto different pads of the elastomer stamp (Figure 38 A).

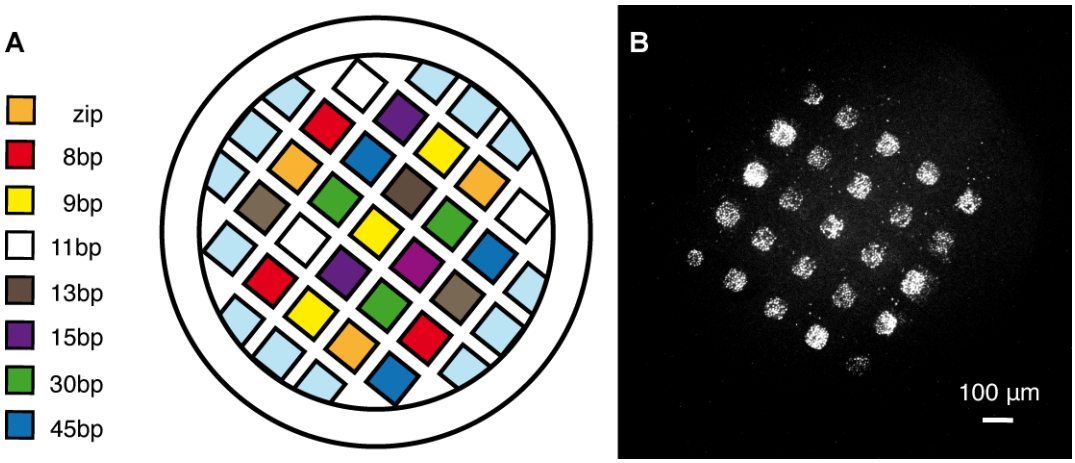

Figure 38 Detailed force measurements of HPA-galNAc interaction on RBCs. **A** For a force analysis of the HPA-galNAc complex, the lectin was deposited on an elastomer stamp together with eight different DNA lengths. **B** The fluorescence picture of the cells after contact shows higher intensities for pads with short DNA duplexes and very low intensities for long DNA.

The fluorescence transfer onto the cells is depicted in Figure 38 B. Again, pads with short DNA duplexes lead to high intensities on the cells, whereas pads with long DNA duplexes transfer little fluorescence to the cells. A detailed data analysis of four different measurements (Figure 39) shows that the maximum fluorescence transfer is only obtained with the zip and 8bp duplex DNA.

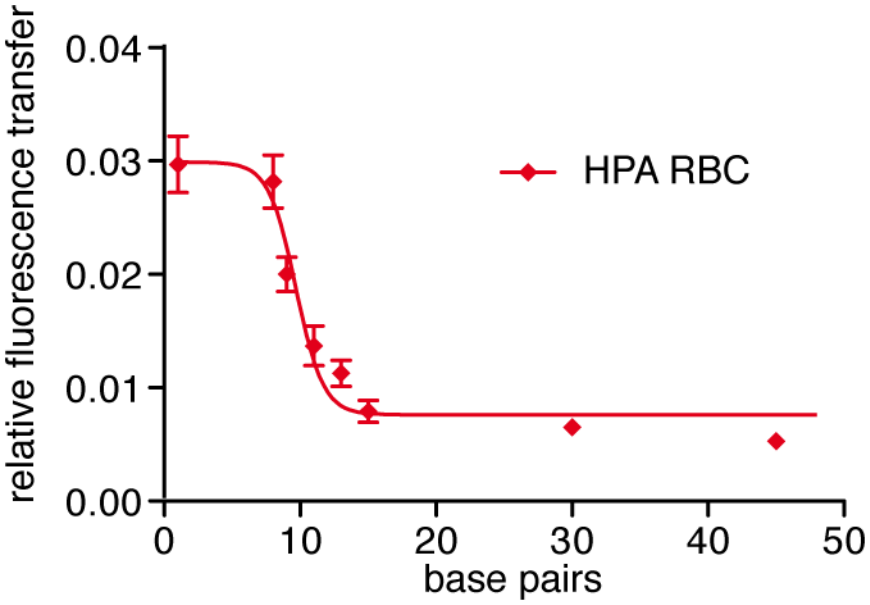

Figure 39 Graph showing detailed force measurements of HPA-galNAc interaction on RBCs. The mean fluorescence transfer of four measurements displays a maximum transfer only for duplexes of 8 bp. An increase in DNA length corresponds to higher reference forces and leads to a transition. For high reference forces exerted by 30 and 45 bp DNA duplexes, the change in intensity is minimal. The 50% value of the Boltzmann sigmoidal fit is 9.7 ± 0.46 bp DNA.

Increasing the reference force leads to a transition towards lower fluorescence transfer. Longer duplexes (15, 30 and 45 bp) produce a minimum in fluorescence transfer. A Boltzmann sigmoidal fit yields a force equivalent of 9.7 ± 0.46 bp DNA for the HPA bound to galNAc. Compared to the force analysis of the CD47 antibody and its receptor, the expected shift to lower forces for the low-affinity ligand HPA is observed. Granbois et al. obtained rupture forces for the galNAc-HPA complex of about 35 pN at a retraction velocity of 6 μm/s [81]. Considering the data Strunz et al. [38] gained from AFM measurements with DNA duplexes, a most probable rupture force of 35 pN at this retraction velocity would be due to a DNA duplex shorter 10 bp. Thus, compared to literature, the force equivalent for HPA is a reasonable value.

6.3.4. Force measurements on M21 cells

The following experiments show that the force analysis with the MFA can be applied on various kinds of cultured living cells and is not restricted to RBCs; force measurements with the CD47 antibody were also conducted on M21 melanoma cells. Again, the stamp was functionalised with the DNA duplexes ranging from zip to 45bp (Figure 40 A).

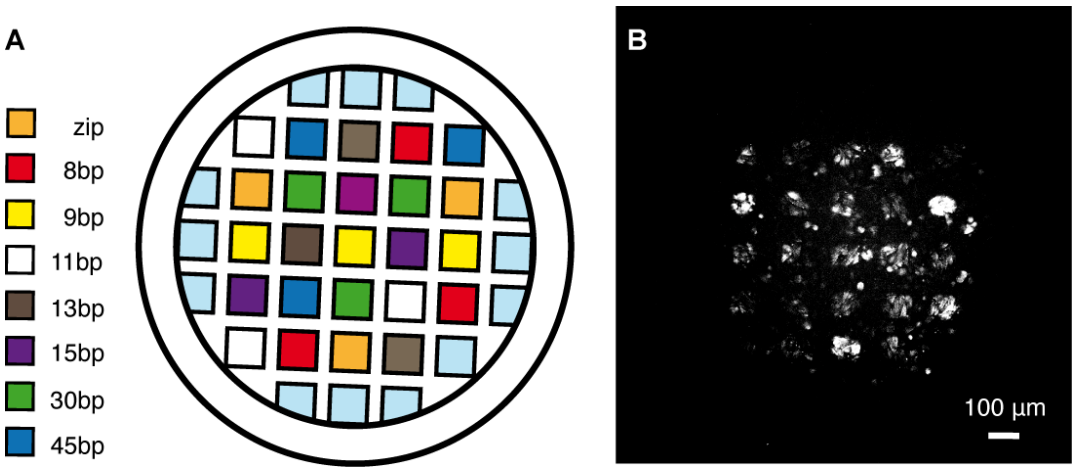

Figure 40 Detailed force measurements of the CD47 receptor on M21 melanoma cells. A The elastomer stamp is functionalised with the CD47 antibody and DNA duplexes of eight different lengths as reference. **B** The fluorescence picture of the cells after contact clearly depicts the maximum fluorescence transfer defined by the zip DNA, and the transfer for 8 bp duplexes is notably higher than for longer reference duplexes.

The picture of the fluorescence transfer on the cells exhibits brighter regions for the zip DNA and short DNA duplexes (Figure 40 B). Explicit data analysis of two measurements reveals two states and a gradient (Figure 41).

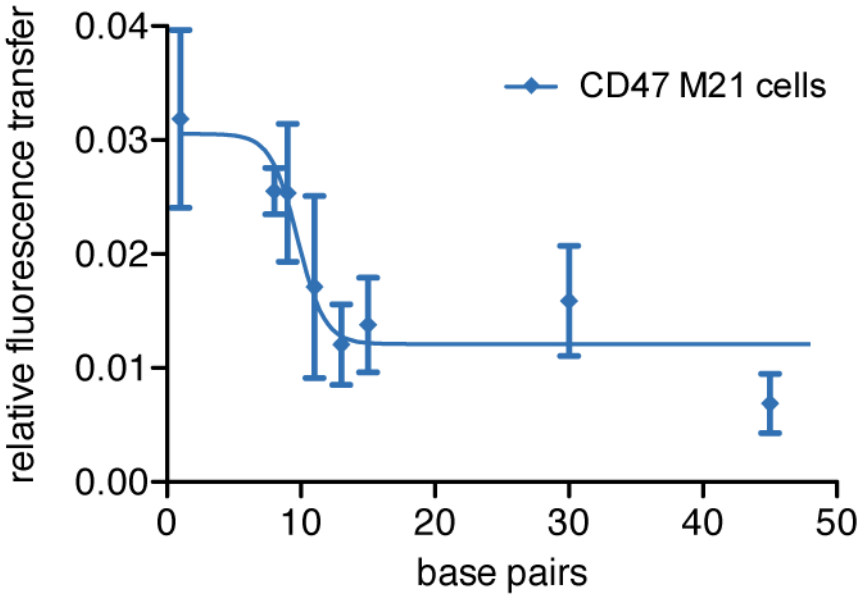

Figure 41 Graph showing force analysis of CD47 receptor on M21 cells. The graph shows the mean fluorescence transfer of two measurements. Again, two states can be distinguished: a maximum and a minimum fluorescence transfer. For the transition, the Boltzmann sigmoidal fit yields a 50% value of 9.8 ± 0.81 bp DNA. Compared to the analysis of the CD47 receptor on RBCs, the binding force for this receptor on M21 cells is shifted to a shorter DNA duplex that corresponds to a lower binding force.

For the force equivalent of the CD47 receptor and its antibody on M21 cells, the Boltzmann fit yields a value of 9.8 ± 0.81 bp DNA. Comparing this to the force equivalent for the CD47 receptor on RBCs, a slightly lower value is found for the M21 melanoma cells. This shift might be generated by variations in the receptor expression that influences the affinity in different cells. Additionally, the signal-to-noise ratio decreases compared to the measurements on RBCs. This might be due to variations in the cell height and a less uniform distribution on the cover slip. Moreover, a lower fluorescence transfer is observed for the M21 cells, which might be caused by a lower receptor density on these cells. However, the obtained signal-to-noise ratio allows for a reliable force measurement conducted directly on living cells.

6.4. Discussion of unspecific fluorescence transfer

To quantify the unspecific fluorescence transfer, the HPA – galNAc interaction is tested on red blood cells of group A and O with DNA reference lengths of 9bp, 15bp, 30bp and 45bp. In the fluorescence images of the cells after contact, a fluorescence transfer onto the cells is observed for blood group A (Figure 42 A) while for blood group O (Figure 42 B) no fluorescence transfer occurs.

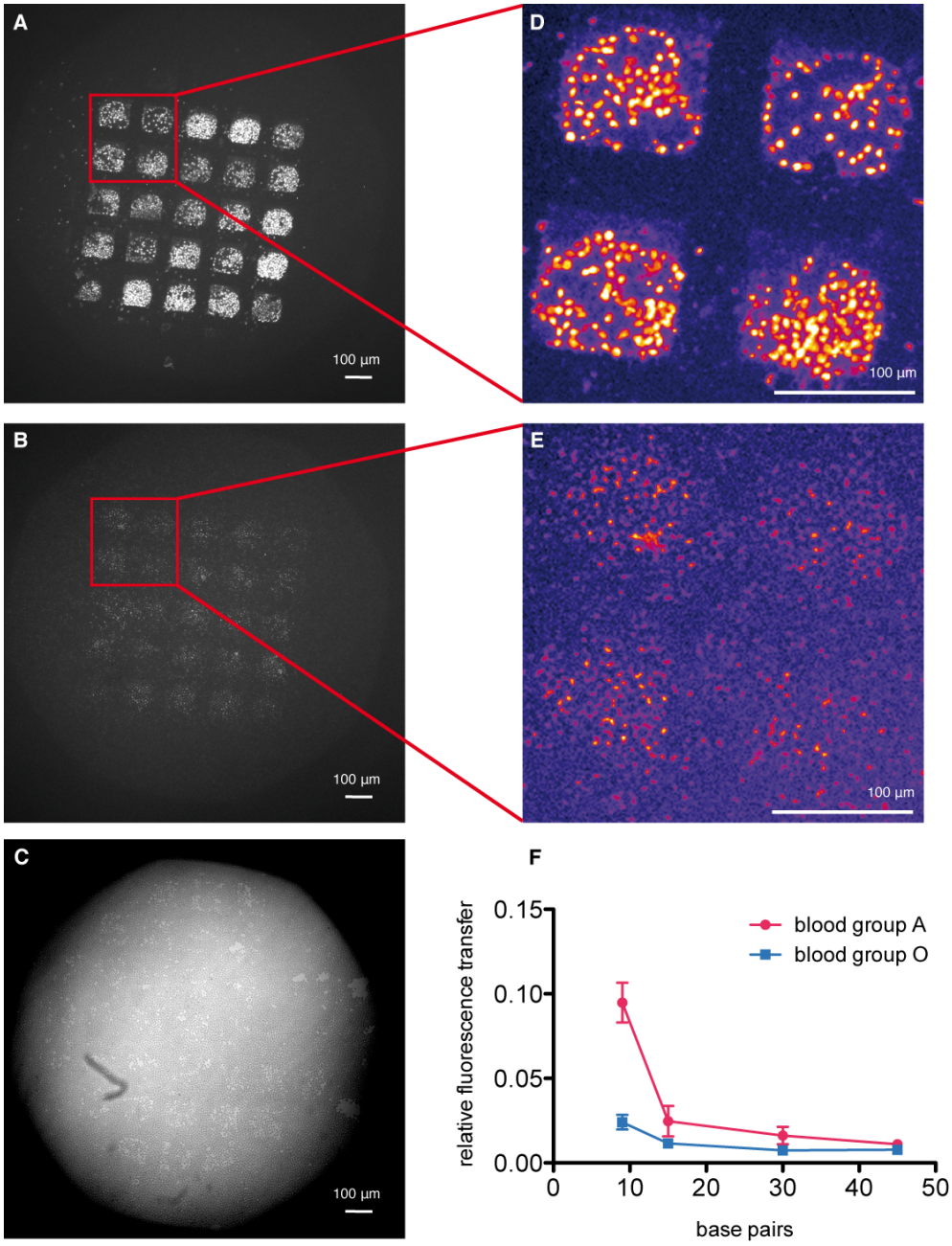

Figure 42 Unspecific fluorescence transfer for the HPA-galNAc interaction. A The fluorescence image of RBCs of blood group A after contact shows a fluorescence transfer on the cells for all DNA reference lengths (9 bp, 15 bp, 30 bp and 45 bp). **B** With the same stamp, no fluorescence transfer is obtained on cells of blood group O. **C** In the transmitted light image of blood group O after contact cells appear lighter in some areas, because several cells are burst. This is due to the rather high contact pressure. **D** Zoomed-in false colour image of blood group A shows fluorescence transfer onto the cells. **E** For blood group O, the zoomed-in false colour image reveals no fluorescence transfer onto the cells, but only onto the glass surface. **F** Data analysis shows a slight increase in unspecific transfer for the 9 bp DNA reference. Still, the specific fluorescence transfer is significantly higher.

The transmitted light image of the cells of blood group O after contact (Figure 42 C) indicates a rather high contact pressure, since in contact areas several cells are burst. This ensures that the non-fluorescent cells of blood group A are no result of weak contact. A zoomed view of the fluorescence images using false colour implies that for blood group A the fluorescence is transferred to the cell surface (Figure 42 D), while for blood group O the unspecific transfer occurs mainly onto the glass surface (Figure 42 E).

A quantitative analysis (Figure 42 F) of this experiment shows that for the short DNA with 9bp the unspecific fluorescence transfer is slightly increased. Due to the high contact force in the experiments aiming at the unspecific interactions, the resulting absolute values for the fluorescence transfer are approximately 4-5x higher than the values obtained in the conventional force measurements. Hence, although the pressure force dependency renders a correction of the measurements with a second independent background measurement difficult, above experiment shows that the unspecific fluorescence transfer only leads to a minor correction of the fluorescence transfer.

When comparing the specific fluorescence transfer with the unspecific fluorescence transfer, a transfer signal is observed for DNA reference lengths up to 30bp although the expected interaction strength is around 10bp. This is, because the DNA duplexes do not have sharp rupture forces, but DNA rupture is a highly statistical process leading to a rupture force distribution with a distinct width. Hence, also for a 30bp reference, the probability of rupture forces below the mean rupture force of a 10bp duplex is non-zero.

7. Conclusion and Outlook

The experiments presented in this thesis show that the MFA on cells offers the perspective of a high throughput screening for receptor profiles on living cells and thus, to gain information about the condition of cells under physiological conditions. On RBCs, the interaction of two different ligands, the CD47 antibody and the blood group specific lectin HPA, with their according receptors are detected. In experiments with two different blood groups, one missing the target for HPA, it is proved that unspecific interactions can be eliminated to a large extent using DNA as a reference force. Despite this force threshold, experiments delivering the CD47 antibody to the according receptor imply that the method still allows distinguishing between healthy red blood cells and deficient cells with low expression levels of the CD47 receptor. Such comparison of different cells is until now only possible for RBCs, since similar contact pressure leads to similar levels of burst cells with lower contrast after the contact process. Nonetheless, a control of the contact force is necessary for a better comparison of different cell types. To improve the control of the contact process, elastomer stamps with a different microstructure might be helpful that additionally exhibit elevated spacers in certain intervals. Still, several parameters like height, width and the distance of these spacers have to be tested. Since such wavers are produced in an elaborate photolithographic process, it is expensive and time-consuming to test several wavers, and within the scope of this work it was refrained from such an approach.

In detailed comparative force experiments on red blood cells, it is demonstrated that the MFA on cells enables a quantitative analysis of the binding behaviour of receptor-ligand interactions. For the galNAc-HPA interaction and the interaction of the CD47 receptor and its antibody, a DNA force equivalent was determined. Additionally, the CD47 interaction was studied on M21 melanoma cells implying that the MFA on cells is applicable also on cultured living cells.

Thus, regarding medical research, it is possible to compare various possible ligands with respect to their binding strength to a certain receptor, and furthermore, signalling pathways might be influenced having a positive effect on the healing of diseases.

For future experiments, the activation and subsequent visualization of such signalling pathways is supposable. In this context, mechanosensitive receptors are an interesting subject to study the force threshold that is necessary to activate signalling. Another interesting question is, in how far adhesion molecules that are offered to the cells, e.g. by a coated glass slide, could influence the binding characteristics of signalling receptors in other parts of the cell.

Altogether, the presented force assay allows for a wide range of applications reaching from the screening of receptors on live-cell surfaces with high specificity to the force analysis of receptor-ligand interactions. In the experiments, single molecules are used as force sensors, and, at the same time, many of such force sensors are tested simultaneously yielding good statistics in only one measurement. Moreover, the MFA on cells is a physiological method that still allows for a high throughput. These qualities make the MFA on cells a highly interesting assay for basic research as well as for drug design.

8. Supplementary Material

8.1. Approach for the improvement of the signal to noise ratio

In experiments with cultured cell lines, the signal to noise ratio is quite low and improvements avoiding background fluorescence are desirable. One approach is to use total internal reflection fluorescence microscopy (TIRFM). For TIRFM, the excitation light is totally reflected at the glass water interface producing an evanescent wave that decays exponentially within a few micrometers. This evanescent wave selectively excites a small volume of the medium with lower refraction, which is the solution side, and thus, is suitable to observe the cell surface excluding background fluorescence [82]. To apply TIRFM in MFA experiments, the setup must be inverted such that the cells grow on the elastomer surface and the force balances are deposited on the glass surface. This way, the fluorophores at the cell surface are excited directly by the evanescent wave. To test the cell growth on the elastomer surface, two stamps, one without and one with microstructure, are coated with collagen. Previously, they are cleaned in an isopropanol water mixture in ultrasonic for 10 min and then autoclaved. A 1:1 collagen water mixture was applied on the stamps for 30 min at 37 °C. Excess collagen was rinsed with water. Additionally, before autoclaving, one stamp was kept in HCL over night and subsequently, passivated with BSA to make the surface more hydrophilic. The experiments with the inverted setup show certain restrictions. On all stamps, the cells grow slowly on the elastomer surface and round up not feeling comfortable (Figure 43, A and B).

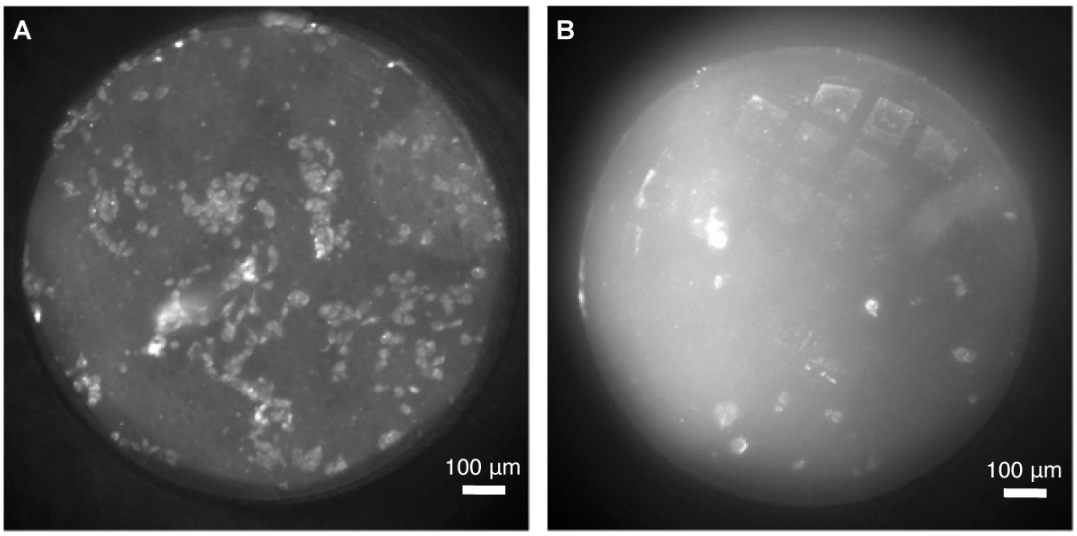

Figure 43 Experiments with inverted setup. A Fluorescence image of cells after contact. Cells are grown on an elastomer surface without microstructure and are stamped onto a functionalised glass surface. As shown in the image, the cells round up, which is a sign of stress. **B** Cells grown on micro-structured elastomer stamp.

Concerning the contact process, the parallel alignment is more complicated, since the light is scattered at the cells on the elastomer surface and interferences are hard to observe. Additionally, fluorescence pictures are not as nice as in other MFA experiments. In conclusion, TIRFM experiments combined with the MFA on cells are tough to realize, and the problems with cell growth on the elastomer surface and the alignment process outweigh possible advantages.

8.2. Velocity dependence

The influence of the retraction velocity is estimated with experiments detecting the CD47 receptor on RBCs. For the measurements, the whole stamps are functionalised with the CD47 antibody and DNA of 20bp or 30bp length, respectively. DNA and biotinylated antibody are linked via NeutrAvidin. The functionalised stamp is brought into contact with the RBCs and retracted with a velocity of 50 nm/s or 5000 nm/s, respectively. The graph in Figure 44 shows the results of the data analysis.

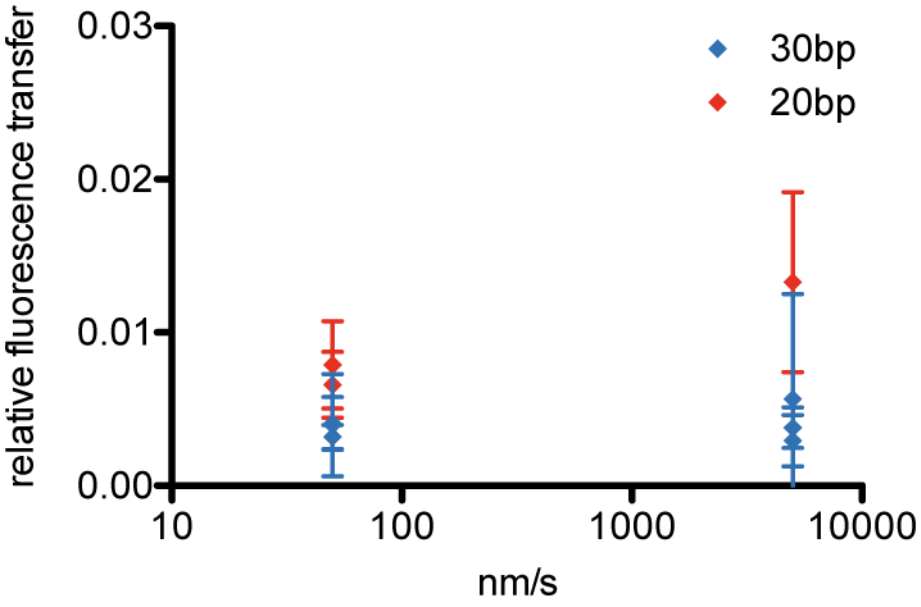

Figure 44 Retraction velocity dependence of fluorescence transfer. For the experiment, an elastomer stamp is functionalised with a 20 bp or 30 bp reference DNA, respectively and the antibody against CD47. Experiments are conducted with retraction velocities of 50 nm/s and 5000 nm/s. For the 30 bp reference, only a slight increase in fluorescence transfer is observed for fast retraction, whereas the 20 bp DNA yields a more obvious increase.

With a reference DNA of 20 bp length, more fluorescence transfer is obtained for a higher retraction velocity. The 30 bp reference strand yields no velocity dependence of the fluorescence transfer. Still, since the contact process is not standardized, but is manually controlled, a comparison of single different measurements is questionable.

8.3. Pressure control – Beads

For a reliable measurement of the velocity dependence, an improved control of the contact pressure is desirable. One approach is to use microscopic beads with a cell's size as spacer. Two different sizes are tested, one mixture with beads in the range of 2-15 µm and a uniform size of 10 µm. For the experiment, the CD47 receptor – antibody interaction is detected on RBCs. In one experiment, beads are attached using 1 µl of 1:100 diluted amino-coated beads mixed with amino-DNA and borate buffer. The mixture is incubated on the stamp surface functionalised

with epoxide groups overnight in salt atmosphere. Unfortunately, beads do not sick to the stamp surface. Repeating the experiment with a 1:10 dilution of beads and rinsing with caution, yields no improvement (Figure 45 A).

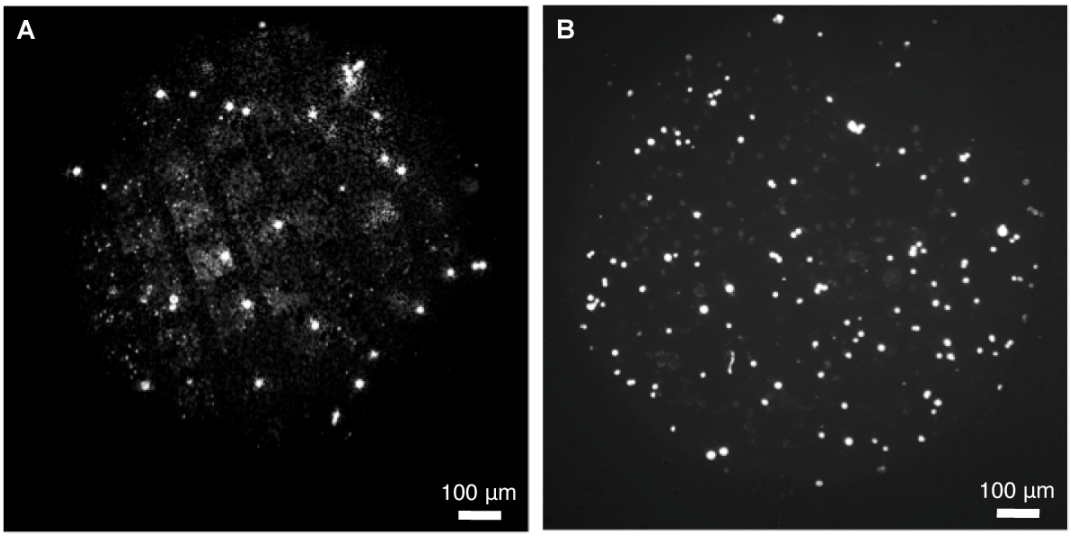

Figure 45 Control of the contact force with beads. A Beads in a mixture of 2-15 µm functionalised with amine groups are attached covalently to epoxide groups on the elastomer surface. During the experiment, beads did not stick to the surface and, as revealed by the image, did not promote an even fluorescence transfer. Moreover, the beads are brightly fluorescent disturbing the measurement. **B** Beads of 10 µm are added to the cells, but float away before contact is made.

In another experiment, beads are added to the cells (Figure 45 B). But upon contact, the beads float around just disturbing the contact process. Bigger beads are pressed hard to the stamp surface deforming the microstructure.

Moreover, the bright fluorescence even more decreases the signal to noise ratio and interferes with the data analysis. Therefore, the approach is unsuitable for a control of the contact pressure.

8.4. Introducing Dry Chemistry & Microplotter

The described microplotter offers a broad field of applications and allows for directed delivery of solutions to the pads representing the mircrostructure of the elastomer stamps. But dispensing liquid volumes in the picolitre range, also entails certain problems. Such small volumes evaporate very quickly, which is a problem

when not only DNA, but also other biomolecules, like proteins, are dispensed. They denaturize under these conditions and hence, precipitate losing their function. To prevent this, a humidity tent encloses the whole plotter such that with an air humidifier a constant humidity of 70 % is ensured. Unfortunately, at high humidity, the electronics does not work reliably, but repeatedly leads to crashes of the whole system. The above-mentioned dry-chemistry approach is a feasible alternative. The sugar trehalose replaces the hydrogen bond of water during evaporation keeping the proteins stable. Still, when using biotinylated antibodies instead of the Lightning Link kit to directly attach the StreptAvidin to the antibody, precipitation occurs frequently (Figure 46 A).

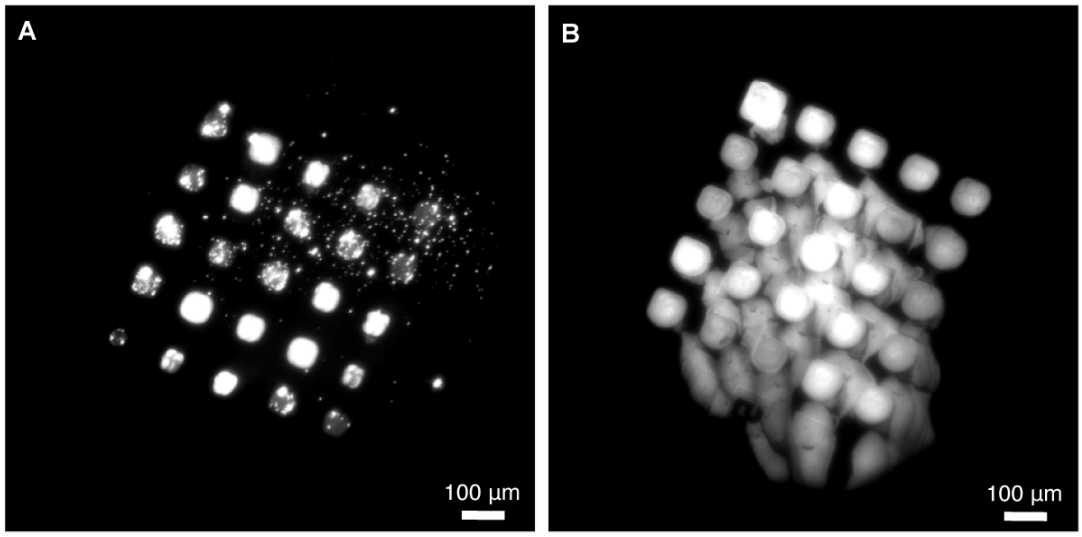

Figure 46 Problems associated with the microplotting process. A Fluorescence image of a stamp functionalised with the microplotter. Bright precipitation occurs frequently if biotinylated ligands are used. Directly attaching the antibody to StreptAvidin with a kit yields better results. **B** Image of a stamp rinsed with 1x PBS after microplotting. The pattern is blurred and differently functionalised pads mix up.

The precipitation also with trehalose might be due to the fact that because of the small capillary and the high viscosity of the solution it was not possible to apply the recommended concentration of trehalose, which is 250 mM [69]. Instead, only 30 mM trehalose was used. Conversely, additional stabilizing molecules in the kit

might cause the absence of precipitation using the Lightning Link kit. Since the precipitation is avoided with the kit, this approach was preferred.

Another problem occurs after the dispensing process. Rinsing the stamps in 1xPBS buffer only leads to blurring of the dispensed pattern. Different solutions even run into each other and make the stamp unusable. This happens, because the whole stamp surface is chemically functionalised with DNA previously to the dispensing process. Spots of complementary DNA and antibody are exclusively on the pads. But dipping the stamps in PBS, which has the same surface tension like water, the excess DNA is swirled and immediately hybridizes to neighbouring fields before it can be rinsed away (Figure 46 B).

To circumvent this, different approaches were tested. Tween and SDS were used at different concentrations to decrease the surface tension. But still, suction leaded to blurring of the pattern. Finally, a single drop of 1xPBS with 0.01 % Tween is pipetted on the stamp before dipping it into the 1xPBS buffer. This way, excess DNA is dissolved and diluted in the drop without suction and the subsequent washing steps did not blur the pattern.

9. References

1. Campbell NA, J. B. Reece. 2003. Biologie. *Spektrum Akademischer Verlag GmbH, Heidelberg, Berlin* 6 Ed, pp 85-87

2. Campbell NA, J. B. Reece. 2003. Biologie. *Spektrum Akademischer Verlag GmbH, Heidelberg, Berlin* 6 Ed, pp 163-170

3. Smok, R. G. and L. M. Gierasch. 2009. Sending signals dynamically. *Science* **324,** 198-203

4. Cavallaro, U. and G. Christofori. 2004. Cell adhesion and signaling by cadherins and Ig-CAMs in cancer. *Nat. Rev. Cancer* **4,** 118-132

5. Parsons, J.T., A. R. Horwitz, and M. A. Schwartz. 2010. Cell adhesion: integrating cytoskeletal dynamics and cellular tension. *Nat. Rev. Mol. Cell Bio.* **11,** 633-643

6. Papusheva, E. and C.-P. Heisenberg. 2010. Spatial organization of adhesion: force-dependent regulation and function in tissue morphogenesis. *EMBO J.* **29,** 2753-2768

7. Simpson, R. J. and D. S. Dorow. 2001. Cancer proteomics: from signaling networks to tumor markers. *Trends Biotechnol.* **19,** 40-48

8. Puchner, E. M. and H. E. Gaub. 2012. Single-molecule mechanoenzymatics. *Annu. Rev. Biophys.* **4,** 497-518

9. Evans, E. A. and D. A. Calderwood. 2007. Forces and bond dynamics in cell adhesion. *Science* **316,** 1148-1153

10. Vogel, V. and M. P. Sheetz. 2009. Cell fate regulation by coupling mechanical cycles to biochemical signaling pathways. *Curr. Opin. Cell Biol.* **21,** 38-46

11. Schwartz, M. A. and D. W. DeSimone. 2008. Cell adhesion receptors in mechanotransduction. *Curr. Opin. Cell Biol.* **20,** 1-6

12. Katz, B.-Z. et al. 2000. Physical state of the extracellular matrix regulates the structure and molecular composition of cell-matrix adhesions. *Mol. Biol. Cell* **11,** 1047-1060

13. Janmey, P. A. and C. A. McCulloch. 2007. Cell Responses to mechanical stimuli. *Annu. Rev. Biomed. Eng.* **9,** 1-34

14. Bershadsky, A., M. Kozlov and B. Geiger. 2006. Adhesion-mediated mechanosensitivity: a time to experiment and a time to theorize. *Curr. Opin. Cell Biol.* **18,** 472-481

15. Alenghat F. J. and D. E. Ingber. 2002. Mechanotransduction: All signals point to cytoskeleton, matrix, and integrins. *Sci. STKE.* **119,** 1-4

16. Puchner, E. M. and H. E. Gaub. 2010. Exploring the conformation-regulated function of titin kinase by mechanical pump and probe experiments with single molecules. *Angew. Chem. Int. Ed.* **49,** 1147-1150

17. Puchner, E. M. et al. 2008. Mechanoenzymatics of titin kinase. *P. Natl. Acad. Sci. USA.* **105,** 13385-13390

18. Zhu, H. and M. Snyder. 2001. Protein arrays and microarrays. *Curr. Opin. Chem. Biol.* **5,** 40-45

19. Chen, H. et al. 2009. Protein chips and nanomaterials for application in tumor marker immunoassays. *Biosens. Bioelectron.* **24,** 3399-3411

20. Zhu, H. and M. Snyder. 2003. Protein chip technology. *Curr. Opin. Chem. Biol.* **7,** 55-63

21. Cunningham F. and C. M. Deber. 2006. Optimizing synthesis and expression of transmembrane peptides and proteins. *Methods (San Diego, CA, U. S.)* **41,** 370-380

22. Bendall, S.C. et al. 2011. Single-cell mass cytometry of differential immune and drug responses across a human hematopoietic continuum. *Science* **332,** 687-696

23. Helenius, J., C.-P. Heisenberg, H. E. Gaub and D. J. Müller. 2008. Single-cell force spectroscopy. *J. Cell Sci*. **121,** 1785-1791

24. Medalsy, I., U. Hensen and D.J. Müller. 2011. Quantifying chemical and physical properties of native membrane proteins at molecular resolution by force-volume AFM. *Angew. Chem. Int. Edit.* **50,** 12103-12108

25. Dufrene, Y. F. and D.J. Müller. 2001.Force nanoscopy of living cells. *Curr. Biol.* **21,** 212-216

26. Friedrichs, J., J. Helenius and D.J. Müller. 2010. Quantifying cellular adhesion to extracellular matrix components by single-cell force spectroscopy. *Nat. Proto.* **10,** 1353-1361

27. Schmitz, J. and K. E. Gottschalk. 2008. Mechanical regulation of cell adhesion. *Soft Matter* **4,** 1373-1387

28. Albrecht, C. et al. 2003. DNA: A programmable force sensor. *Science* **301,** 367-370

29. Albrecht, C.H., H. Clausen-Schaumann and H. E. Gaub. 2006. Differential analysis of biomolecular rupture forces. *J. Phys.: Condens. Matter.* **18,** 581-599

30. Severin, P. M. D. and H. E. Gaub. 2012. DNA-Protein binding force chip. *Small* **8,** 3269-3273

31. Dose, C., D. Ho, H. E. Gaub, P. B. Dervan and C. H. Albrecht. 2007. Recognition of "Mirror-Image" DNA by small molecules. *Angew. Chem. Int. Ed.* **46,** 8384-8387

32. Severin, P. M. D., D. Ho, and H. E. Gaub. 2011. A high throughput molecular force assay for protein–DNA interactions. *Lab Chip* **11,** 856-862

33. Ho, D., K. Falter , P. M. D. Severin and H. E. Gaub. 2009. DNA as a force sensor in an aptamer-based biochip for ATP. *Anal. Chem.* **81,** 3159–3164

34. Limmer, K., D. Aschenbrenner and H. E. Gaub. 2013. Sequence-specific inhibition of Dicer measured with a force-based microarray for RNA ligands. *Nucleic Acids Res.* 1-9

35. Blank, K. et al. 2003. A force-based protein biochip. *Proc. Natl. Acad. Sci. USA.* **100,** 11356-11360

36. Evans E, K. Ritchie. 1999. Strength of a weak bond connecting flexible polymer chains. *Biophys. J.* **76,** 2439-2447

37. Bell GI 1978. Models for the specific adhesion of cells to cells. *Science* **200,** 618-627.

38. Strunz, T., K. Oroszlan, R. Schäfer and H.-J. Güntherodt. 1999. Dynamic force spectroscopy of single DNA molecules. *Proc. Natl. Acad. Sci. USA.* **96,** 11277-11282

39. Adapted from: Campbell NA, J. B. Reece. 2003. Biologie. *Spektrum Akademischer Verlag GmbH, Heidelberg, Berlin* 6 Ed, pp 343

40. Campbell NA, J. B. Reece. 2003. Biologie. *Spektrum Akademischer Verlag GmbH, Heidelberg, Berlin* 6 Ed, pp 342-345

41. Wang, X., T. Ha. 2013. Defining Single Molecular Forces Required to Activate Integrin and Notch Signaling *Science* 340, 991-994

42. Adapted from: Strunz, T., K. Oroszlan, R. Schäfer and H.-J. Güntherodt. 1999. Dynamic force spectroscopy of single DNA molecules. *Proc. Natl. Acad. Sci. USA*. **96,** 11277-11282

43. Adapted from: Livnah, O. et al. 1993. Three-dimensional structures of avidin and the avidin-biotin complex. *Proc. Natl. Acad. Sci. USA*. **90,** 5076-5080

44. Green, N. M. 1963. The nature of the biotin-binding site. *Biochem. J.* **89,** 599-609

45. Data sheet Piercenet "NeutAvidin protein and conjugates", Thermo Fisher Scientific Inc., Rockford, IL.
http://www.piercenet.com/product/neutravidin-protein-conjugates

46. Freitag, S. et al. 1997. Structural studies of the streptavidin binding loop. *Protein Sci.* **6,** 1157-1166

47. Campbell NA, J. B. Reece. 2003. Biologie. *Spektrum Akademischer Verlag GmbH, Heidelberg, Berlin* 6 Ed, pp 133-135

48. Campbell NA, J. B. Reece. 2003. Biologie. *Spektrum Akademischer Verlag GmbH, Heidelberg, Berlin* 6 Ed, pp 129-133

49. Lehninger, Nelson, Cox. 1994. Prinzipien der Biochemie. *Spektrum Akademischer Verlag GmbH, Heidelberg, Berlin, Oxford* pp 311-326

50. Campbell NA, J. B. Reece. 2003. Biologie. *Spektrum Akademischer Verlag GmbH, Heidelberg, Berlin* 6 Ed, pp 166

51. Adapted from Lehninger, Nelson, Cox. 1994. Prinzipien der Biochemie. *Spektrum Akademischer Verlag GmbH, Heidelberg, Berlin, Oxford* pp 315

52. Klinke,R, H.-C. Pape, s. Silbernagl. 2003. Physiologie. *Georg Thieme Verlag KG, Stuttgart), 4 Ed*, pp 229-232

53. Sanchez J.-F. et al. 2006. Biochemical and structural analysis of Helix pomatia agglutinin. *J. Biol. Chem.* **281,** 20171-20180

54. Torres B. V. and D. F. Smith. 1988. Purification of Forssman and human blood group A glycolipids by affinity chromatography on immobilized Helix pomatia lectin. *Anal. Biochem.* **170,** 209–219

55. Adapted from Sanchez J.-F. et al. 2006. Biochemical and structural analysis of Helix pomatia agglutinin. *J. Biol. Chem.* **281,** 20171-20180

56. Mouro-Chanteloup I et al. 2003. Evidence that red cell skeleton protein 4.2 interacts with the Rh membrane complex member CD47. *Blood* **101(1)**, 338-344

57. Brown, E. J. and W. A. Frazier. 2001. Integrin-associated protein (CD47) and ist ligands. *Trends Cell Biol.* **11,** 130-135

58. Adapted from Brown, E. J. and W. A. Frazier. 2001. Integrin-associated protein (CD47) and ist ligands. *Trends Cell Biol.* **11,** 130-135

59. Liu Y et al. 2001. The role of CD47 in neutrophil transmigration. *J. Biol Chem.* **276(43),** 40156-40166.

60. Dahl, K. N., C. M. Westhoff and D.E. Discher. 2003. Fractional attachment of CD47 (IAP) to the erythrocyte cytoskeleton and visual colocalization with Rh protein complexes. *Blood*. **101,** 1194-1199

61. Oldenborg, P. A. et al. 2000. Role of CD47 as a Marker of Self on Red Blood Cells. *Science* **288,** 2051-2054

62. Campbell NA, J. B. Reece. 2003. Biologie. *Spektrum Akademischer Verlag GmbH, Heidelberg, Berlin* 6 Ed, pp 1095-1096

63. Adapted from Klinke, R, H.-C. Pape, s. Silbernagl. 2003. Physiologie. *Georg Thieme Verlag KG, Stuttgart), 4 Ed*, pp 240

64. Adapted from Campbell NA, J. B. Reece. 2003. Biologie. *Spektrum Akademischer Verlag GmbH, Heidelberg, Berlin* 6 Ed, pp 1095

65. Adapted from Lehninger, Nelson, Cox. 1994. Prinzipien der Biochemie. *Spektrum Akademischer Verlag GmbH, Heidelberg, Berlin, Oxford* pp 209

66. Adapted from Klinke, R, H.-C. Pape, s. Silbernagl. 2003. Physiologie. *Georg Thieme Verlag KG, Stuttgart), 4 Ed*, pp 230

67. Xia, Y. and G. M. Whitesides. 1998. Soft lithography. *Annu. Rev. Mater. Sci*. **28,** 153-184

68. Crowe, J. H. et al. 1987. Stabilization of dry phospholipid bilayers and proteins by sugars. *Biochem. J.* **242,** 1-10

69. Dráber, P., E. Dráberová, Martina Nováková. 1994. Stability of monoclonal IgM antibodies freeze-dried in the presence of trehalose. *J. Immunol. Methods* **181,** 37-43

70. Allison, S.D. et al. 1999. Hydrogen Bonding between Sugar and Protein Is Responsible for Inhibition of Dehydration-Induced Protein Unfolding. *Arch. Biochem. Biophys.* **365,** 289-298

71. Adapted from http://www.bio-ope.com/doc/CyDye.asp

72. Adapted from Sonoplot, Inc. 2010. GIX^{TM} MICROPLOTTER^{TM} II Manual. pp 4

73. Sonoplot, Inc. 2010. GIX^{TM} MICROPLOTTER^{TM} II Manual. pp 3-5

74. Larson, B. 2005. New technologies for fabricating biological microarrays. *Dissertation at the University of Wisconsin, Madison* pp 37-46

75. Rädler, J., E. Sackmann 1993. Imaging optical thicknesses and separation distances of phospholipid vesicles on solid surfaces. *J. Phys. II France* **3,** 227-248

76. Morfill, J. L., 2005. Hochauflösende Einzelmolekülkraftspektroskopie von doppelsträngiger DNA. *Diplomarbeit an der Ludwig-Maximilians-Universität München* pp 67-71

77. De Gennes, P. G. 2001. Force and kinetic barriers to unzipping of the DNA double helix. *C. R. Acad. Sci., Ser. IV Phys. Astrophys. 2*, 1505

78. Oldenborg P.-A. 2004. Role of CD47 in erythroid cells and in autoimmunity. *Leucemia Lymphoma* **45,** 1319-1327

79. Arlt, F., U. Stein 2009. Colon cancer metastasis: MACC1 and Met as metastatic pacemakers. *Int. J. Biochem. Cell B.* **41,** 2356-2359

80. Batlle, E. et al. 2000. The transcription factor Snail is a repressor of *E-cadherin* gene expression in epithelial tumour cells. *Nat. Cell Biol.* **2,** 84-89

81. Grandbois, M., W. Dettmann, M. Benoit and H. E. Gaub. 2000. Affinity imaging of red blood cells using an atomic force microscope. *J. Histochem. Chemochem.* **48,** 719-724

82. Axelrod, D. 1981. Cell-substrate contacts illuminated by total internal reflection fluorescence. *J. Cell Biol.* **89,** 141-145

10. List of figures

11. Publications

P1:

U. Wienken and Gaub, H. E. Stamping vital cells - A force-based ligand-receptor assay. *Biophys. J.* (Accepted for publication October 2013)

Stamping vital cells – A force-based ligand receptor assay

Uta Wienken and Hermann E. Gaub*

Chair of Experimental Physics & Center for NanoScience,

Ludwig-Maximilians-University München,

Amalienstrasse 54,

80799 Munich, Germany

Email: gaub@physik.uni-muenchen.de

Phone: + 49 (0) 89 2180 3172

ABSTRACT

Gaining information about receptor profiles on cells and subsequently finding the most efficient ligands for these signalling receptors, remain challenging tasks in stem cell and cancer research as well as drug development. We introduce a live-cell method with great potential in both screening for surface receptors and analysing binding forces of different ligands. The technique is based on the molecular force assay, a parallel format high throughput experiment on a single-molecule level. On human red blood cells, we demonstrate the detection of the interaction of N-acetyl-α-D-galactosaminyl residues with the lectin *helix pomatia* agglutinine and of the CD47 receptor with its antibody. The measurements are performed under nearly physiological conditions and still provide a highly specific binding signal. Moreover, with a detailed comparative force analysis on two cell types with different morphology, we show that our method even allows the determination of a DNA force equivalent for the interaction of the CD47 receptor and its antibody.

INTRODUCTION

Surface receptors and their interactions are a major focus of biomedical and pharmaceutical research due to their fundamental role in both signal transduction (1) and cell adhesion (2-4) as well as their involvement in cancer development and progression (5). In addition to the biochemical aspects of cell regulation and signalling, mechanical aspects play an important role (6-15) and must be considered. Still, the analysis of the binding behaviour of such proteins remains challenging (16). In recent years, biochip technologies have steadily gained importance not only as a research tool for detecting protein-protein interactions in general, but also as a diagnostic device. Offering the possibility of screening for a vast amount of specific marker proteins in parallel many different protein biochip formats have been developed (17,18). Though fast and cost-saving, the principle of microarrays is unfortunately afflicted with certain restrictions. To probe protein-protein interactions in a highly parallel format, proteins have to be immobilized on a surface. Such non-physiological conditions hold the possibility of denaturation of the protein. Considering the influence of conformational changes on protein-protein interactions, this method might easily lead to wrong results, such as unspecific binding of non-target molecules or non-binding of the natural target (18). An assay with membrane proteins seems even more problematic, because their hydrophobic transmembrane region makes it nearly impossible to immobilize such proteins on a surface. Consequently, they can only be probed if it is possible to do protein expression with the extracellular or intracellular domain or analyse single domains (19).

In this article we introduce a new live-cell assay that is based on the molecular force assay (MFA), established by Albrecht et al. (20). So far, the MFA was only applied to probe molecules immobilized on glass surfaces. The application of the MFA on cells offers the possibility of screening for receptors on the cell membrane with high throughput. Furthermore, it even allows access to the binding properties of such receptors under nearly physiological conditions.

MATERIALS AND METHODS

Production of elastomer stamps and chemical treatment. The stamps consisting of the silicone elastomer Sylgard (Dow Corning, Midland, MI) are fabricated as described by Xia et al. (21). They are 1 mm high and 1 mm in diameter with a square microstructure of 100 x 100 μm^2 and 5 μm in height. The pads' centres have a distance of 41 μm from each other. Before chemical modification, the stamps are ultrasonically cleaned in 50% aqueous isopropanol solution for ten minutes, irradiated for another ten minutes in an UV cleaner, activated in 12,5 % HCl over night, and rinsed afterwards. Subsequently, the stamps are incubated for 30 minutes in (3-glycidoxypropyl)-trimethoxysilane (ABCR, Karlsruhe, Germany) to generate epoxide groups on the surface. After rinsing excess silane with isopropanol and ddH_2O, the stamps are stored in argon atmosphere at 6°C until usage. For DNA functionalisation, the stamp is incubated in a borate buffered solution of amino-modified DNA in a saturated salt atmosphere over night resulting in a covalent bond between stamp surface and DNA. For further treatment, the stamp is rinsed with water, passivated with a 4% bovine serum albumin (Carl Roth, Karlsruhe, Germany) solution for 10 min and finally rinsed with water and dried with N_2.

Molecules. For all experiments an amino-modified 45 bp DNA strand was coupled via the amino-epoxy reaction to the elastomer surface. A 5x hexaethyleneglycol (HEGL) spacer followed by a polyT spacer (10x thymine) prevents interactions of the DNA with the surface. The reference DNA complexes are generated by binding complementary DNA strands of different length to the amino-modified strand. The strands of varying length consist of 8, 9, 11, 13, 15, 30, 45 nucleotides of complementary sequence followed by a Cy5 fluorescence dye and a biotin modification separated by a polyT spacer (5x thymine). For a minimum force measurement, a 20-nucleotide zipper-like DNA was used. In experiments with 15 to 45 bp the GC content of DNA is 60%, for shorter duplexes it is in a range between 62 and 67%. All DNA strands are purchased from IBA (Göttingen, Germany). The CD47 antibody (Klon CC2C5, BioLegend, San Diego, CA) and the lectin *helix pomatia* agglutinin (HPA) (Sigma Aldrich, St. Louis, MO) were covalently linked to streptavidin using Lightning-Link streptavidin (Innova Biosciences, Cambridge, UK).

Modification of the stamp surface. Different solutions of complementary biotin-modified DNA strands with a Cy5 fluorescence dye marker and streptavidin-modified antibodies are mixed in a 1:1 stoichiometry in 1x phosphate buffered saline (PBS) solution with 30mM trehalose and are deposited with the microarray plotter (GIX I microplotter, SonoPlot, Middleton, WI) on the microstructure of the stamp. After 5 minutes, the stamp is washed in 1x PBS, 1x PBS with 0.1% tween, and again 1x PBS for one minute each and then blocked with 4% bovine serum albumin for ten minutes. Finally, the stamp is rinsed and kept in 1x PBS till usage. The measurements are conducted with solutions of 0.56 μM streptavidin-modified CD47 antibody and 0.56 μM streptavidin-modified HPA, which are combined with biotin-modified DNA strands of different length (zip, 8, 9, 11, 13, 15, 30, 45 base pairs).

Cell culture. Human red blood cells (RBCs) are taken freshly from the finger pad of healthy volunteers, washed with 1x PBS, and centrifuged five times to separate the cells from the blood plasma. RBCs in 1x PBS suspension are then seeded on a poly-L-lysine (Biochrom, Berlin, Germany) -covered glass cover slip and incubated for 30 min at 37°C. RBCs are afterwards rinsed three times with 1x PBS to remove non-adherent cells. Measurements are performed in 1x PBS.

The human melanoma cell line M21 is provided by D. L. Morton (University of California, Los Angeles, CA) and is cultured in RPIM 1640 medium (GIBCO, Life Technologies, Paisley, UK) supplemented with 10% fetal bovine serum and 5 mM glutamine at 37°C in 5% CO_2 atmosphere. At least 24h prior to experiments, cells are harvested with 0.01% EDTA and seeded on a glass cover slip. Directly before measurements, the culture medium is removed, and cells are rinsed three times with 1x PBS. The measurements are performed in CO_2-independent L-15 Leibovitz medium without phenol red (GIBCO, Paisley, UK).

Experimental setup. The MFA measurements are conducted with a modified inverse epi-fluorescence microscope (Axio Observer. Z1, Zeiss, Oberkochen, Germany) (23). For the alignment of elastomer stamp and cells, the probe stage can be positioned in x-y-direction. The elastomer stamp is adhered to a small glass cover slip with 12 mm in diameter and is attached at the glass block of the stamping unit by an elastomer connecting piece.
The cell surface is approached by a high-precision stepper motor (PI, Karlsruhe, Germany) and then brought into close proximity by a piezo actuator (piezosystem, Jena, Germany). The parallel alignment of the stamp to the cell surface is done by micrometer screws (OWIS, Staufen, Germany) and monitored by reflection interference contrast microscopy. Illumination is performed using high power LEDs (627 nm peak wavelength, Thorlabs, Dachau, Germany) for fluorescence imaging and using a mercury arc lamp (Osram, Munich, Germany) for interference contrast microscopy.

Fluorescence analysis.
Fluorescence pictures of the cells are recorded with an Andor iXon camera (Andor Technology, Belfast, UK) and analysed with a self-written Labview software (National Instruments, München, Germany). For analysis, fluorescence pictures with 10x magnitude displaying the complete stamping pattern are recorded. The data we gain is fluorescence intensity, which is proportional to the incoming light intensity. To account for the heterogeneity of the illumination profile, the pictures are corrected with a picture of the illumination. The background intensity is measured in the non-fluorescent area between the pads. Several background measurements are averaged and then subtracted. For the analysis of the fluorescent areas, a grid is overlaid and aligned in the pictures of the stamp and of the cells after stamping. According to the grid, the mean intensity of the areas is measured, and afterwards, the mean intensity of the fluorescent areas on the cells is divided by the mean intensity of the corresponding pads on the stamp. In this way, we gain the relative fluorescence transfer of the cells. Hence, a relative fluorescence transfer of 0.05 means that 5% of the ligands on the stamp are transferred to the cells.

RESULTS AND DISCUSSION

Experimental approach. The MFA allows an analysis of binding forces of receptor-ligand interactions on a single molecule level by performing ensemble measurements. A molecular reference complex with known binding force is compared to the binding force of a probe complex. Both complexes are clamped in series between two surfaces. When separated, the molecular complex with the weaker bond is more likely to rupture, and a fluorescent label indicates the outcome of the experiment (20,22). In conventional MFA experiments, reference and probe consist of DNA or RNA duplexes. The typical setup (23) offers the possibility to analyse e.g. the effect of a single base pair mismatch or nucleic acid binding molecules (20-27). The setup for the *in vitro* analysis of membrane proteins with the MFA differs in some aspects. Most importantly, one surface is exchanged for a layer of living cells exposing certain receptors. These cell surface receptors and their possible ligands serve as probe, while the reference still consists of DNA. The DNA reference complex is immobilized on an elastomer surface. The specific ligand for a cell surface receptor is linked to the reference complex via a biotin-avidin chemistry (Fig. 1A).

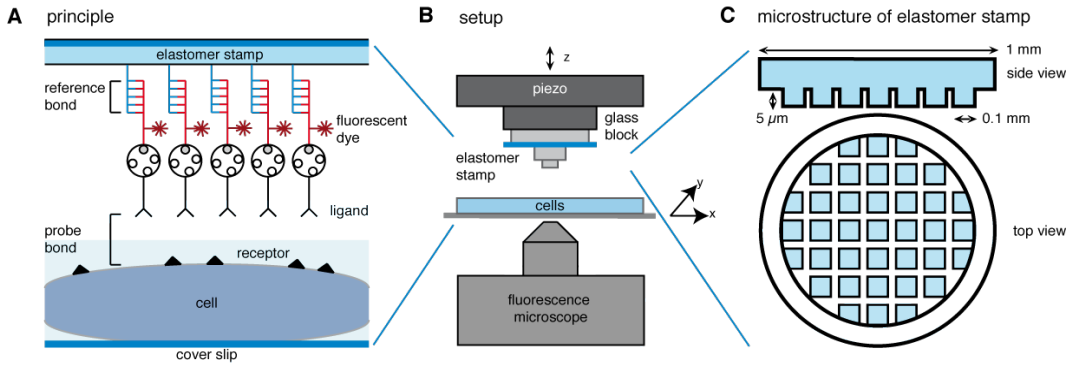

FIGURE 1 Experimental setup. *(A) The principle design of force balances in this experiment is illustrated. A reference bond and the probe bond are clamped in series between two surfaces; one is an elastomer stamp and the other is a cell's surface that exposes the receptor to analyse. The elastomer stamp is functionalised with the reference bond that consists of a DNA duplex with biotin, to which the probe molecule is linked via streptavidin. Both surfaces are brought into close contact and then are retracted. The weaker of the two bonds is more likely to rupture. A fluorescent dye at the reference complex displays the outcome of the experiment. (B) The experiment is monitored with an epi-fluorescence microscope with an x-y-stage and an additional glass block to which the functionalised elastomer stamp is adhered. The glass block can be accurately adjusted in z-position with a piezo, and its tilt can be levelled out with micrometer screws to ensure that both surfaces are parallel. (C) A scheme of the microstructure of the elastomer stamp is shown. The stamp is 1mm in diameter with elevated pads of 100x100µm.*

When contacting the cells with the elastomer stamp, reference and probe are clamped in series between rubber and cell surface. Like in standard MFA experiments, the molecular complex with the weaker bond is more likely to rupture, when separating the surfaces, and a fluorescent label at the reference complex indicates the outcome of the experiment. These single molecule measurements are now performed in a highly parallel format by functionalising the elastomer stamp with such molecular balances. However, in contrast to conventional MFA experiments, the number of force balances on the elastomer surface is much higher than the number of receptors at the cell surface. Consequently, with this setup there are many more incomplete than complete force balances, and thus, the ratio of the fluorescence intensity of the two surfaces provides no information about the strength of binding forces. The only parameter relevant for this experiment is the fluorescence transfer onto the cells.

A scheme of the experimental setup is shown in Fig. 1B. Before conducting the experiment, the stamp is prepared with DNA force balances of various strengths. Each pad can be functionalised with different force balances by a micro plotter. To abate suction and turbulence during the retraction of the stamp, the elastomer stamp has a microstructure with elevated pads of 100 x 100 μm shown in Fig. 1C. During the experiment, the cell surface is approached by a high-precision stepper motor and then brought into close proximity by a piezo actuator. As the exact parallel alignment of the elastomer surface and the cells is crucial to ensure an all-over contact for the whole elastomer surface with the cells during the experiment, the tilt of the glass block can be adjusted with micrometer screws. The parallel alignment is controlled by interference contrast microscopy allowing for adjustments in the nanometre range.

After the cells have been in contact with the functionalised stamp for one minute, the stamp is retracted with a velocity of 50 nm/s. The precise definition of the retraction speed is controlled using the piezo actuator. After separation, fluorescence images of the stamped cells are taken. Fig. 2A shows a typical 10x magnification fluorescence image, which is then used for detailed analysis of a complete experiment.

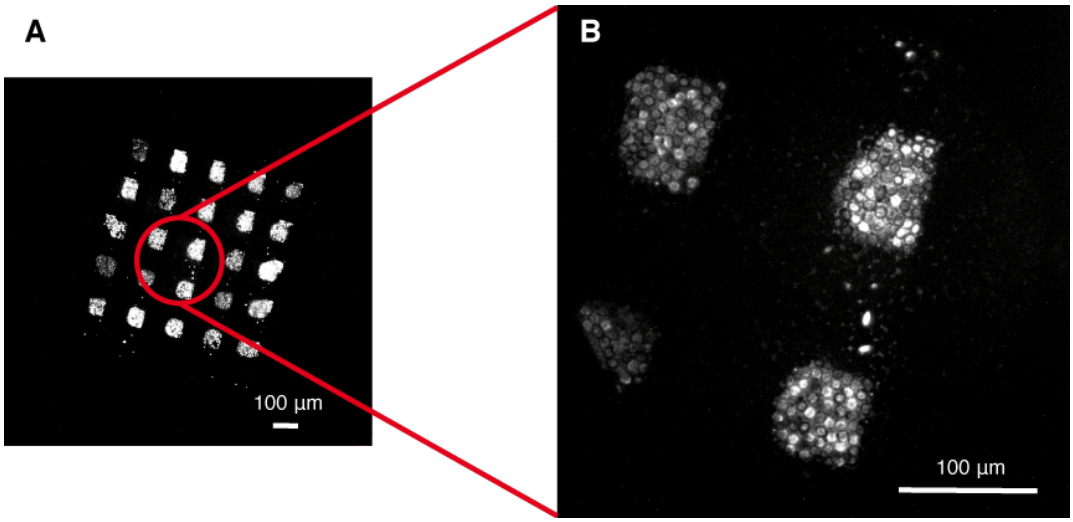

FIGURE 2 Fluorescence pictures of RBCs after contact. *(A) The picture with 10x magnitude depicts the fluorescence pattern of the pads. (B) At 40x magnitude, single fluorescently labelled blood cells are visible.*

The fluorescence picture with 40x magnitude gives a more detailed view of single blood cells (Fig. 2B). They are only labelled in areas where the functionalised pads of the stamp were in contact.

Screening assay. The experiment described in the following shows that the application of the MFA on cells is a valuable method to screen for multiple cell surface receptors in parallel. This is of great interest for medical research and drug development, since the lack or over-expression of surface receptors often is linked to diseases (28,29). We demonstrate the high specificity of detection for this method with two different ligands. The first ligand is an antibody against the CD47 receptor. The CD47 receptor is a transmembrane protein found on nearly every human cell in an appropriate density (30). The second ligand is the lectin HPA (31) that binds to N-acetyl-α-D-galactosaminyl residues (galNAc), a special glycolipid rest in the glycocalix of human red blood cells (RBCs). This glycolipid rest is exposed in a high density on RBCs of only blood group A. On RBCs of blood group O or B galNAc is absent (32). Grandbois et al. previously analysed this receptor-ligand complex with the AFM. They obtained rupture forces of about 35 pN for a single bond rupture of the galNAc-HPA complex at a retraction velocity of 6 µm/s (33). According to Strunz et al. (34), this corresponds to a DNA duplex shorter 10 bp. Since the rupture force of the DNA duplex is given by a rupture force distribution with non-zero width, it is possible to obtain a specific fluorescence transfer in a force range around the distribution's mean value. Given the unknown rupture force of the CD47 receptor and its antibody, a DNA reference force higher than 10bp was chosen to cover a broad range of possible interaction strengths. With the used 15 bp DNA reference complex, additionally, the non-specific fluorescence transfer could be reduced. HPA was deposited with a microplotter on every second

pad in a chessboard-like pattern, and the CD47 antibody was transferred to the remaining pads (Fig. 3, A and B).

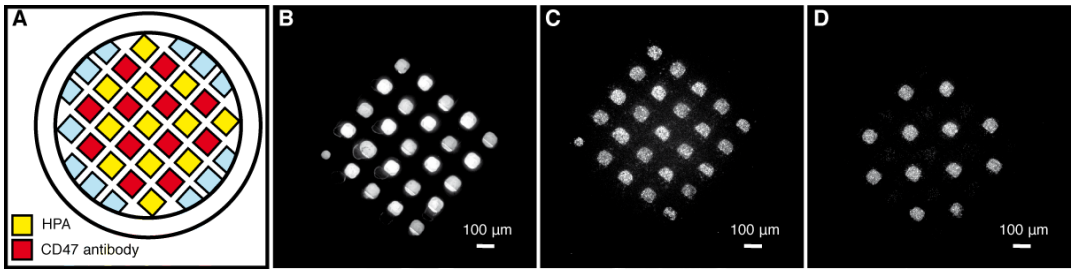

FIGURE 3 Detection of CD47 receptor and galNAc on human RBCs. *(A) Force balances consisting of a 15 bp DNA duplex as reference force and the CD47 antibody or the lectin HPA, respectively, are deposited in a chessboard-like pattern. (B) The fluorescence picture shows the elastomer stamp after functionalisation. With one stamp, two different experiments are conducted. (C) Post-contact fluorescence picture demonstrates that we obtain a fluorescence signal for both the CD47 receptor and galNAc on cells of blood group A with slightly different intensities. This difference might be due to different ligand densities on the cells or a lower binding force of the receptor-ligand complex. (D) In the fluorescence image of the cells of blood group O after contact, no fluorescence transfer is observed for the pads functionalised with the lectin. This is due to the absence of galNAc in blood group O and clearly demonstrates the reduction of unspecific interactions with this method.*

The first pad is always excluded from the measurements, because it is the starting and end point for the plotting process. Here, different solutions might accidently mix up. With only one stamp, two different experiments are conducted, first on RBCs of blood group A, and second on blood group O. This is possible, because the number of receptors on the cells is much lower than the number of ligands on the stamp.

In the first experiment, the RBCs of blood group A precisely exhibit the pattern on the microstructure of the elastomer as a fluorescence transfer pattern (Fig. 3C) indicating that both galNAc and the CD47 receptor are exposed on the cells. The fluorescence transfer for HPA is higher than for CD47 antibody. One explanation could be a higher galNAc density on the cell surface. A higher binding force of galNAc to HPA, on the other hand, would lead to the same result, since the DNA duplex is more likely to rupture. Repeating the experiment with the same stamp on RBCs of blood group O, we only obtained the chessboard-like pattern of the CD47 antibody (Fig. 3D). Clearly, we gained no fluorescence transfer for the lectin HPA on blood group O. This directly shows the absence of galNAc on blood group O. Furthermore, these results strongly suggest the elimination of unspecific interactions with this method, since the force to open the 15 bp DNA strand exceeds the strength of possible unspecific interactions. Similar experiments with a 9 bp DNA strand confirm the results. These experiments demonstrate that the MFA on living cells in combination with the microplotter technique is a powerful tool for the parallel screening for cell surface receptors.

Force measurements on RBCs. Since the MFA is primarily a method for highly sensitive force measurements (20), using the MFA on cells to reveal binding characteristics of the receptor-ligand bond seems a logical direction. The comparison of binding forces of different ligands provides valuable information about the interaction parameters, and hence, is of high interest for basic research and drug development. By performing a comparative force measurement, we circumvent elaborate direct force measurements like AFM experiments. Instead, we compare the binding force of the receptor-ligand complex of interest to a reference molecule that in case of the DNA is easier to analyse than the receptor-ligand complex (34). DNA is very well suited for those comparative force measurements, since the rupture force between duplexes may be programmed in a wide range by choosing attachment geometry, overlap length, and sequence (34,35). In a single experiment, the pads of the elastomer stamp are functionalised with different DNA lengths linked to the ligand. The ligand binds to the receptor in contact with the cell surface, and upon retraction, the reference or the probe bond ruptures in a stochastic process. The shorter the DNA duplex the weaker is the reference bond and the more readily it breaks resulting in a fluorescence transfer to the cell surface. Dependent on the length of the DNA duplexes and on the according strength of the reference bonds, we expect to obtain three regimes. For high reference forces corresponding to long DNA duplexes, we expect a minimum fluorescence transfer. On the other hand, for short DNA duplexes with a low reference force, we should obtain saturation of fluorescence transfer. In between these two regimes we expect a gradient, and specifically, the case that the probability of bond rupture is 50%. This is, when the reference force equals the force of the probe bond.
We conducted detailed force analyses with the CD47 antibody and the HPA on RBCs. For the analysis of the CD47 receptor, we functionalised an elastomer stamp with force balances consisting of the CD47 antibody and eight different lengths of DNA double strands (zip, 8, 9, 11,13, 15, 30 and 45 bp) corresponding to different reference forces (Fig. 4A).

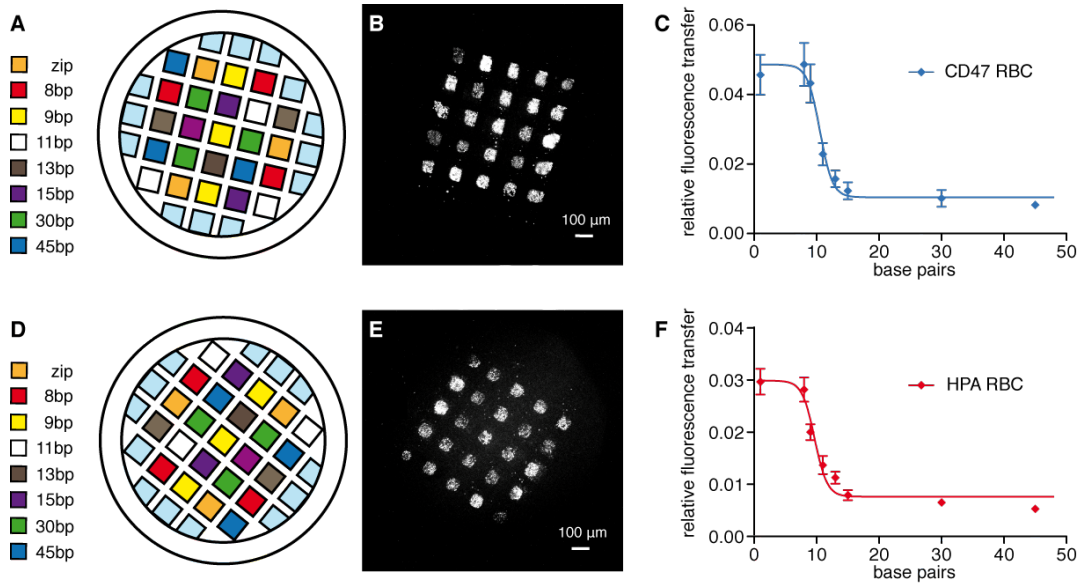

FIGURE 4 Detailed force measurements on RBCs for CD47 antibody and HPA. *(A) A stamp is functionalised with force balances consisting of the CD47 antibody and DNA duplexes of eight different lengths varying from 8 to 45 bp that correspond to different reference forces increasing with DNA length. The maximum fluorescence transfer is defined by a 20 bp DNA strand that opens base pair by base pair like a zipper and is named zip DNA. It is thermodynamically stable and mirrors the binding force of a single DNA base pair. (B) The fluorescence picture of the cells after contact already depicts higher fluorescence intensities for lower reference forces. (C) The mean fluorescence transfer of three measurements is shown in the graph. For low reference forces (8 and 9 bp duplexes), we obtain the maximum transfer defined by the zip DNA. With increasing DNA length, which represents an increasing reference force, we observe a rapid decrease in fluorescence intensity. When further increasing the DNA length to 45 bp, the intensity stays nearly constant. A Boltzmann sigmoidal fit displays a 50% value of 10.5 ± 0.32 bp DNA. (D) For a force analysis of the HPA-galNAc complex, the lectin was deposited on an elastomer stamp together with eight different DNA lengths. (E) The fluorescence picture of the cells after contact similarly shows higher intensities for pads with short DNA duplexes and very low intensities for long DNA. (F) The mean fluorescence transfer of four measurements displays a maximum transfer only for duplexes of 8 bp. An increase in DNA length corresponds to higher reference forces and leads to a transition. For high reference forces exerted by 30 and 45 bp DNA duplexes, the change in intensity is minimal. The 50% value of the Boltzmann sigmoidal fit is 9.7 ± 0.46 bp DNA.*

For a maximum transfer, we use a 20bp DNA, called “zip DNA” that opens one base pair after the other. This offers the advantage that it is a thermodynamically stable strand that mirrors the rupture force of a single base pair. Zip DNA, therefore, defines the maximum fluorescence transfer. The geometry of the

remaining duplexes is designed in a way that the force affects both 5'-ends of the double strand resulting in a shear force. The fluorescence image of the RBCs after the contact process (Fig. 4B) already reveals that pads with short DNA duplexes (corresponding to low reference forces) lead to more fluorescence transfer onto cells than pads with long DNA as a reference force. The graph obtained by explicit data analysis of three similar measurements (Fig. 4C) shows the maximum fluorescence transfer for the zip DNA and the short 8 and 9 bp DNA duplexes. This indicates that the binding force of antibody and receptor exceeds the reference force in this regime. A further increase in the number of base pairs corresponding to higher reference forces leads to a rapid change in fluorescence intensity. For long strands (30 and 45 bp), the fluorescence intensity hardly decreases indicating that the binding force of the DNA duplex is higher than the force of antibody and receptor. A fit with a Boltzmann sigmoidal function displays a force equivalent of 10.5 ± 0.32 bp DNA duplex for the CD47 antibody and its receptor. Having a closer look at the data points, the sigmoidal fit represents only an approximation for our data. For the long DNA strands, we still observe a decrease in fluorescence transfer with increasing DNA length, even if the DNA length exceeds the DNA force equivalent of the interaction. This can be explained by the non-zero width of the rupture force distribution of the DNA reference. Thus, we obtain a specific transfer also for long DNA strands with interaction strengths stronger than the force equivalent. In contrast to this, in the screening assay shown in Figure 3, the cells lack the necessary receptor for a specific transfer. Hence, the experiment without the according receptor yields only unspecific fluorescence transfer, which is significantly below the specific transfer.

In a similar experiment, a second receptor-ligand complex consisting of the glycolipid rest galNAc and its ligand HPA was analysed. Since the affinity of the HPA for galNAc is only in the 10^{-4} M regime (33), a shift to lower forces is expected. For the rupture forces analysis, balances with HPA and again eight different DNA lengths (zip, 8, 9, 11, 13, 15, 30, 45 bp) are bound onto different pads of the elastomer stamp (Fig. 4D). The fluorescence transfer onto the cells is depicted in Fig. 4E. Again, pads with short DNA duplexes lead to high intensities on the cells, whereas pads with long DNA duplexes transfer little fluorescence to the cells. A detailed data analysis of four different measurements (Fig. 4F) shows that the maximum fluorescence transfer is only obtained with the zip and 8bp duplex DNA. Increasing the reference force leads to a transition towards lower fluorescence transfer. Longer duplexes (15, 30 and 45 bp) produce a minimum in fluorescence transfer. A Boltzmann sigmoidal fit yields a force equivalent of 9.7 ± 0.46 bp DNA for the HPA bound to galNAc. Compared to the force analysis of the CD47 antibody and its receptor, we obtain the expected shift to lower forces for the low-affinity ligand HPA. Granbois et al. obtained rupture forces for the galNAc-HPA complex of about 35 pN at a retraction velocity of 6 μm/s (33). Considering the data Strunz et al. (34) gained from AFM measurements with DNA duplexes, a most probable rupture force of 35 pN at this retraction velocity would be due to a DNA duplex shorter 10 bp. Thus, compared to literature, the force equivalent for HPA is a reasonable value.

Force analyses on M21 cells. We demonstrate in the following that the force analysis with the MFA can be applied on different types of living cells with differing morphology and is not restricted to RBCs; we also conducted force analyses with the CD47 antibody on M21 melanoma cells. Again, we functionalised the stamp with the same DNA duplexes (Fig. 5A).

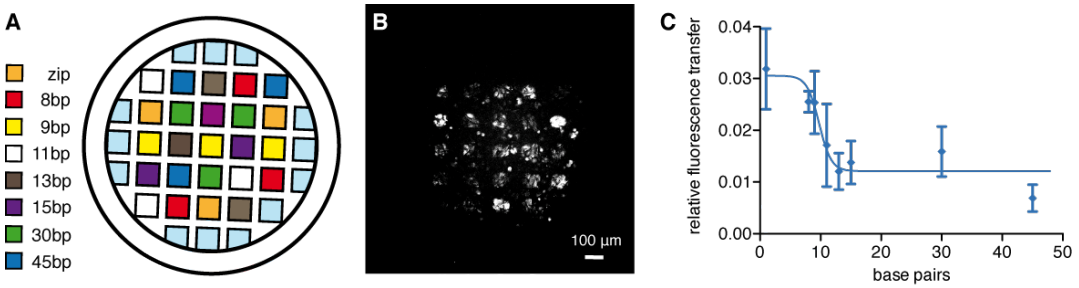

FIGURE 5 Force analysis of the CD47 receptor on M21 melanoma cells. *(A) The elastomer stamp is functionalised with the CD47 antibody and DNA duplexes of eight different lengths as reference. (B) The fluorescence picture of the cells after contact clearly depicts the maximum fluorescence transfer defined by the zip DNA, and the transfer for 8 bp duplexes is notably higher than for longer reference duplexes. (C) The graph shows mean fluorescence transfer of two measurements. Again, two states can be distinguished: a maximum and a minimum fluorescence transfer. For the transition the Boltzmann sigmoidal fit yields a 50% value of 9.8 ± 0.81 bp DNA. Compared to the analysis of the CD47 receptor on RBCs, the binding force for this receptor on M21 cells is shifted to a shorter DNA duplex that corresponds to a lower binding force.*

The picture of the fluorescence transfer on the cells exhibits brighter regions for the zip DNA and short DNA duplexes (Fig. 5B). Explicit data analysis of two measurements reveals two states and a gradient (Fig. 5C). For the force equivalent for the CD47 receptor and its antibody on M21 cells, the Boltzmann fit yields a value of 9.8 ± 0.81 bp DNA. Comparing this to the force equivalent for the CD47 receptor on RBCs, a slightly lower value is found for the M21 melanoma cells. This shift might be generated by variations in the receptor expression that influences the affinity in different cells. Additionally, the signal-to-noise ratio decreases compared to the measurements on RBCs. This might be due to variations in the cell height and a less uniform distribution on the cover slip. Moreover, a lower fluorescence transfer is observed for the M21 cells, which might be caused by a lower receptor density on these cells. However, the obtained signal-to-noise ratio allows for a reliable force analysis conducted directly on living cells.

CONCLUSION

Considering the highly important role of membrane proteins in physiological and pathological processes, and thus, their potential for medical and pharmaceutical research, there is a great demand for methods for the in vitro analysis of cell surface receptors. However, the research on membrane proteins remains challenging, and methods for their investigation are rare. One method to deal with transmembrane proteins is to stain living or fixed cells with specific fluorescently labelled ligands and analyse them by flow cytometry. For the staining process, cells are incubated with the ligand for a certain time and then washed to get rid of the excess ligand (36). Still, there is the possibility that in the absence of the target the ligand binds unspecifically and with lower affinity to another molecule on the cell surface, thereby leading to a false positive result. By using stains with different emission wavelengths, it is possible to detect a few different types of surface molecules at the same time, yet this method does not yield any information about the binding properties of the receptor under investigation. Employing the AFM, the mechanical properties of receptor-ligand complexes on cells can be analysed in detail, and rupture forces can be measured very accurately on a single molecule level (37-41). On the other hand, this technique is very time-consuming and, thereby, not suitable for a high throughput screening for membrane receptors on cells.

In this article we demonstrated that the MFA applied on living cells is a powerful method to do parallel screenings for cell surface receptors at nearly physiological conditions. At the same time, by delivering the ligand to the cell surface against a certain reference force, the method excludes unspecific interactions that might lead to biased results. The possibility to do a parallel screening for receptors on living cells without unspecific interactions makes this application attractive for healthcare and drug design. Moreover, we proved that it is possible to determine a DNA force equivalent for the receptor of interest by the variation of DNA reference forces. We have shown that the force equivalent for the low-affinity binder HPA is lower than for the CD47 antibody on RBCs. Additionally, we determined the force equivalent for the CD47 receptor on M21 melanoma cells and demonstrated that our method can be applied on living cells of cultured cell lines. Altogether, by the analysis of binding forces, our method provides access to the force threshold that is e.g. necessary for a specific delivery of molecules on vital cells. Moreover, we gain highly valuable information about binding characteristics of receptors that help finding and evaluating possible ligands in cancer research and drug design. In summary, these qualities make the MFA on cells a powerful, effective, and widely applicable tool for health care, research, and drug development.

ACKNOWLEDGEMENTS

The authors thank Katja Limmer, Daniela Aschenbrenner, Marcus Otten, Dr. Philip Severin, and Dr. Martin Benoit for helpful discussions and Katherine Erlich for suggestions on the manuscript. Furthermore we thank Dr. Diana Pippig and Katja Limmer for being healthy volunteers for the RBC experiments. The authors thank the ERG and the DFG for support.

REFERENCES

1. Smok, R. G. and L. M. Gierasch. 2009. Sending signals dynamically. *Science* **324,** 198-203
2. Cavallaro, U. and G. Christofori. 2004. Cell adhesion and signaling by cadherins and Ig-CAMs in cancer. *Nat. Rev. Cancer* **4,** 118-132
3. Parsons, J.T., A. R. Horwitz, and M. A. Schwartz. 2010. Cell adhesion: integrating cytoskeletal dynamics and cellular tension. *Nat. Rev. Mol. Cell Bio.* **11,** 633-643
4. Papusheva, E. and C.-P. Heisenberg. 2010. Spatial organization of adhesion: force-dependent regulation and function in tissue morphogenesis. *EMBO J.* **29,** 2753-2768
5. Simpson, R. J. and D. S. Dorow. 2001. Cancer proteomics: from signaling networks to tumor markers. *Trends Biotechnol.* **19,** 40-48
6. Puchner, E. M. and H. E. Gaub. 2012. Single-molecule mechanoenzymatics. *Annu. Rev. Biophys.* **4,** 497-518
7. Evans, E. A. and D. A. Calderwood. 2007. Forces and bond dynamics in cell adhesion. *Science* **316,** 1148-1153
8. Vogel, V. and M. P. Sheetz. 2009. Cell fate regulation by coupling mechanical cycles to biochemical signaling pathways. *Curr. Opin. Cell Biol.* **21,** 38-46
9. Schwartz, M. A. and D. W. DeSimone. 2008. Cell adhesion receptors in mechanotransduction. *Curr. Opin. Cell Biol.* **20,** 1-6
10. Katz, B.-Z. et al. 2000. Physical state of the extracellular matrix regulates the structure and molecular composition of cell-matrix adhesions. *Mol. Biol. Cell* **11,** 1047-1060
11. Janmey, P. A. and C. A. McCulloch. 2007. Cell Responses to mechanical stimuli. *Annu. Rev. Biomed. Eng.* **9,** 1-34
12. Bershadsky, A., M. Kozlov and B. Geiger. 2006. Adhesion-mediated mechanosensitivity: a time to experiment and a time to theorize. *Curr. Opin. Cell Biol.* **18,** 472-481
13. Alenghat F. J. and D. E. Ingber. 2002. Mechanotransduction: All signals point to cytoskeleton, matrix, and integrins. *Sci. STKE.* **119,** 1-4
14. Puchner, E. M. and H. E. Gaub. 2010. Exploring the conformation-regulated function of titin kinase by mechanical pump and probe experiments with single molecules. *Angew. Chem. Int. Ed.* **49,** 1147-1150
15. Puchner, E. M. et al. 2008. Mechanoenzymatics of titin kinase. *P. Natl. Acad. Sci. USA.* **105,** 13385-13390
16. Zhu, H. and M. Snyder. 2001. Protein arrays and microarrays. *Curr. Opin. Chem. Biol.* **5,** 40-45
17. Chen, H. et al. 2009. Protein chips and nanomaterials for application in tumor marker immunoassays. *Biosens. Bioelectron.* **24,** 3399-3411
18. Zhu, H. and M. Snyder. 2003. Protein chip technology. *Curr. Opin. Chem. Biol.* **7,** 55-63
19. Cunningham F. and C. M. Deber. 2006. Optimizing synthesis and expression of transmembrane peptides and proteins. *Methods (San Diego, CA, U. S.)* **41,** 370-380

20. Albrecht, C. et al. 2003. DNA: A programmable force sensor. *Science* **301,** 367-370
21. Xia, Y. and G. M. Whitesides. Soft lithography. 1998. *Annu. Rev. Mater. Sci*. **28,** 153-184
22. Albrecht, C.H., H. Clausen-Schaumann and H. E. Gaub. 2006. Differential analysis of biomolecular rupture forces. *J. Phys.: Condens. Matter.* **18,** 581-599
23. Severin, P. M. D., D. Ho, and H. E. Gaub. 2011. A high throughput molecular force assay for protein–DNA interactions. *Lab Chip* **11,** 856-862
24. Ho, D., K. Falter , P. M. D. Severin and H. E. Gaub. 2009. DNA as a force sensor in an aptamer-based biochip for ATP. *Anal. Chem.* **81,** 3159–3164
25. Limmer, K., D. Aschenbrenner and H. E. Gaub. 2013. Sequence-specific inhibition of Dicer measured with a force-based microarray for RNA ligands. *Nucleic Acids Res.* 1-9
26. Severin, P. M. D. and H. E. Gaub. 2012. DNA-Protein binding force chip. *Small* **8,** 3269-3273
27. Dose, C., D. Ho, H. E. Gaub, P. B. Dervan and C. H. Albrecht. 2007. Recognition of "Mirror-Image" DNA by small molecules. *Angew. Chem. Int. Ed.* **46,** 8384-8387
28. Oldenborg, P. A. et al. 2000. Role of CD47 as a Marker of Self on Red Blood Cells. *Science* **288,** 2051-2054
29. Petitclerc, E. et al. 1999. Integrin aVb3 promotes M21 melanoma growth in human skin by regulating tumor cell survival. *Cancer Res.* **59,** 2724-2730
30. Brown, E. J. and W. A. Frazier. 2001. Integrin-associated protein (CD47) and ist ligands. *Trends Cell Biol.* **11,** 130-135
31. Sanchez J.-F. et al. 2006. Biochemical and structural analysis of Helix pomatia agglutinin. *J. Biol. Chem.* **281,** 20171-20180
32. Torres B. V. and D. F. Smith. 1988. Purification of Forssman and humanblood group A glycolipids by affinity chromatography on immobilized Helix pomatia lectin. *Anal. Biochem.* **170,** 209–219
33. Grandbois, M., W. Dettmann, M. Benoit and H. E. Gaub. 2000. Affinity imaging of red blood cells using an atomic force microscope. *J. Histochem. Chemochem.* **48,** 719-724
34. Strunz, T., K. Oroszlan, R. Schäfer and H.-J. Güntherodt. 1999. Dynamic force spectroscopy of single DNA molecules. *Proc. Natl. Acad. Sci. USA.* **96,** 11277-11282
35. Wang, X. and T. Ha. 2013. Defining single molecular forces required to activate integrin and Notch signalling. *Science* **340,** 991-994
36. Bendall, S.C. et al. 2011. Single-cell mass cytometry of differential immune and drug responses across a human hematopoietic continuum. *Science* **332,** 687-696
37. Helenius, J., C.-P. Heisenberg, H. E. Gaub and D. J. Müller. 2008. Single-cell force spectroscopy. *J. Cell Sci*. **121,** 1785-1791
38. Medalsy, I., U. Hensen and D.J. Müller. 2011. Quantifying chemical and physical properties of native membrane proteins at molecular resolution by force-volume AFM. *Angew. Chem. Int. Edit.* **50,** 12103-12108
39. Dufrene, Y. F. and D.J. Müller. 2001.Force nanoscopy of living cells. *Curr. Biol.* **21,** 212-216

40. Friedrichs, J., J. Helenius and D.J. Müller. 2010. Quantifying cellular adhesion to extracellular matrix components by single-cell force spectroscopy. *Nat. Proto.* **10,** 1353-1361
41. Schmitz, J. and K. E. Gottschalk. 2008. Mechanical regulation of cell adhesion. *Soft Matter* **4,** 1373-1387

SUPPORTING MATERIAL for

Stamping vital cells – A force-based ligand receptor assay

Uta Wienken and Hermann E. Gaub*

Chair of Experimental Physics & Center for NanoScience,
Ludwig-Maximilians-University München,
Amalienstrasse 54,
80799 Munich, Germany
Email: gaub@physik.uni-muenchen.de
Phone: + 49 (0) 89 2180 3172

Discussion of unspecific fluorescence transfer. To quantify the unspecific fluorescence transfer, we tested the HPA –galNAc interaction on red blood cells of group A and O with DNA reference lengths of 9bp, 15bp, 30bp and 45bp. In the fluorescence images of the cells after contact fluorescence transfer onto the cells is observed for blood group A (Fig. S1A), while for blood group O (Fig. S1B) no fluorescence transfer occurs.

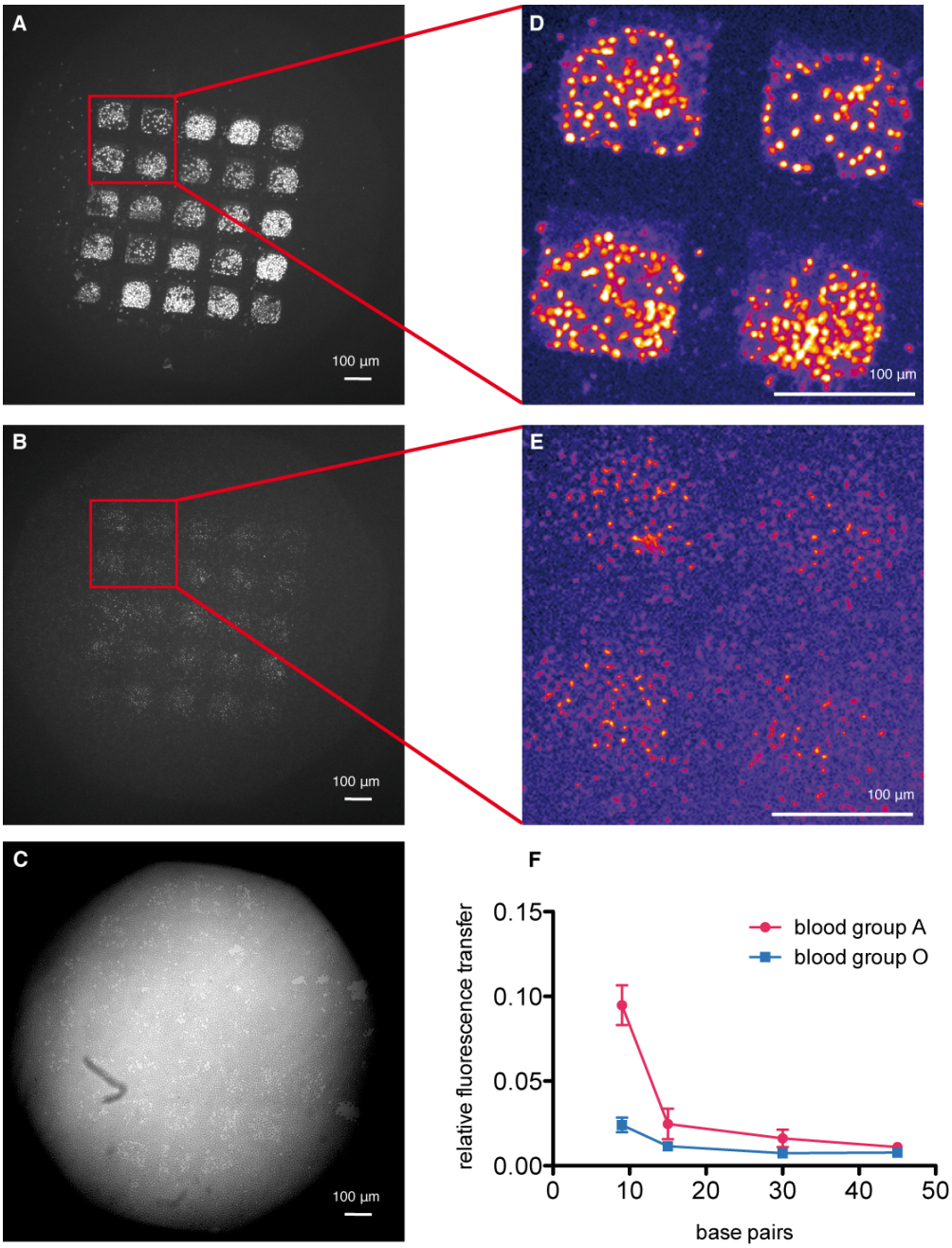

FIGURE S1 Unspecific fluorescence transfer for the HPA-galNAc interaction. *(A) The fluorescence image of RBCs of blood group A after contact shows a fluorescence transfer on the cells for all DNA reference lengths (9 bp, 15 bp, 30 bp and 45 bp). (B) With the same stamp no fluorescence transfer is obtained on cells of blood group O. (C) In the transmitted light image of blood group O after contact cells appear lighter in some areas, because several cells are burst. This is due to the rather high contact pressure. (D) Zoomed-in false colour image of blood group A shows fluorescence transfer onto the cells. (E) For blood group O the zoomed-in false colour image reveals no fluorescence transfer onto the cells, but only onto the glass surface. (F) Data analysis shows a slight increase in unspecific transfer for the 9 bp DNA reference. Still, the specific fluorescence transfer is significantly higher.*

The transmitted light image of the cells of blood group O after contact (Suppl. Fig. 1C) indicates a rather high contact pressure, since in contact areas several cells burst. This ensures that the non-fluorescent cells of blood group A are no result of weak contact. A zoomed view of the fluorescence images using false colour implies that for blood group A the fluorescence is transferred to the cell surface (Fig. S1D), while for blood group O the unspecific transfer occurs mainly onto the glass surface (Fig. S1E).
A quantitative analysis (Fig. S1F) of this experiment shows that for the short DNA with 9bp the unspecific fluorescence transfer is slightly increased. Due to the high contact force in the experiments aiming at the unspecific interactions, the resulting absolute values for the fluorescence transfer are approximately 4-5x higher than the values obtained in the force analyses. Hence, although the pressure force dependency renders a correction of the measurements with a second independent background measurement difficult, above experiment shows that the unspecific fluorescence transfer only leads to a minor correction of the fluorescence transfer.
When comparing the specific fluorescence transfer with the unspecific fluorescence transfer, a transfer signal is observed for DNA reference lengths up to 30bp, although the expected interaction strength is around 10bp. This is, because the DNA duplexes do not have sharp rupture forces, but DNA rupture is a highly statistical process leading to a rupture force distribution with a distinct width. Hence, also for 30bp the probability of rupture forces below the mean rupture force of a 10bp duplex is non-zero.

Discussion of the influence of contact force and contact time. The contact force is the pressure exerted on the cells during the experiment. It has an effect on the amount of fluorescence transfer on the cells: The stronger the contact force the higher the fluorescence transfer. This is due to the morphology of the cells, as some areas, like the border area on RBCs, are elevated and make contact before other parts of the cell. At higher contact forces, the cells are deformed, which leads to a fluorescence transfer on a larger area of the cell surface.
However, since the cells are quite sensitive to pressure and may burst, we do not aim for full contact in our experiments.
Due to the extensive parallel alignment of the stamp with the glass surface, a comparable contact force is obtained for all pads on one stamp. This allows comparing the fluorescence values of the pads and, thus, allows comparing the rupture forces.
The fluorescence transfer values of independent experiments with varying contact force can therefore not be compared.

The contact time has no significant effect on the fluorescence transfer. However, for longer contact times the cells suffer from deformation, which leads to apoptosis or the bursting of cell membranes. Contact times shorter than 60s are difficult to realize, as the cell surface has to be approached very carefully to avoid too high contact forces.

12. Acknowledgements

I'd like to thank all the people that supported me and contributed to my work. First of all, I thank Hermann Gaub for enabling this thesis, for his scientific support, his inspiring ideas and discussions, and for the flexible schedule line. I thank the whole "Gambicrew" for giving me a great time making it a pleasure to work, even in more frustrating days. I thank:

The "Stempler" for their team spirit:

Katja Limmer and Daniela Aschenbrenner and Anita Ladenburger for the enjoyable tea sessions and not only scientific conversations.

Philip Severin and Dominik Ho for scientific inspiration and funny nights having curry wurst and beer.

Diana Pippig for helpful scientific discussions.

Angelika Kardinal for always giving me a warm welcome and taking care of my cells.

Thomas Nikolaus for support concerning surface chemistry.

Christopher Hitz for support in experimental preparation.

Especially, I thank my family that is so important to me and always gives me strength and backing. I thank:

My husband, Christoph Wienken, for being my very best friend and giving me motivation and comfort in all situations.

My little daughter, Paula Wienken, for letting the sun shine every day.

My parents, Kornelia and Uwe Steinbach, for always being there and supporting me in going my way.

My parents in law, Jutta and Egon Wienken, for being good friends and giving manifold support.